US005755226A

United States Patent [19]

Carim et al.

[11] Patent Number: 5,755,226

[45] Date of Patent: May 26, 1998

[54] **METHOD AND APPARATUS FOR NONINVASIVE PREDICTION OF HEMATOCRIT**

[75] Inventors: **Hatim M. Carim**, West St. Paul; **Orlin B. Knudson**, Vadnais Heights; **Bruce P. Ekholm**, Inver Grove Heights; **David P. Erickson**, Stillwater; **William J. Kelliher, Jr.**, Shoreview; **Michael J. Rude**, St. Paul, all of Minn.

[73] Assignee: **Minnesota Mining and Manufacturing Company**, St. Paul, Minn.

[21] Appl. No.: **711,612**

[22] Filed: **Sep. 10, 1996**

Related U.S. Application Data

[62] Division of Ser. No. 189,600, Jan. 31, 1994, Pat. No. 5,553,615.

[51] **Int. Cl.**[6] **A61B 5/00**

[52] **U.S. Cl.** **128/633**; 128/664; 356/39

[58] **Field of Search** 128/633, 664, 128/665, 666; 356/39, 40, 41

[56] **References Cited**

U.S. PATENT DOCUMENTS

3,923,397	12/1975	Shuck	356/39
4,227,814	10/1980	Soodak et al.	356/410
4,303,336	12/1981	Cullis	356/39
4,407,290	10/1983	Wilber	128/633
4,447,150	5/1984	Heinermann	356/41
4,548,211	10/1985	Marks	128/694
4,562,843	1/1986	Djordjevich et al.	128/672
4,586,313	5/1986	Hamaguri	128/633
4,621,643	11/1986	New, Jr. et al.	128/633
4,653,498	3/1987	New, Jr. et al.	128/633
4,685,464	8/1987	Goldberger	128/633
4,745,279	5/1988	Karkar et al.	250/343
4,776,340	10/1988	Moran et al.	128/634
4,805,623	2/1989	Jobsis	128/633
4,819,752	4/1989	Zelin	128/633
4,832,484	5/1989	Aoyagi et al.	356/41
4,869,254	9/1989	Stone et al.	128/633
4,883,353	11/1989	Hausman et al.	356/41
4,936,679	6/1990	Mersch	356/41
4,975,581	12/1990	Robinson et al.	250/339
5,078,136	1/1992	Stone et al.	128/633
5,101,825	4/1992	Gravestein et al.	128/633
5,137,023	8/1992	Mendelson et al.	128/633
5,193,543	3/1993	Yelderman	128/633
5,200,345	4/1993	Young	436/63
5,233,991	8/1993	Wright	128/653.2

(List continued on next page.)

FOREIGN PATENT DOCUMENTS

0 419 223 A2	3/1991	European Pat. Off.	G01N 21/35
0 476 192 A2	3/1992	European Pat. Off.	G01N 21/35
WO 92/13482	8/1992	WIPO	A61B 5/00
WO 93/13706	7/1993	WIPO	A61B 5/00

OTHER PUBLICATIONS

Claim 1 for U.S. Pat. No. 5,456,253, *Biomedical Technology Information Service*, Dec. 1, 1995.

(List continued on next page.)

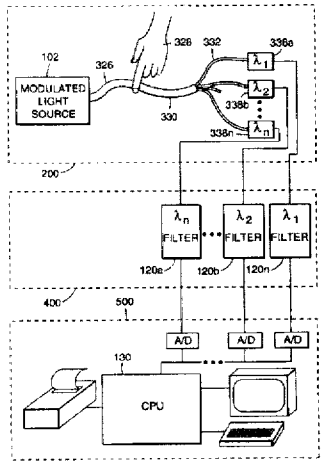
Primary Examiner—Jennifer Bahr
Assistant Examiner—Eric F. Winakur
Attorney, Agent, or Firm—Gary L. Griswold; Walter N. Kirn; Kari H. Bartingale

[57] **ABSTRACT**

A method and apparatus for the direct noninvasive prediction of hematocrit in mammalian blood using photoplethysmography techniques and data processing. The method and apparatus also include optional prediction of other analytes of interest: percent oxygen saturation of mammalian blood and methemoglobin of stored blood. The method and apparatus can be used for the immediate, periodic, or continuous noninvasive diagnosis or monitoring of hematocrit levels in mammalian patients without pain to the patient or exposure of the health care practitioner to the blood of the patient.

11 Claims, 32 Drawing Sheets

Microfiche Appendix Included
(2 Microfiche, 128 Pages)



U.S. PATENT DOCUMENTS

5,277,181	1/1994	Mendelson et al.	128/633
5,297,548	3/1994	Pologe	128/633
5,337,745	8/1994	Benaron	128/633
5,355,880	10/1994	Thomas et al.	128/633
5,372,136	12/1994	Steuer et al.	128/633
5,406,223	4/1995	Vulih et al.	330/258
5,553,613	9/1996	Parker	128/633

OTHER PUBLICATIONS

The CRIT-Line™ System Brochure, In-Line Diagnostics Corporation.

Noninvasive Blood Volume Monitoring Brochure, In-Line Diagnostics Corporatiion, 1993.

Cope et al., "A CCD Spectrophotometer to Quantitate the Concentration of Chromophores in Living Tissue Utilising the Absorption Peak of Water at 975 nm", *Adv, Exp. Med. Biol.*, Proc. 150TT88 Cont. Plenum.

Dickensheets et al., Pathlength Independent Spectrophotometric Measurement of Hemoglobin in Solution:, IEEE 11th Annual Conference, pp. 1090–1091 (1989).

Focus, "Near-Infrared Spectrometry in Clinical Analysis", *Analytical Chemistry*, vol. 58, No. 8, (1986).

Honigs, "Near Infrared Analysis", *Analytical Instrumentation*, 14(1), pp. 1–62 (1985).

Lee et al., "Measurement of Percent Carboxyhemoglobin with Pulse-Oximetry Technique", IEEE 10th Annual International Conference, pp. 1781–1782 (1988).

Lee et al., "Simultaneous Measurement of Percent Carboxyhemoglobin and Functional Oxygen Saturation", IEEE 11th Annual International Conference, pp. 1092–1093 (1989).

Ozanich, "Non Invasive Method For Determination of Blood pH based on Visible NIR Spectroscopy", University of Washington Ph.D. Dissertation: Chapter 3 Determination of Hematocrit By Short-Wave-Near -Infrared Spectrophotometry and Chapter 4 In-Vivo Spectrophotometry and Imaging of Biological Samples, pp. 1–3, catalogued Feb. 11, 1993.

Pries et al., "Microphotometric Determination of Hematocrit in Small Vessels", American Physiological Society H167–H177 (1983).

Schmitt, "Measurement of blood hematocrit by dual-wavelength near-IR photoplethsmography", SPIE, vol. 1641, pp. 150–161 (1992).

Steinke et al., "Reflectance measurements of hematocrit and oxyhemoglobin saturation", *Am J. Physiol. (U.S.)*, 22(1), pp. H147–H153 (1987).

Steur et al., Evaluation of a noninvasive hematocrit monitor: A new technology, *Amer. Clin. Lab.*, 10(6):20 (1991).

Takatani et al., "Experimental and Clinical Evaluatiion of a Noninvasive Reflectance Pulse Oximeter Sensor", *Journal of Clinical Monitoring*, vol. 8, No. 4, pp. 257–266 (1992).

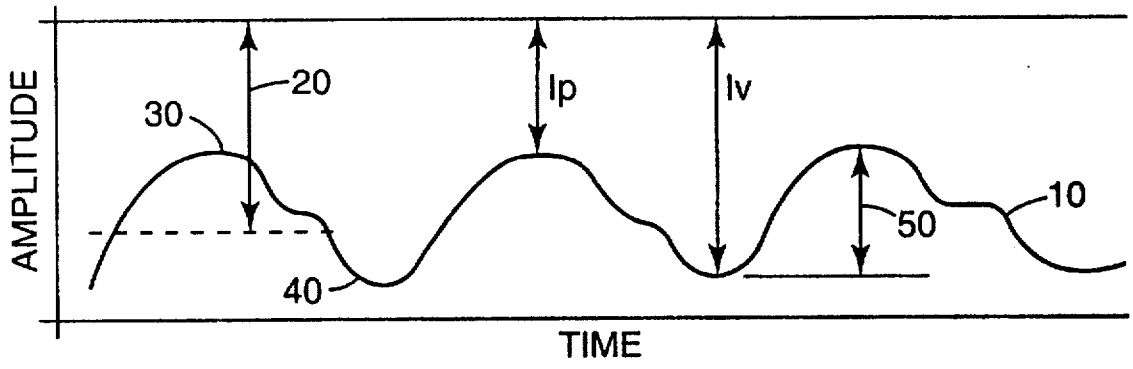


Fig. 1

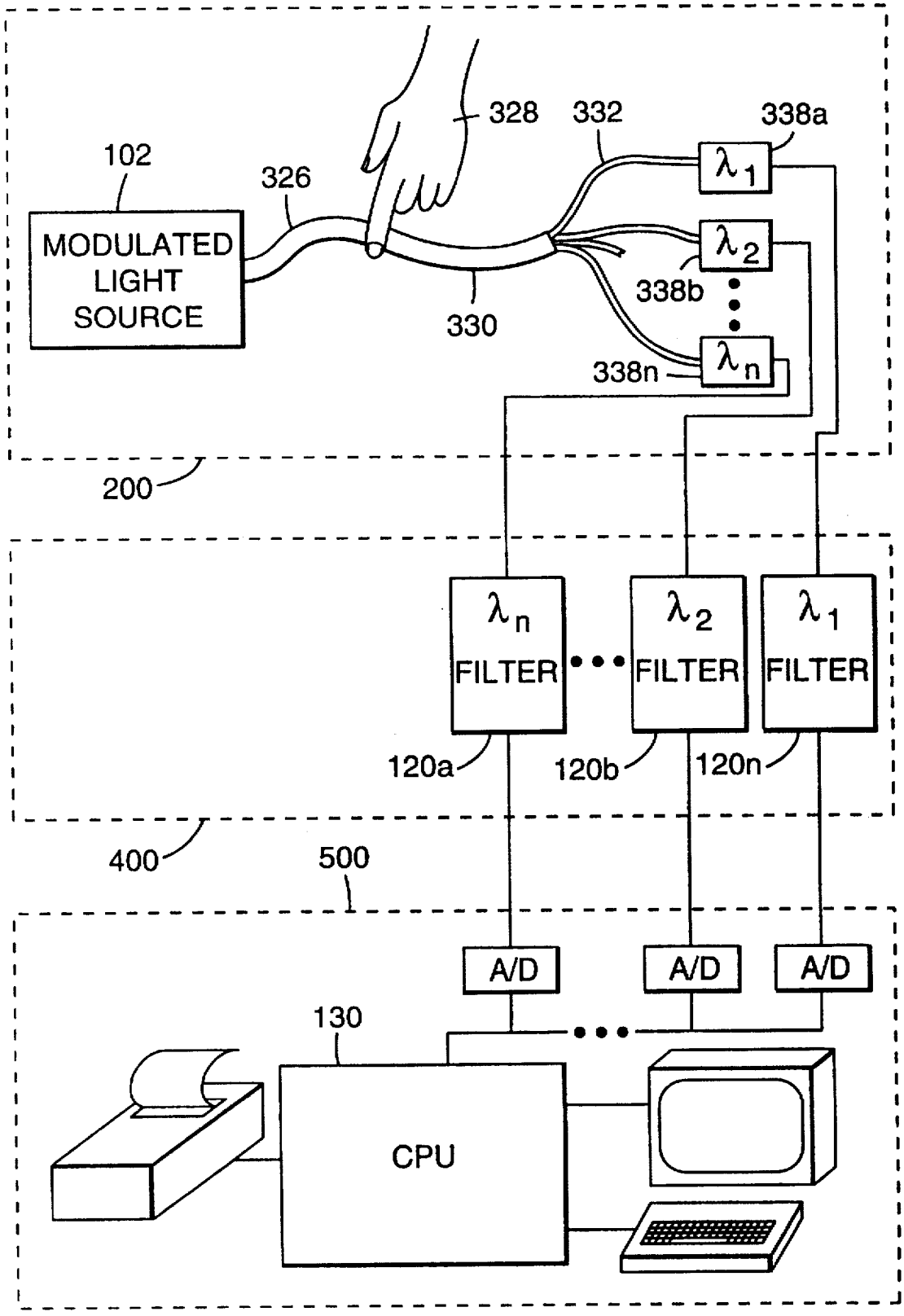

102
MODULATED LIGHT SOURCE
326
328
330
332
338a
338b
338n
λ1
λ2
λn
200
λn FILTER
λ2 FILTER
λ1 FILTER
120a
120b
120n
400
500
A/D
A/D
A/D
130
CPU

Fig. 2

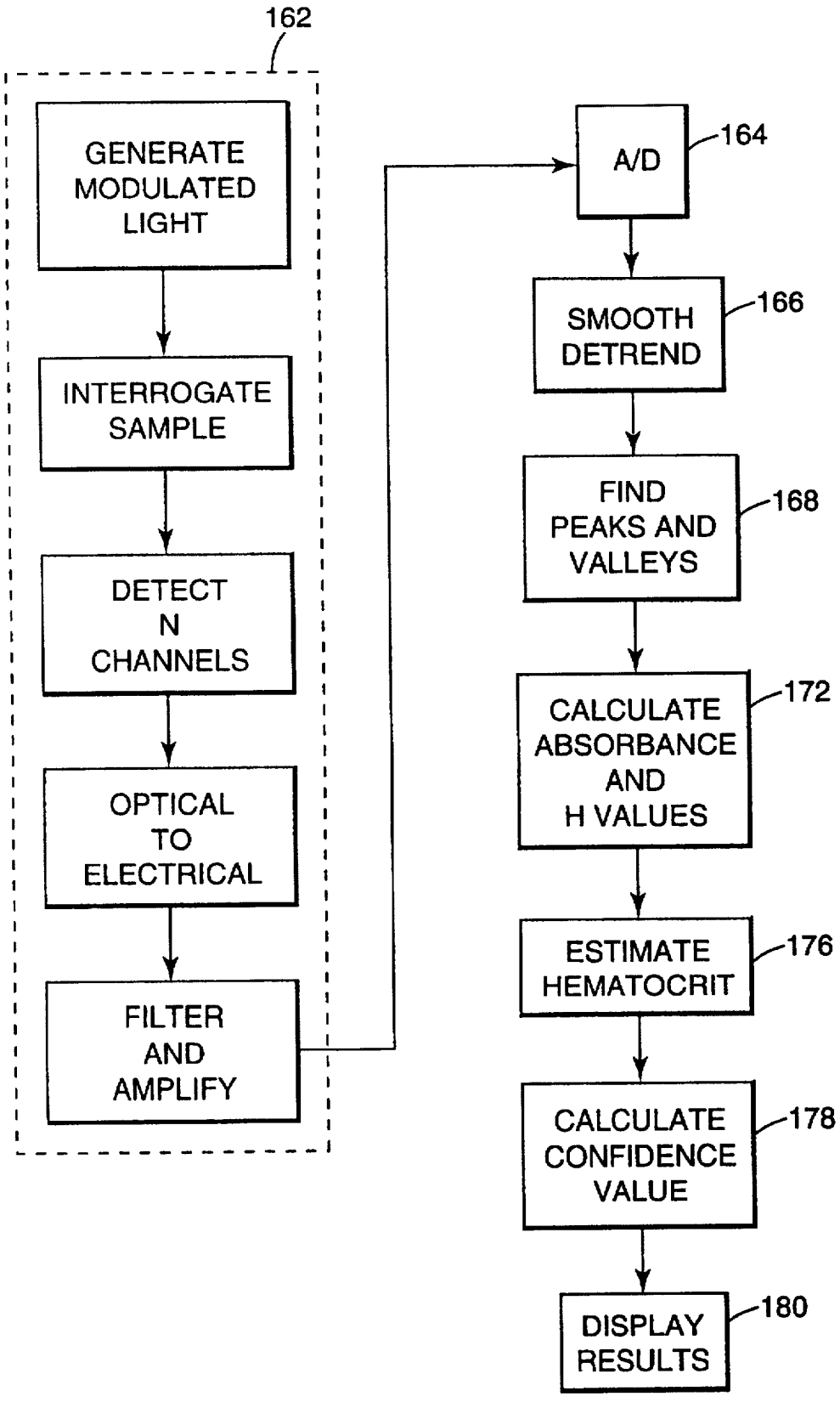

162
GENERATE MODULATED LIGHT
INTERROGATE SAMPLE
DETECT N CHANNELS
OPTICAL TO ELECTRICAL
FILTER AND AMPLIFY
A/D
164
SMOOTH DETREND
166
FIND PEAKS AND VALLEYS
168
CALCULATE ABSORBANCE AND H VALUES
172
ESTIMATE HEMATOCRIT
176
CALCULATE CONFIDENCE VALUE
178
DISPLAY RESULTS
180

Fig. 3

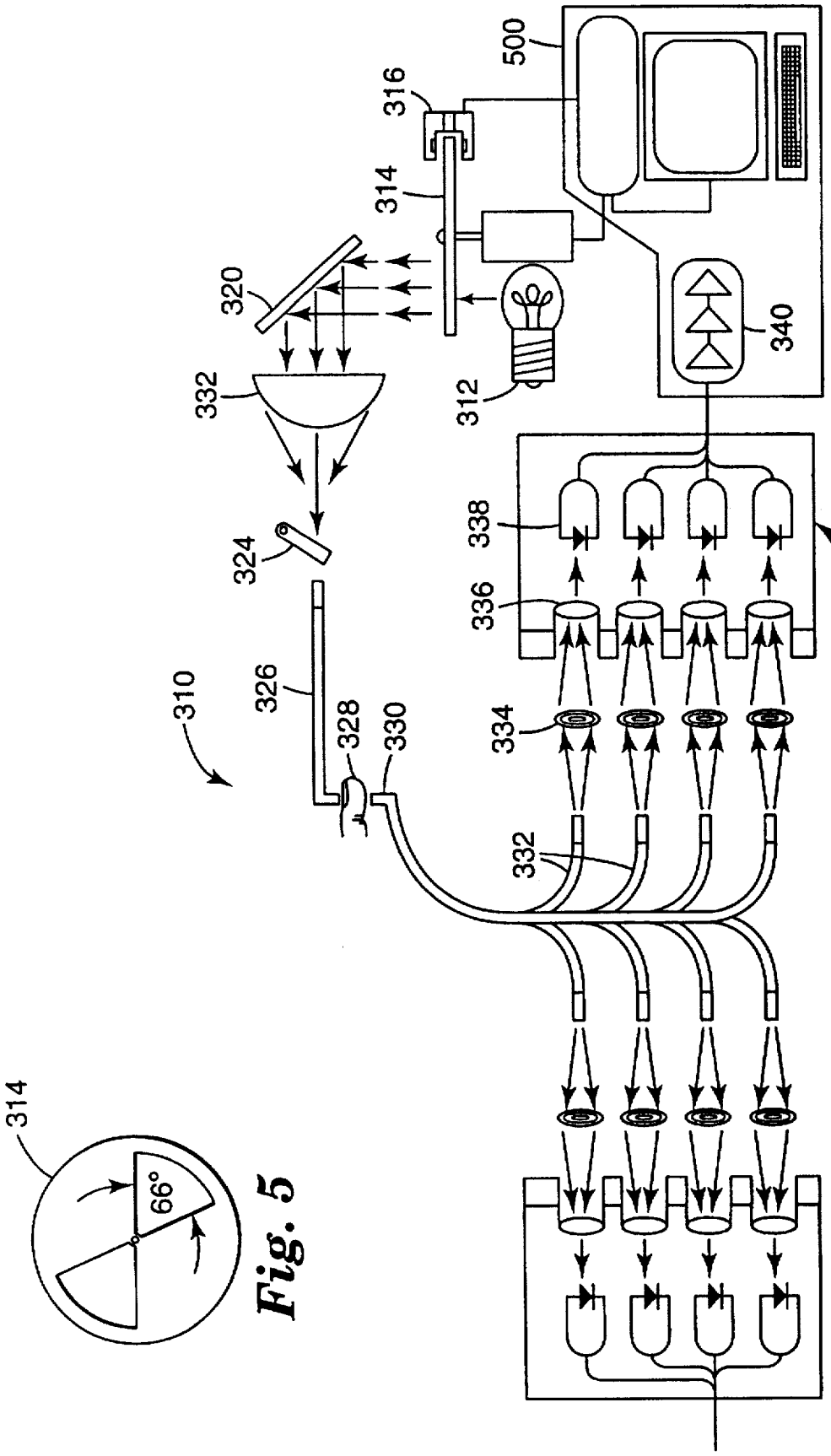

500
316
314
320
332
312
340
338
336
374
324
326
310
328
330
334
332

Fig. 4

314
66°

Fig. 5

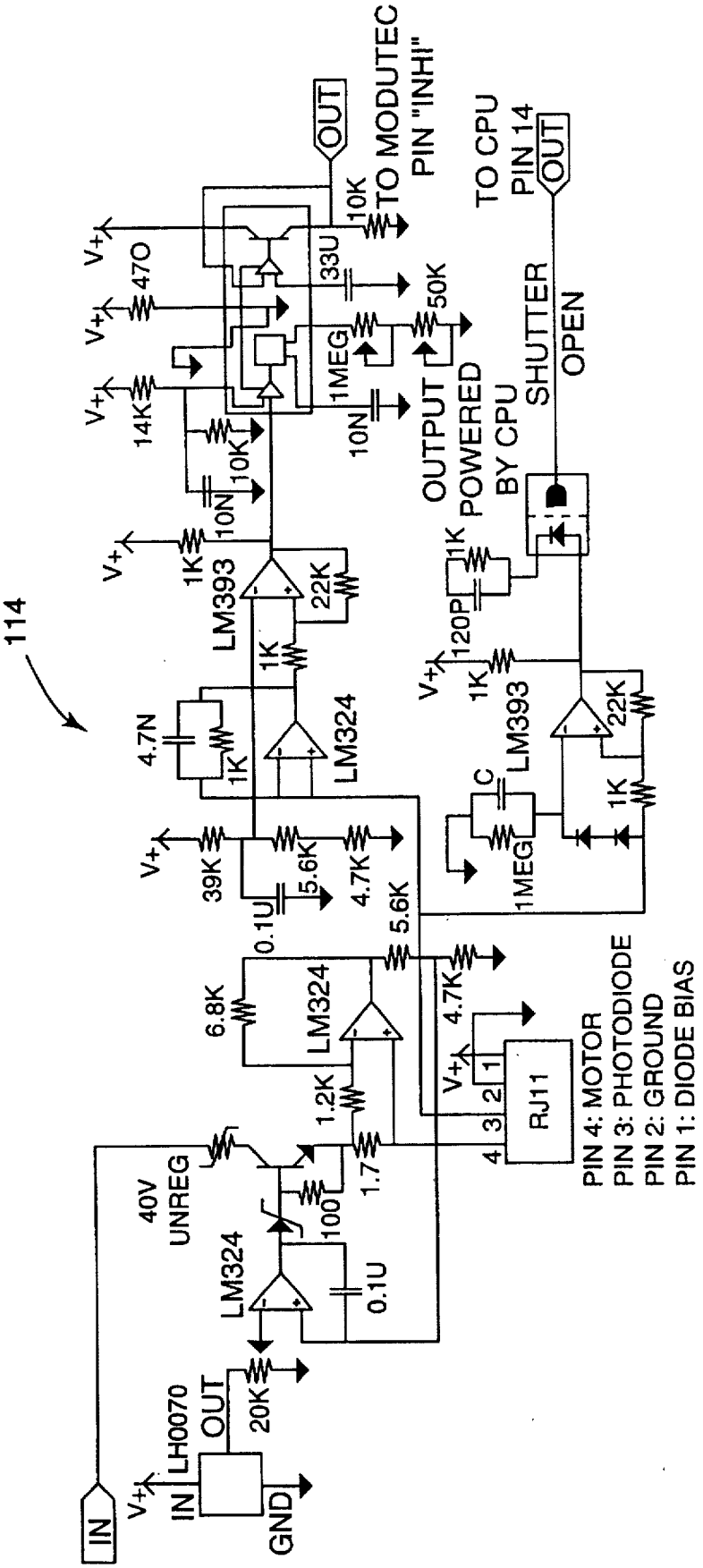

114
IN
V+
LH0070
IN
OUT
GND
20K
40V
UNREG
LM324
100
1.7
0.1U
1.2K
6.8K
LM324
0.1U
39K
5.6K
4.7K
5.6K
4.7K
RJ11
1
2
3
4
PIN 4: MOTOR
PIN 3: PHOTODIODE
PIN 2: GROUND
PIN 1: DIODE BIAS
4.7N
1K
LM324
LM393
22K
1K
1K
14K
10K
10N
1K
10K
10N
47O
33U
1MEG
50K
10N
OUTPUT
POWERED
BY CPU
1K
120P
C
1MEG
LM393
22K
1K
TO CPU
PIN 14
OUT
SHUTTER
OPEN
OUT
10K
TO MODUTEC
PIN "INH"

Fig. 6

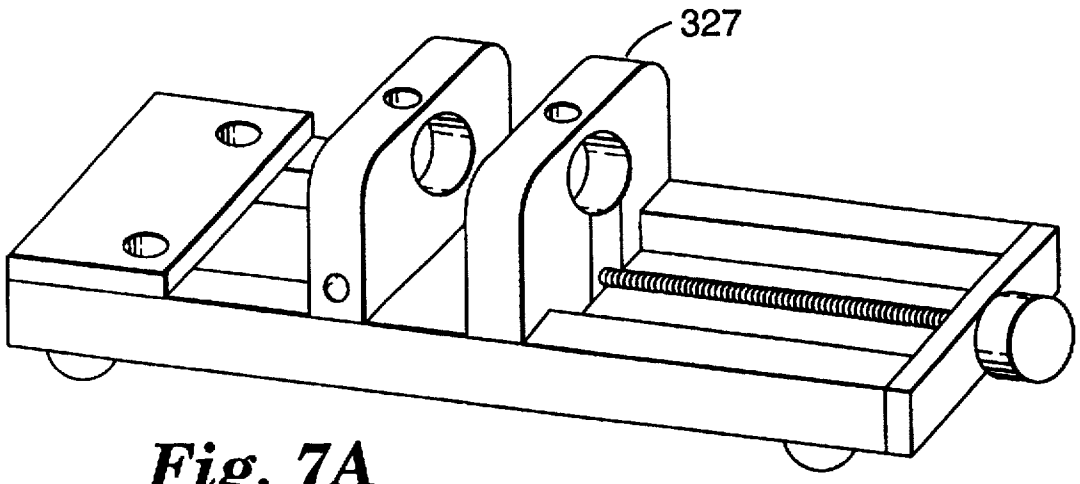


Fig. 7A

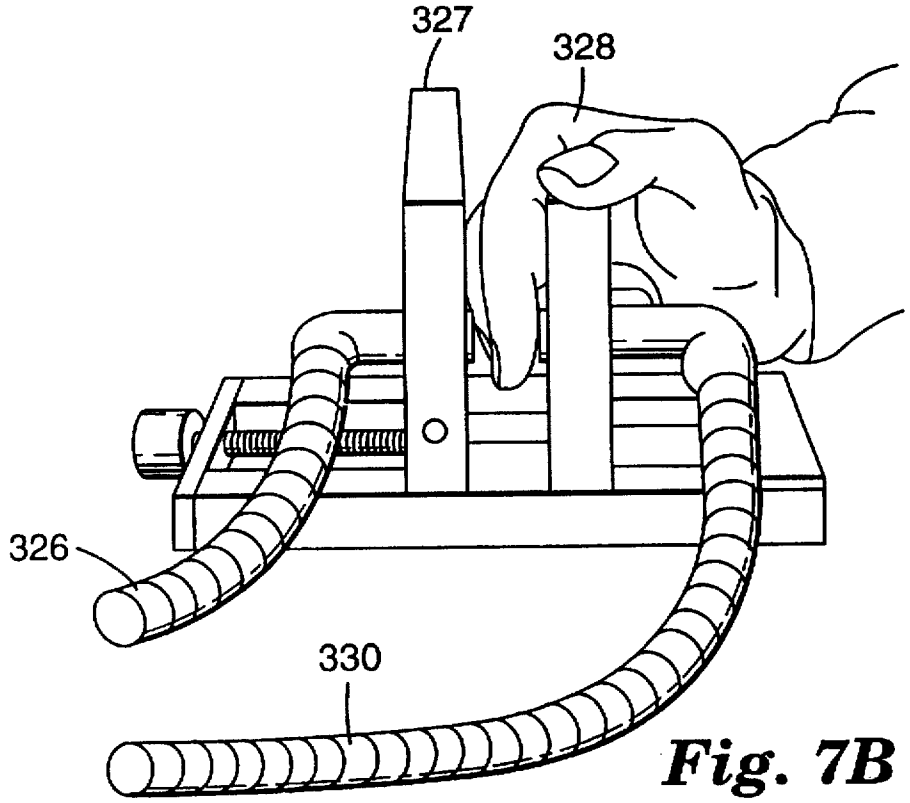


Fig. 7B

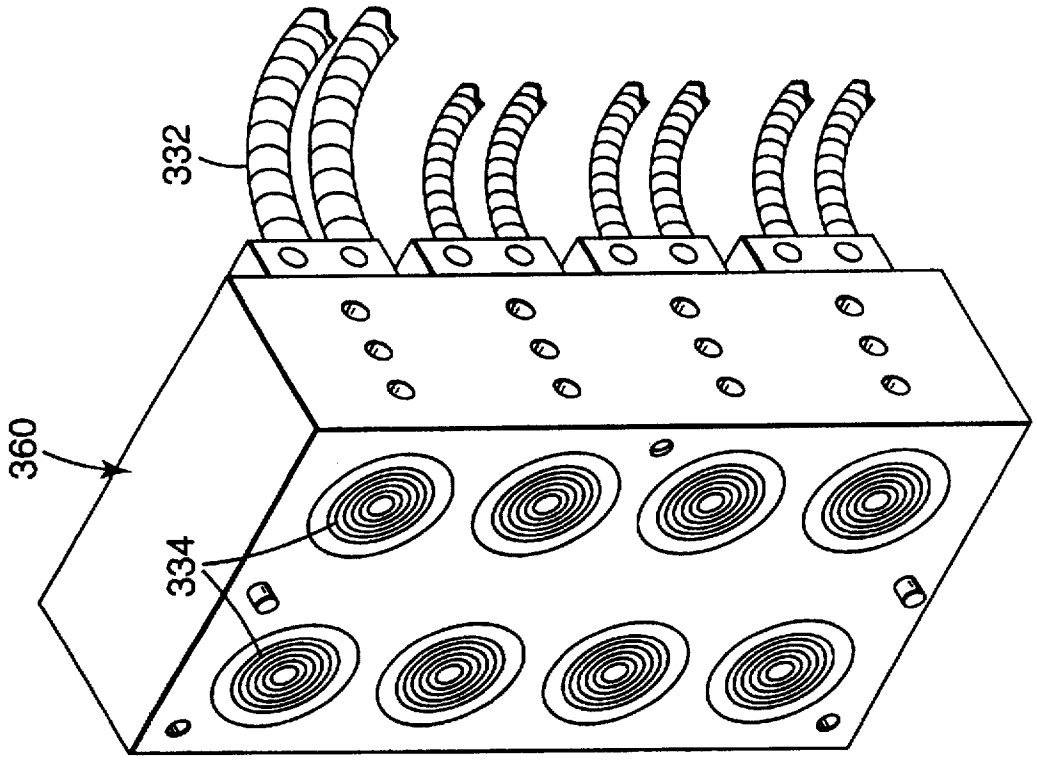


Fig. 8B

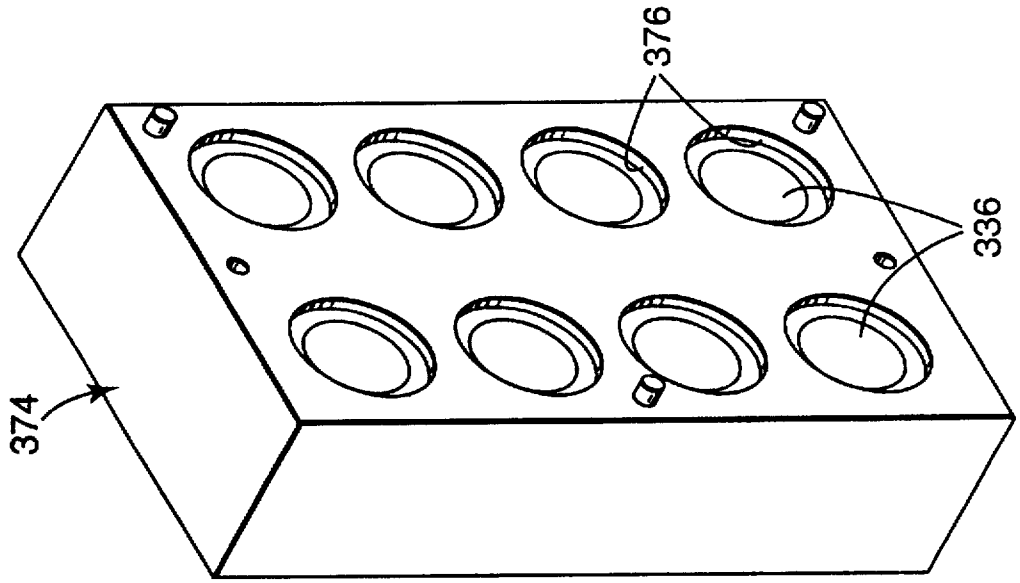


Fig. 8A

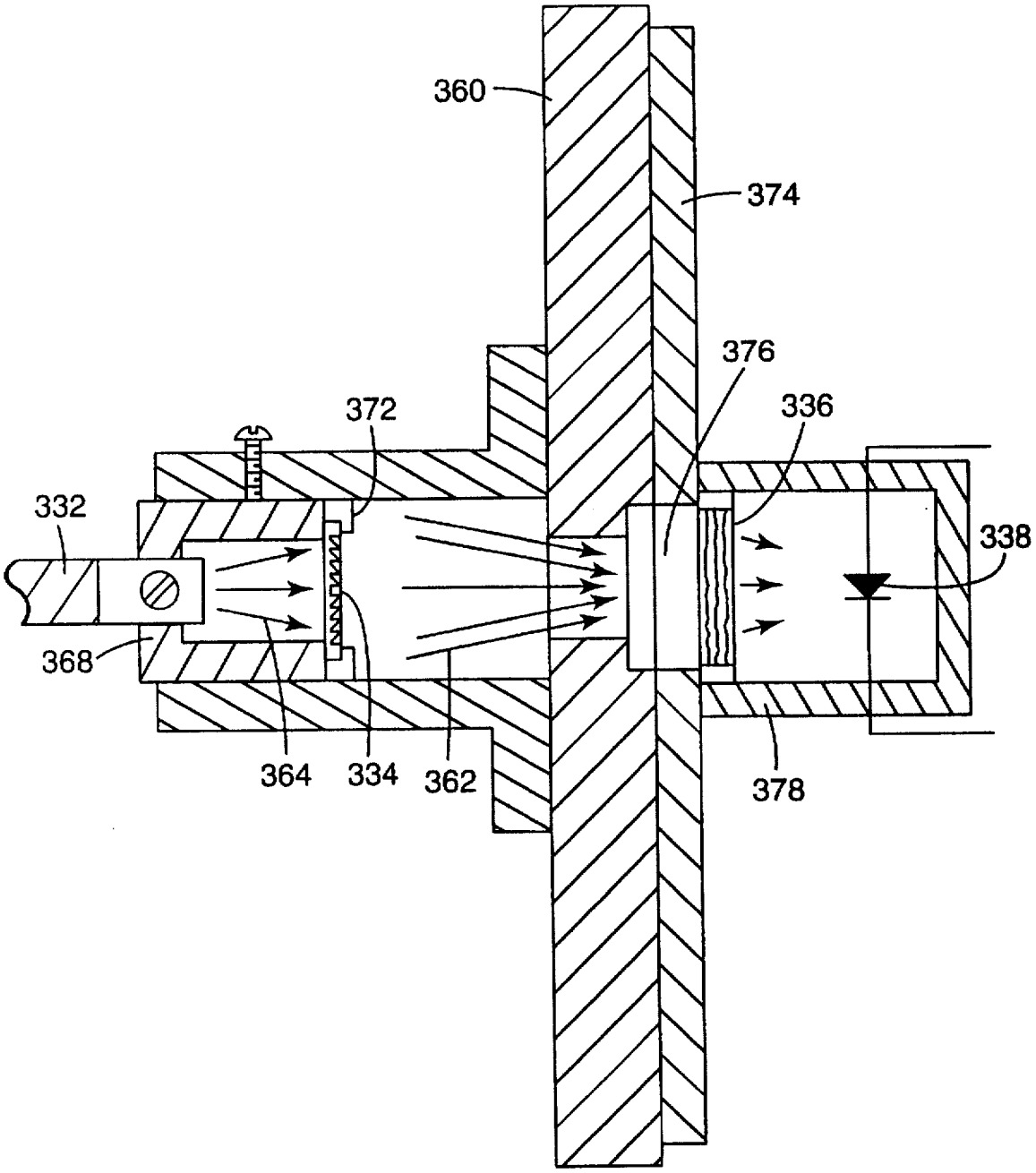


Fig. 9

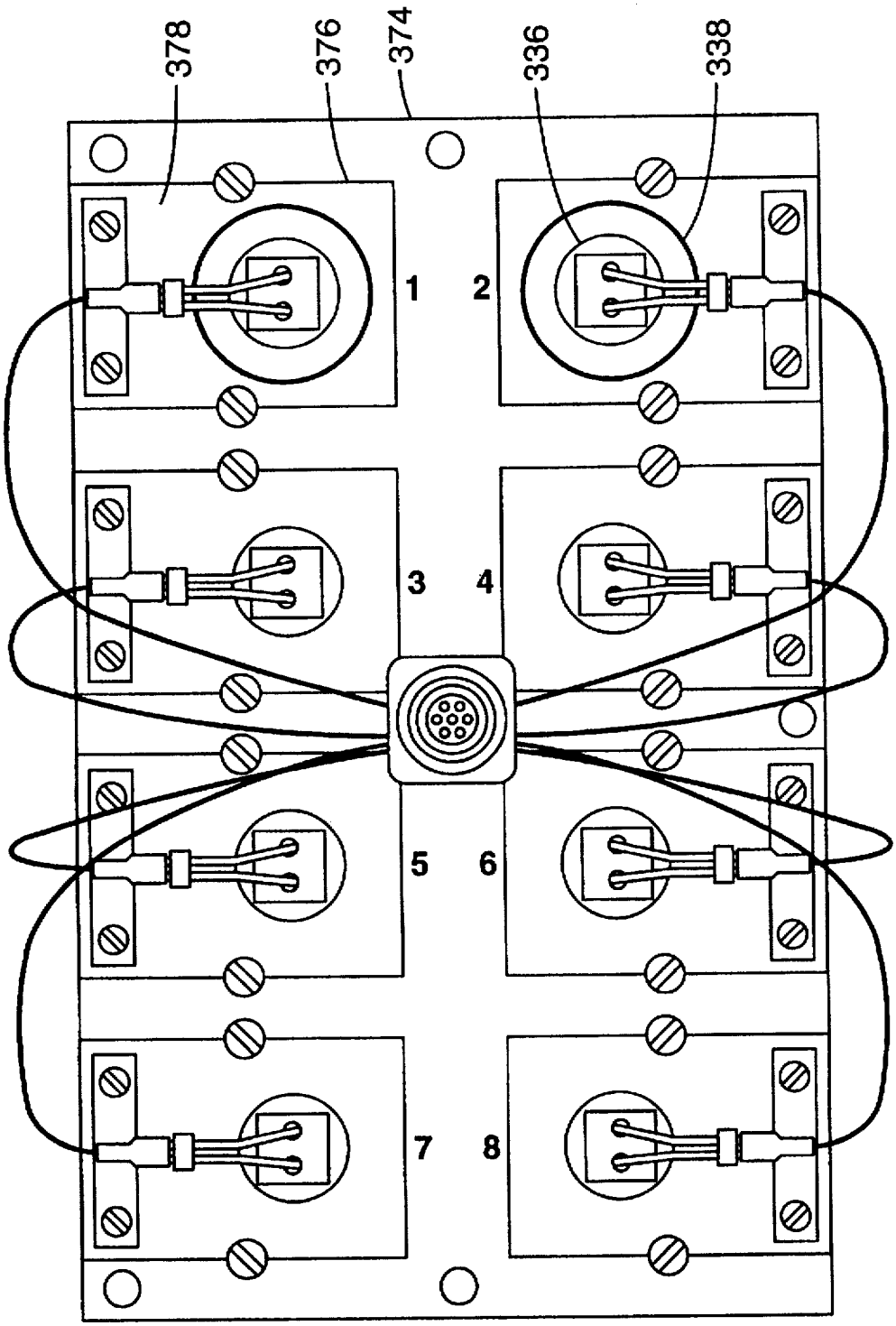


Fig. 10

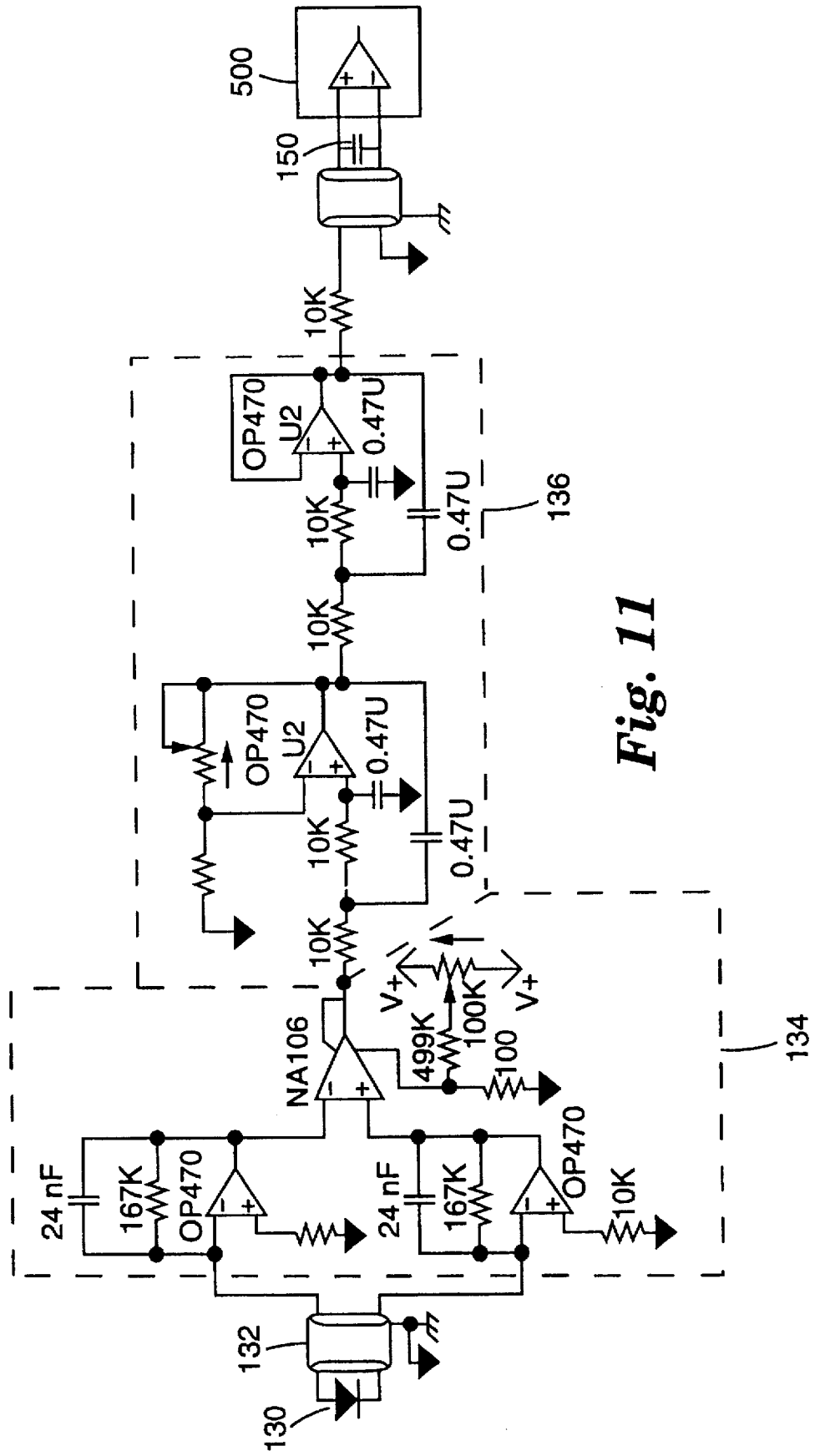

500
150
10K
OP470
U2
0.47U
10K
0.47U
136
10K
OP470
U2
0.47U
10K
0.47U
10K
V+
V+
100K
499K
100
NA106
134
24 nF
167K
OP470
24 nF
167K
OP470
10K
132
130

Fig. 11

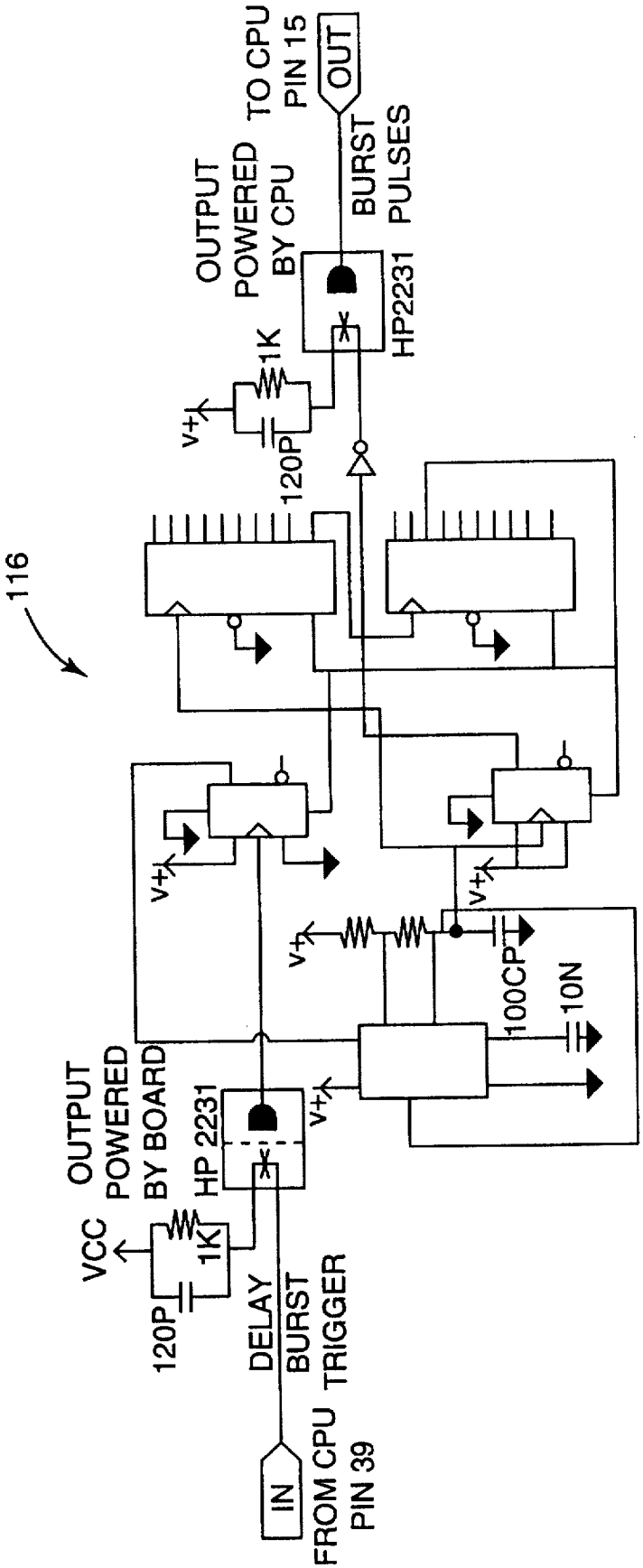

116
OUTPUT POWERED BY BOARD
HP 2231
VCC
1K
120P
DELAY
BURST TRIGGER
FROM CPU PIN 39
IN
V+
100CP
10N
OUTPUT POWERED BY CPU
HP2231
1K
120P
BURST PULSES
TO CPU PIN 15
OUT

Fig. 12

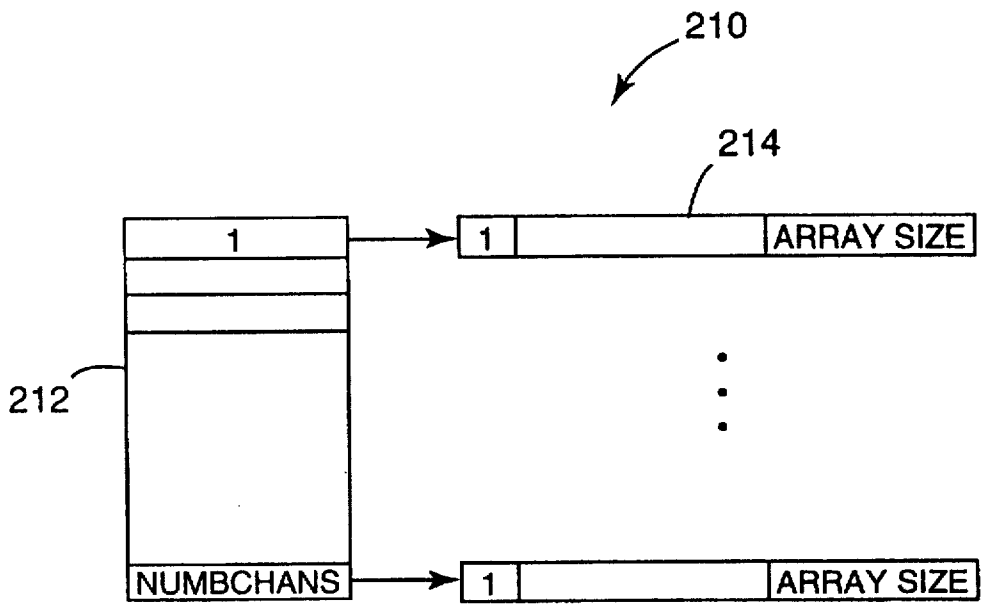


Fig. 13A

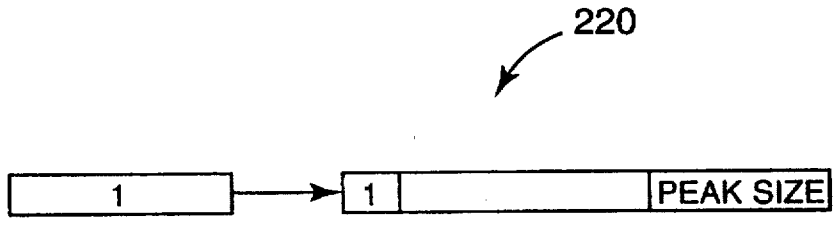


Fig. 13B

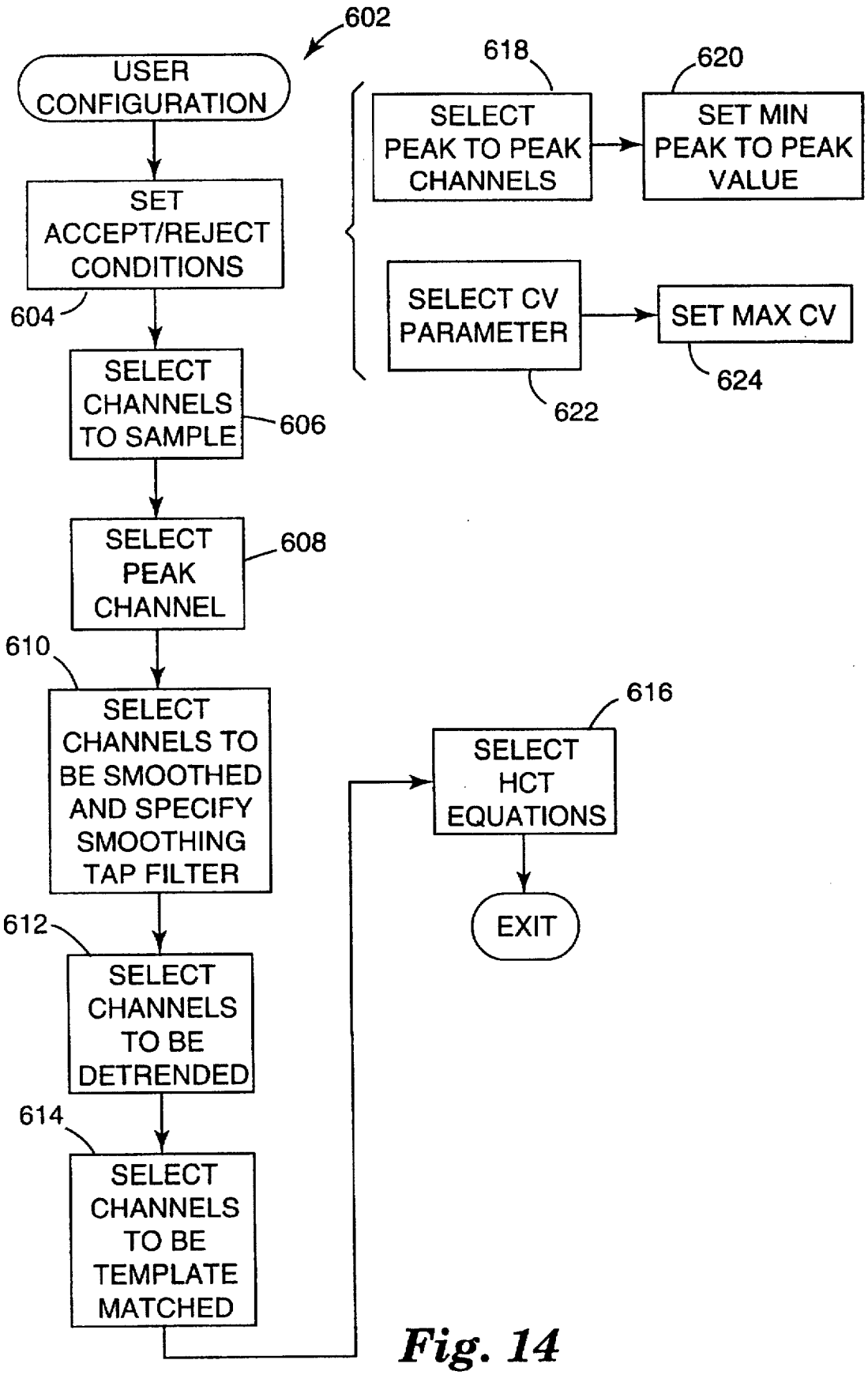

602
USER CONFIGURATION
SET ACCEPT/REJECT CONDITIONS
604
SELECT CHANNELS TO SAMPLE
606
SELECT PEAK CHANNEL
608
610
SELECT CHANNELS TO BE SMOOTHED AND SPECIFY SMOOTHING TAP FILTER
612
SELECT CHANNELS TO BE DETRENDED
614
SELECT CHANNELS TO BE TEMPLATE MATCHED
618
SELECT PEAK TO PEAK CHANNELS
620
SET MIN PEAK TO PEAK VALUE
SELECT CV PARAMETER
622
SET MAX CV
624
616
SELECT HCT EQUATIONS
EXIT

Fig. 14

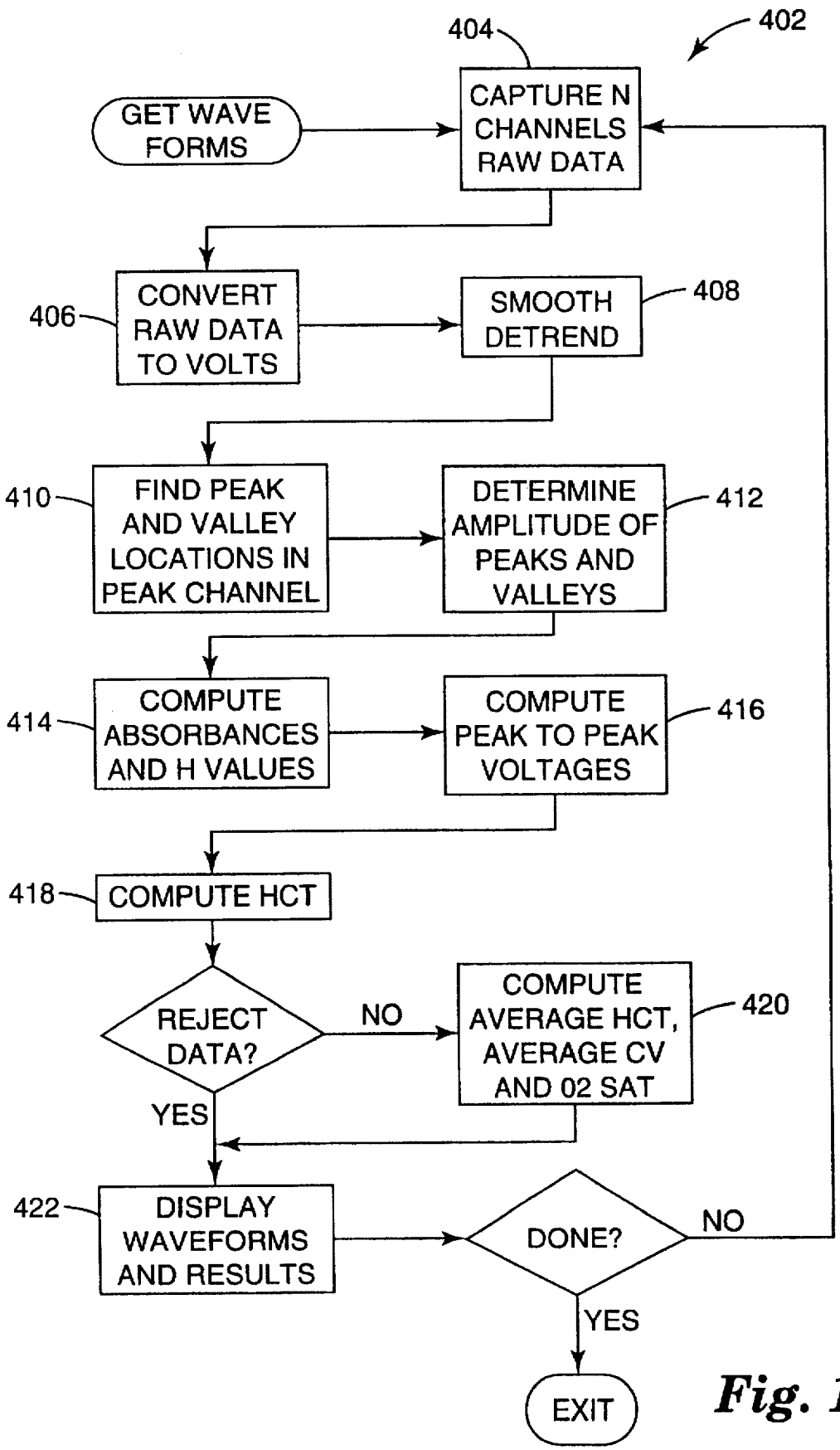

402
404
GET WAVE FORMS
CAPTURE N CHANNELS RAW DATA
406
CONVERT RAW DATA TO VOLTS
SMOOTH DETREND
408
410
FIND PEAK AND VALLEY LOCATIONS IN PEAK CHANNEL
DETERMINE AMPLITUDE OF PEAKS AND VALLEYS
412
414
COMPUTE ABSORBANCES AND H VALUES
COMPUTE PEAK TO PEAK VOLTAGES
416
418
COMPUTE HCT
REJECT DATA?
NO
COMPUTE AVERAGE HCT, AVERAGE CV AND 02 SAT
420
YES
422
DISPLAY WAVEFORMS AND RESULTS
DONE?
NO
YES
EXIT

Fig. 15

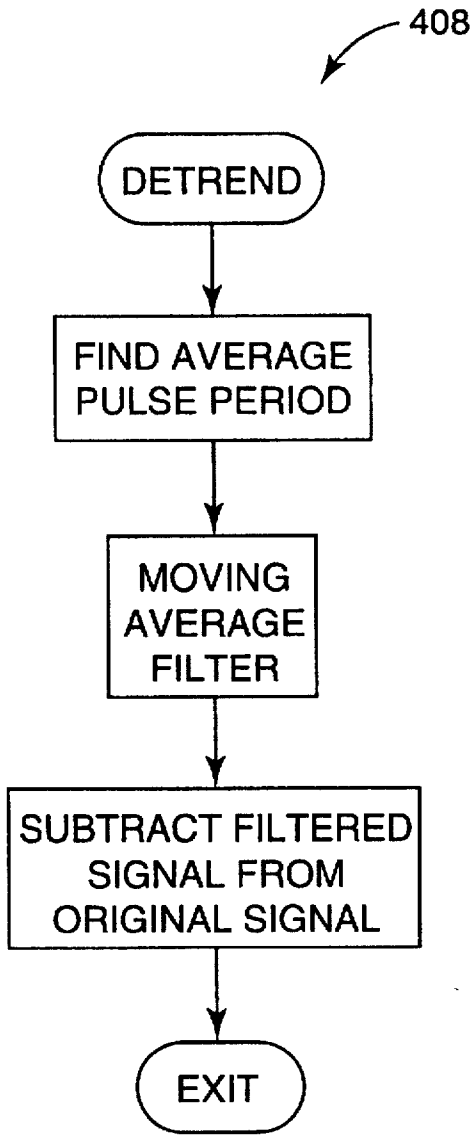

408
DETREND
FIND AVERAGE PULSE PERIOD
MOVING AVERAGE FILTER
SUBTRACT FILTERED SIGNAL FROM ORIGINAL SIGNAL
EXIT

Fig. 16

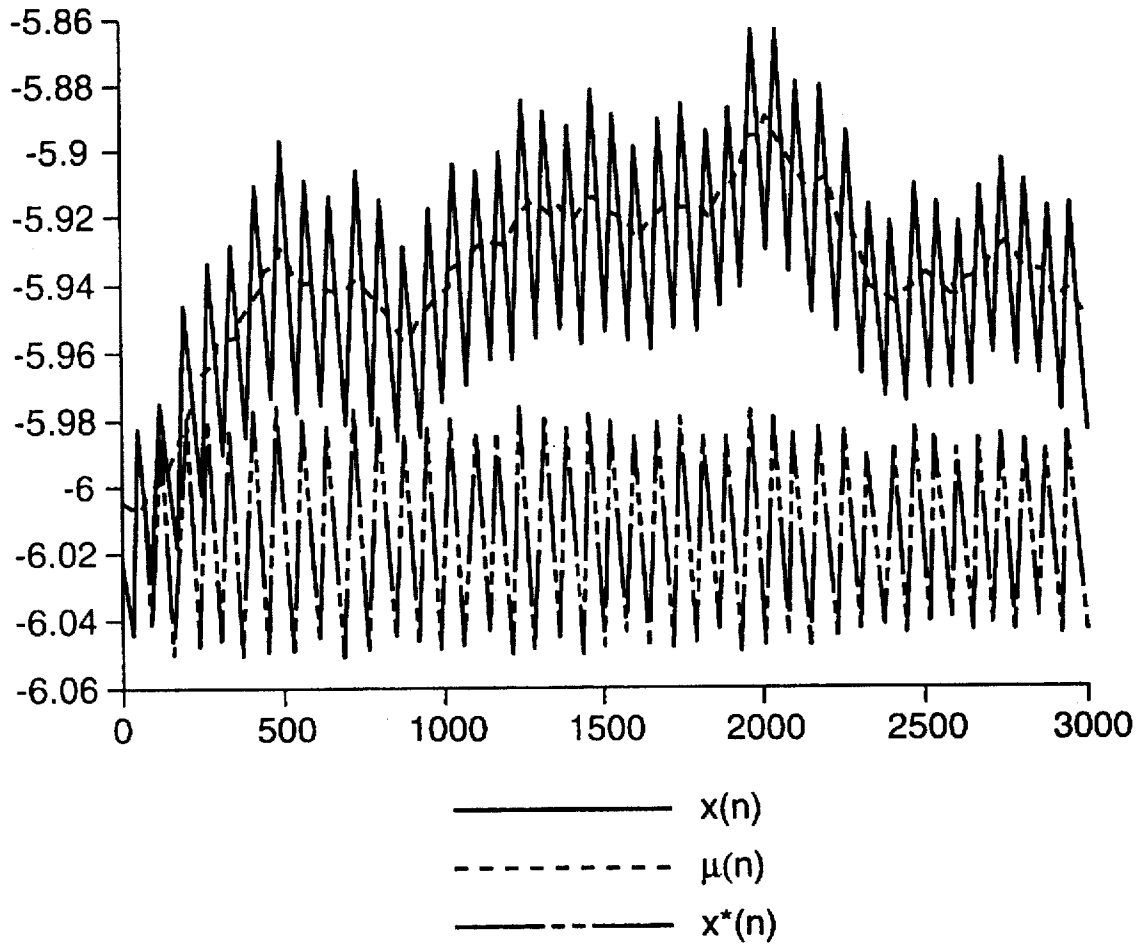

-5.86
-5.88
-5.9
-5.92
-5.94
-5.96
-5.98
-6
-6.02
-6.04
-6.06
0
500
1000
1500
2000
2500
3000
x(n)
μ(n)
x*(n)

Fig. 17

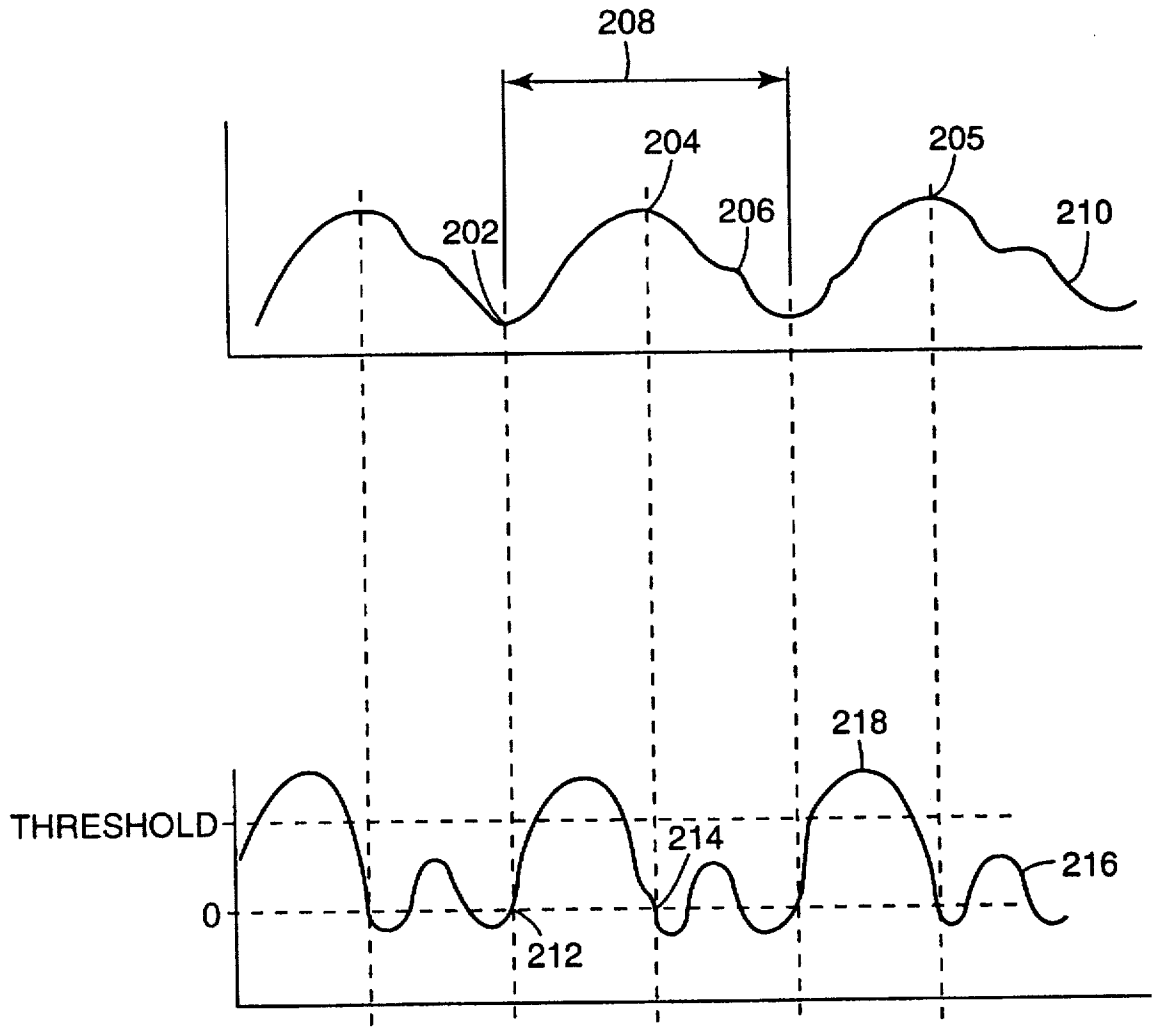


Fig. 18

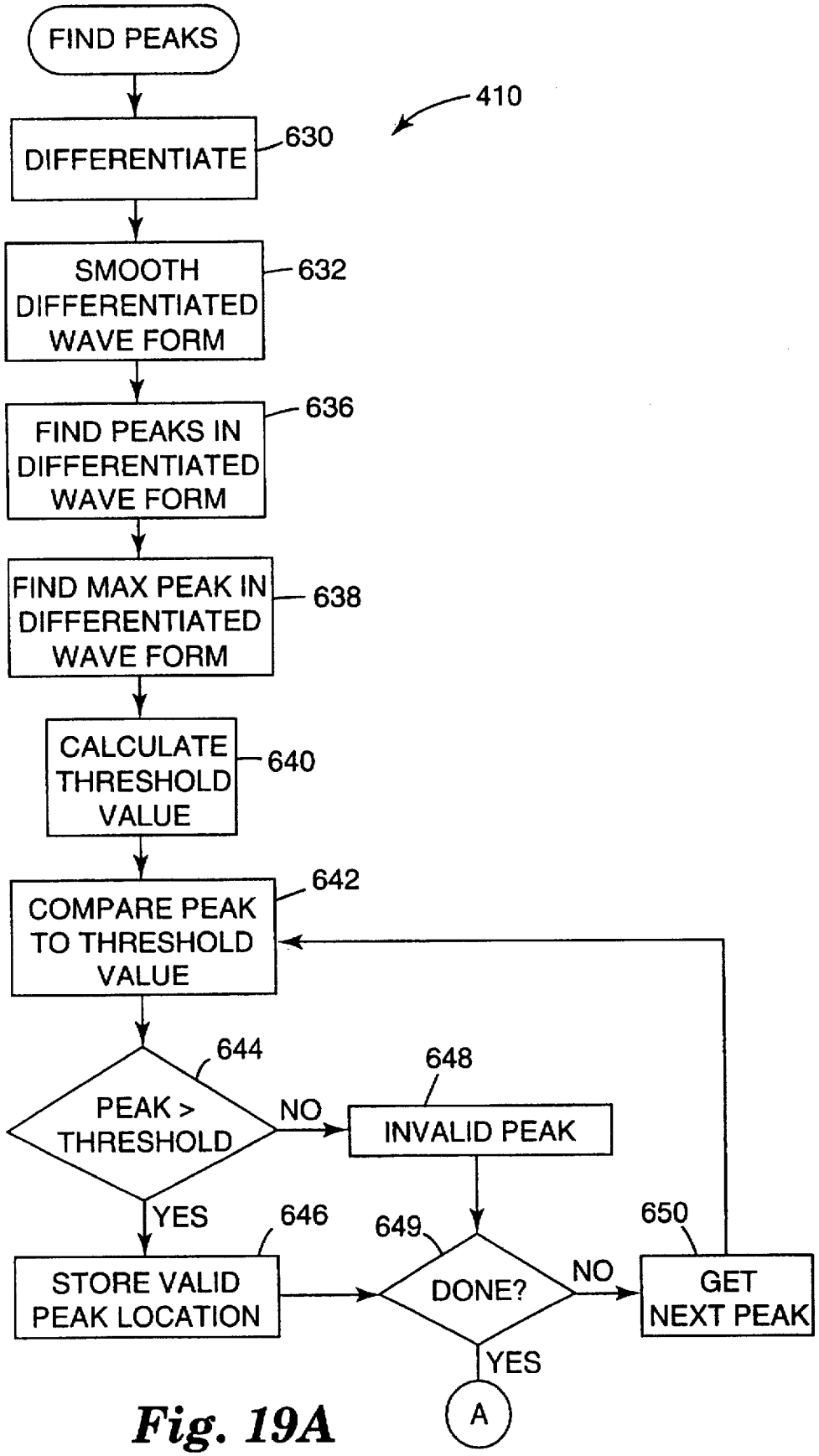

FIND PEAKS
410
DIFFERENTIATE
630
SMOOTH DIFFERENTIATED WAVE FORM
632
FIND PEAKS IN DIFFERENTIATED WAVE FORM
636
FIND MAX PEAK IN DIFFERENTIATED WAVE FORM
638
CALCULATE THRESHOLD VALUE
640
COMPARE PEAK TO THRESHOLD VALUE
642
644
PEAK > THRESHOLD
NO
648
INVALID PEAK
YES
646
649
650
STORE VALID PEAK LOCATION
DONE?
NO
GET NEXT PEAK
YES
A

Fig. 19A

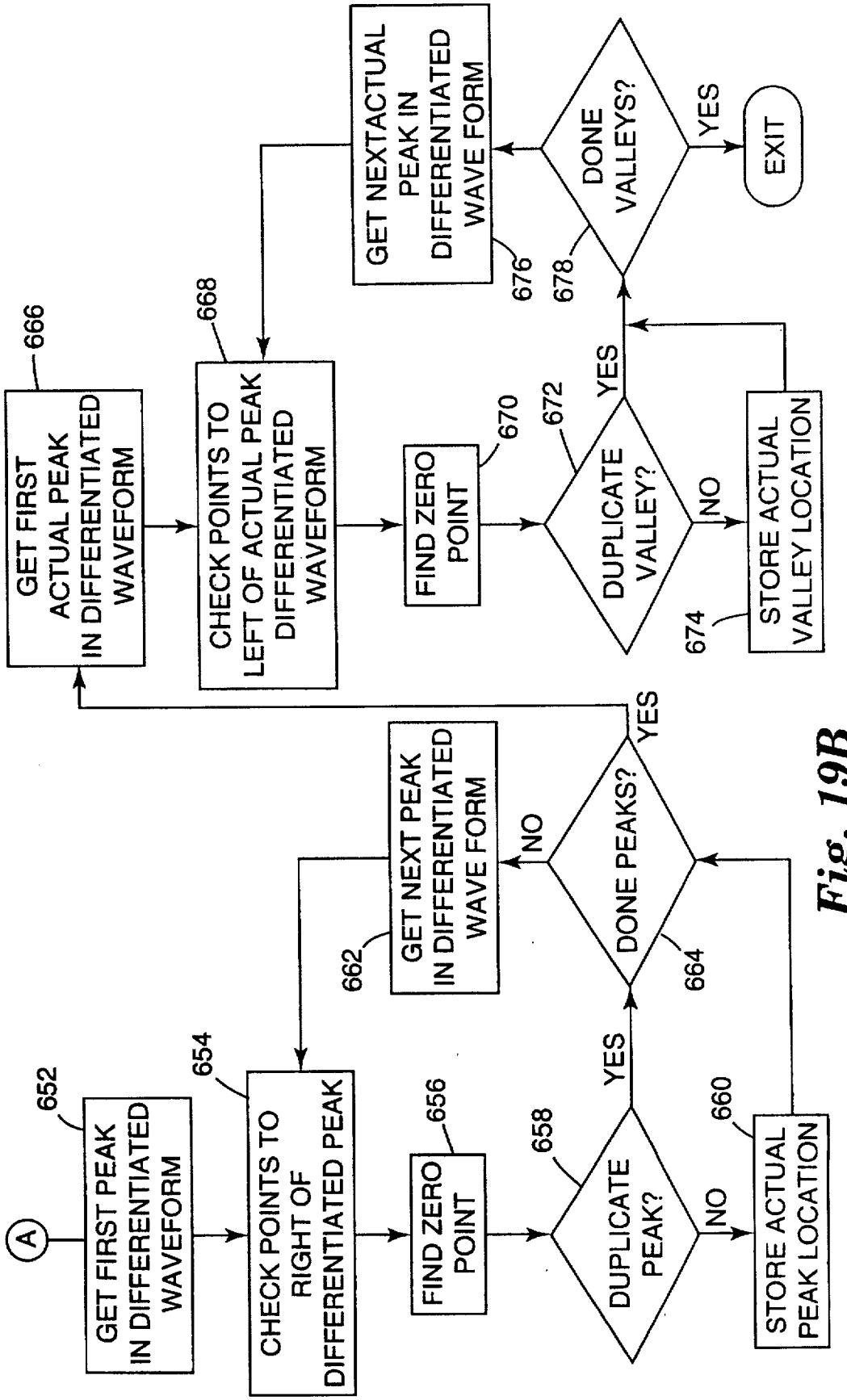

A
652
GET FIRST PEAK IN DIFFERENTIATED WAVEFORM
654
CHECK POINTS TO RIGHT OF DIFFERENTIATED PEAK
656
FIND ZERO POINT
658
DUPLICATE PEAK?
YES
NO
660
STORE ACTUAL PEAK LOCATION
662
GET NEXT PEAK IN DIFFERENTIATED WAVE FORM
664
DONE PEAKS?
NO
YES
666
GET FIRST ACTUAL PEAK IN DIFFERENTIATED WAVEFORM
668
CHECK POINTS TO LEFT OF ACTUAL PEAK DIFFERENTIATED WAVEFORM
670
FIND ZERO POINT
672
DUPLICATE VALLEY?
NO
YES
674
STORE ACTUAL VALLEY LOCATION
676
GET NEXTACTUAL PEAK IN DIFFERENTIATED WAVE FORM
678
DONE VALLEYS?
YES
EXIT

Fig. 19B

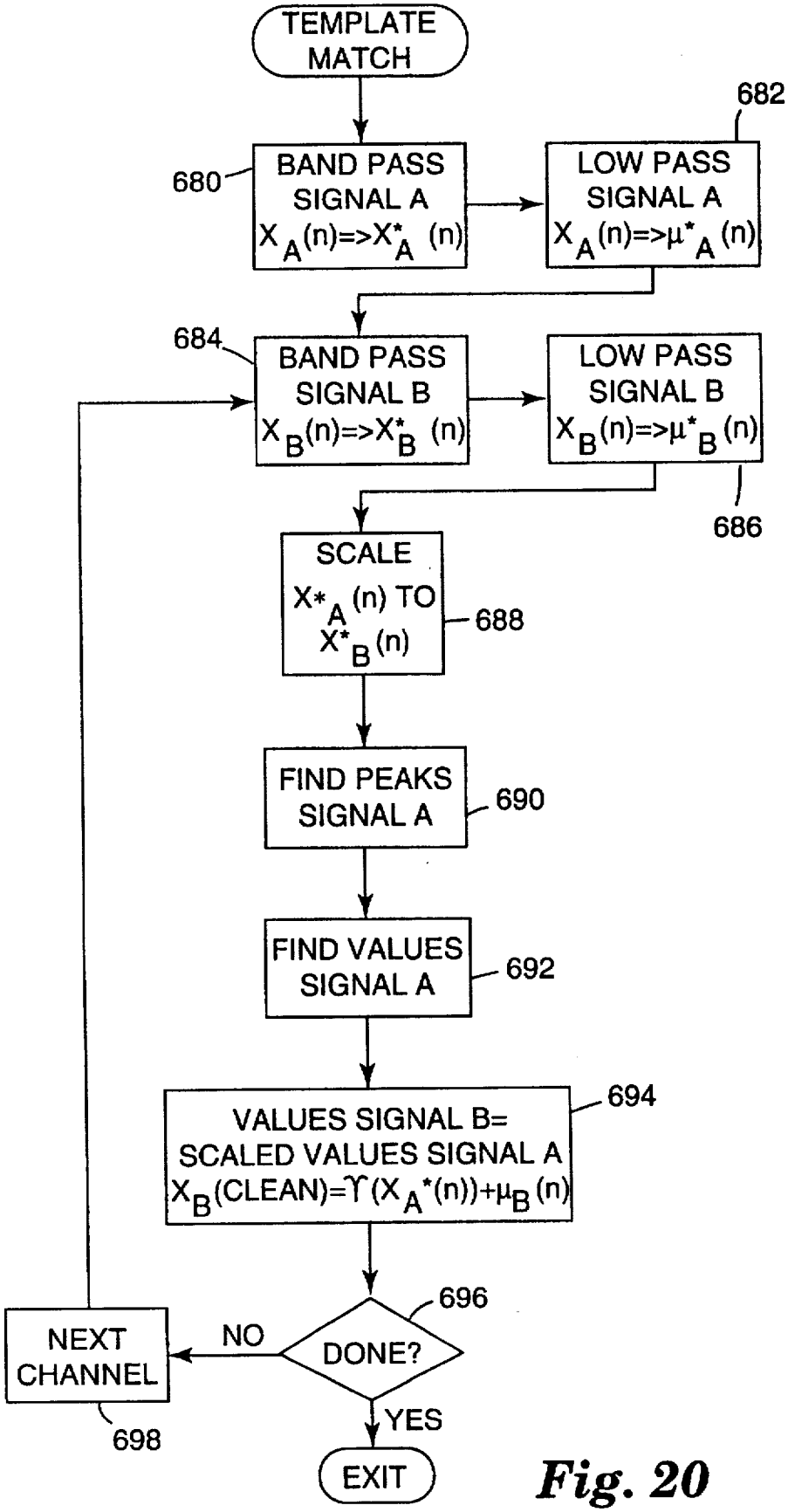

TEMPLATE MATCH
680
BAND PASS SIGNAL A
$X_A(n) => X^*_A(n)$
682
LOW PASS SIGNAL A
$X_A(n) => \mu^*_A(n)$
684
BAND PASS SIGNAL B
$X_B(n) => X^*_B(n)$
LOW PASS SIGNAL B
$X_B(n) => \mu^*_B(n)$
686
SCALE
$X^*_A(n)$ TO $X^*_B(n)$
688
FIND PEAKS SIGNAL A
690
FIND VALUES SIGNAL A
692
VALUES SIGNAL B= SCALED VALUES SIGNAL A
$X_B(CLEAN) = \Upsilon(X_A^*(n)) + \mu_B(n)$
694
696
DONE?
NO
NEXT CHANNEL
698
YES
EXIT

Fig. 20

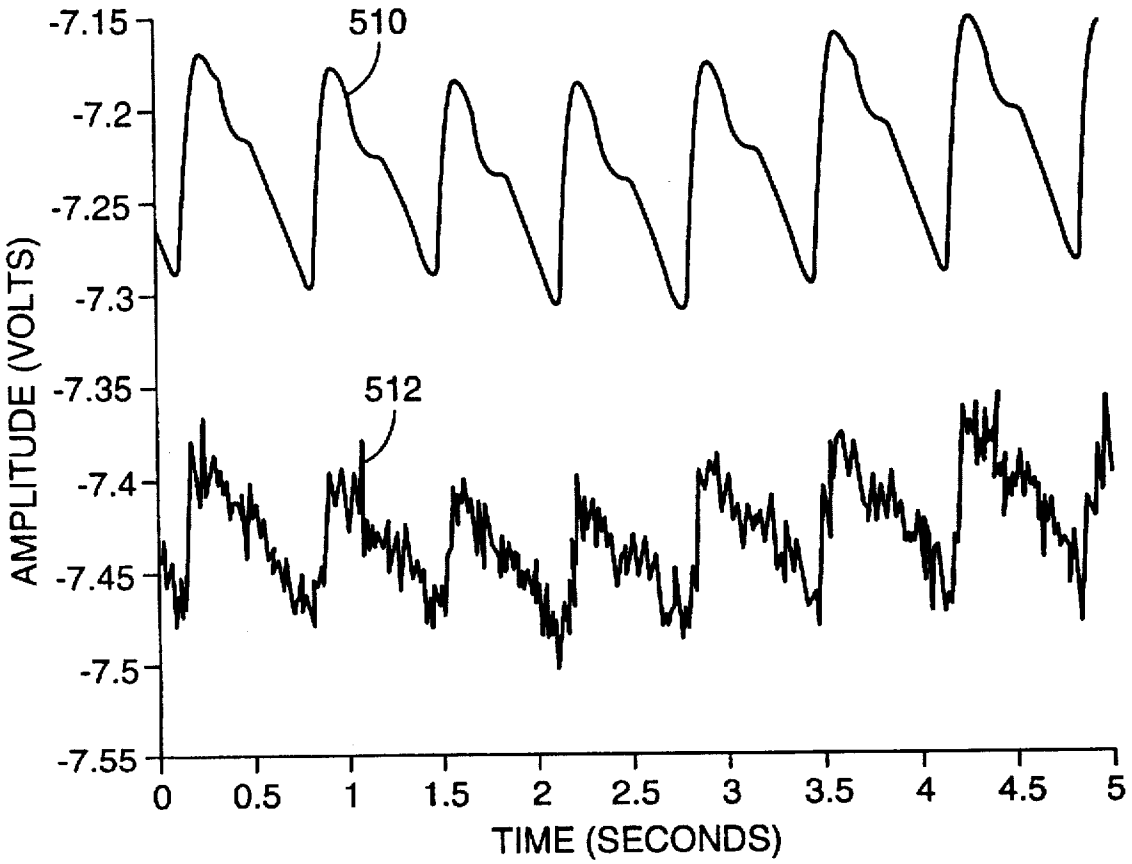

-7.15
-7.2
-7.25
-7.3
-7.35
-7.4
-7.45
-7.5
-7.55
AMPLITUDE (VOLTS)
510
512
0
0.5
1
1.5
2
2.5
3
3.5
4
4.5
5
TIME (SECONDS)

Fig. 21A

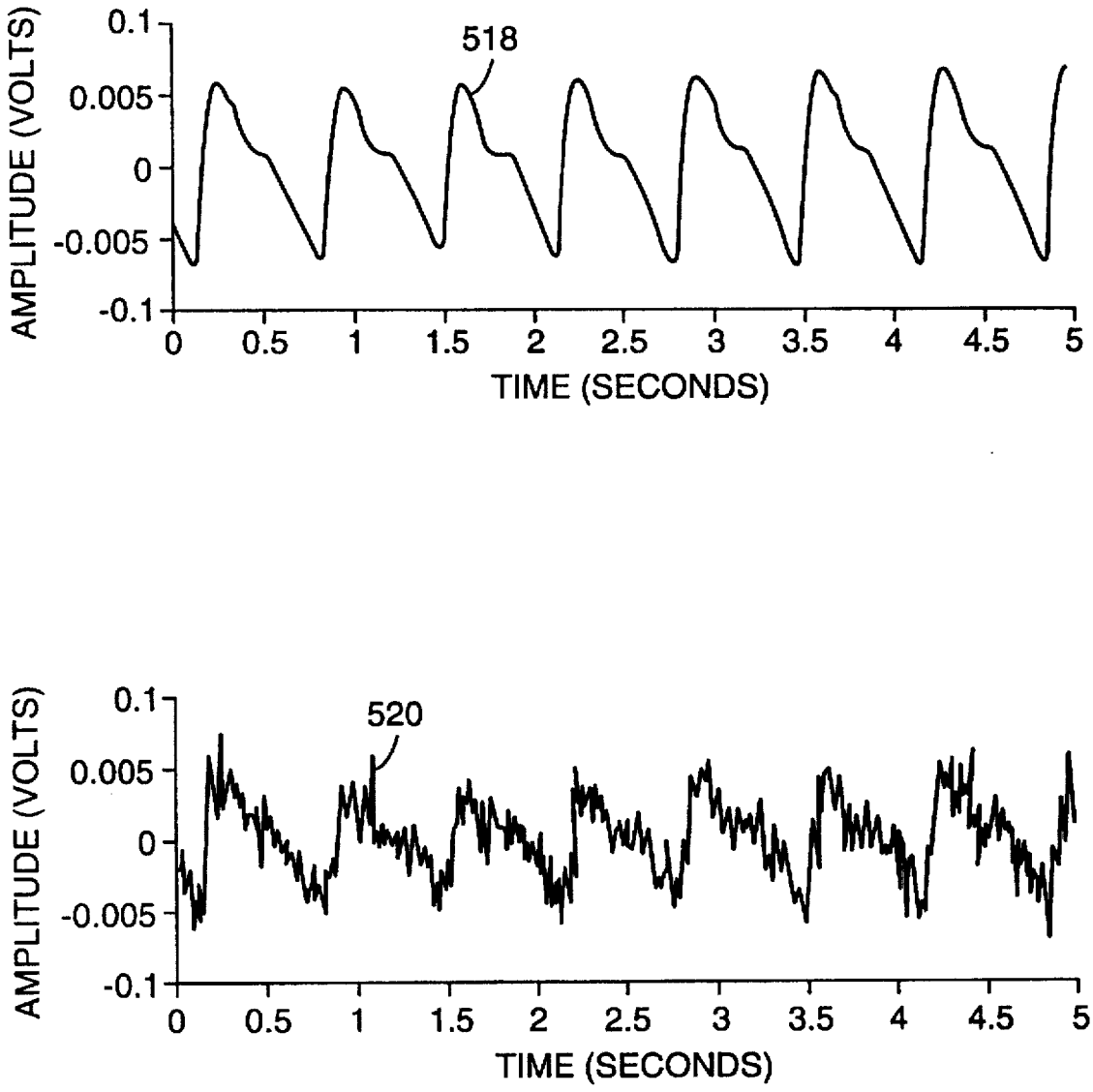

AMPLITUDE (VOLTS)
0.1
0.005
0
-0.005
-0.1
518
0
0.5
1
1.5
2
2.5
3
3.5
4
4.5
5
TIME (SECONDS)
AMPLITUDE (VOLTS)
0.1
0.005
0
-0.005
-0.1
520
0
0.5
1
1.5
2
2.5
3
3.5
4
4.5
5
TIME (SECONDS)

Fig. 21B

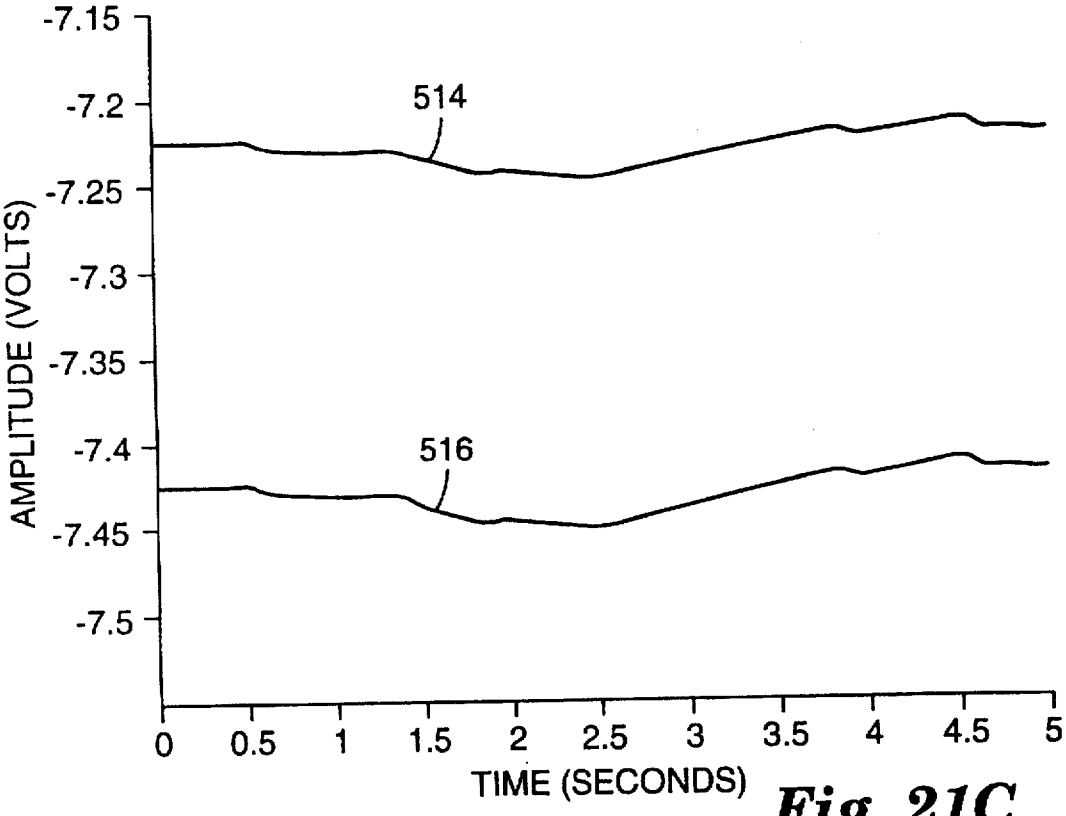


Fig. 21C

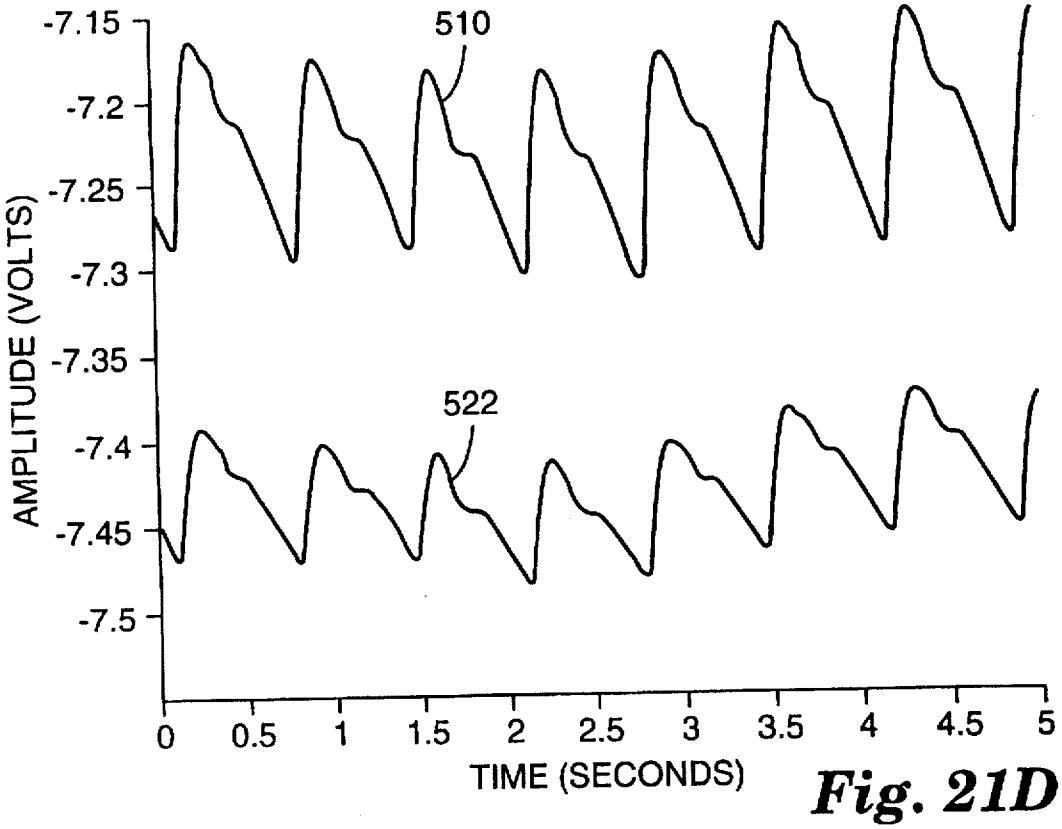


Fig. 21D

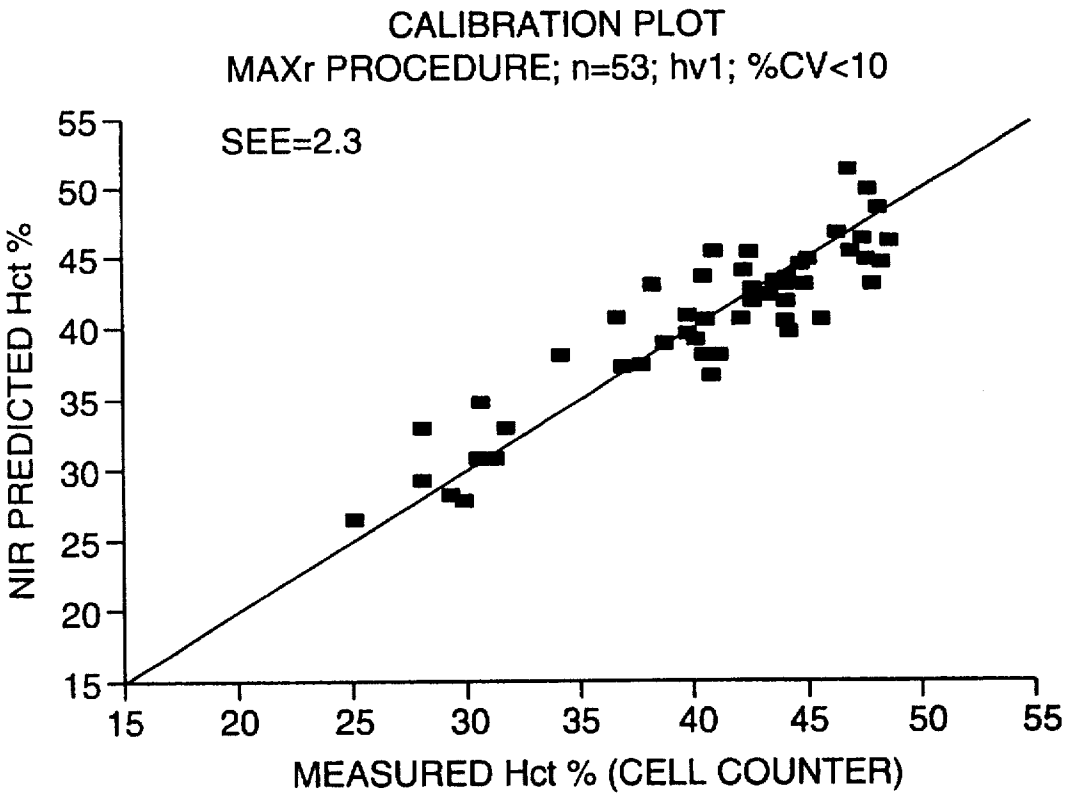

CALIBRATION PLOT
MAXr PROCEDURE; n=53; hv1; %CV<10
SEE=2.3
NIR PREDICTED Hct %
MEASURED Hct % (CELL COUNTER)
15
20
25
30
35
40
45
50
55

Fig. 22

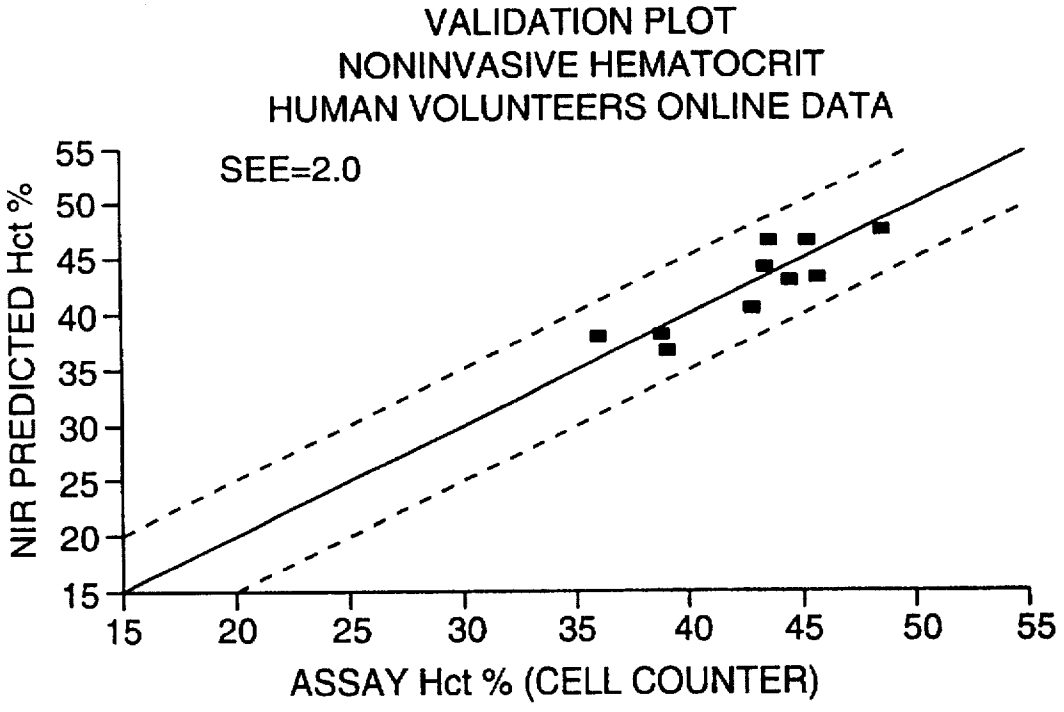

VALIDATION PLOT
NONINVASIVE HEMATOCRIT
HUMAN VOLUNTEERS ONLINE DATA
SEE=2.0
NIR PREDICTED Hct %
ASSAY Hct % (CELL COUNTER)
15
20
25
30
35
40
45
50
55

Fig. 23

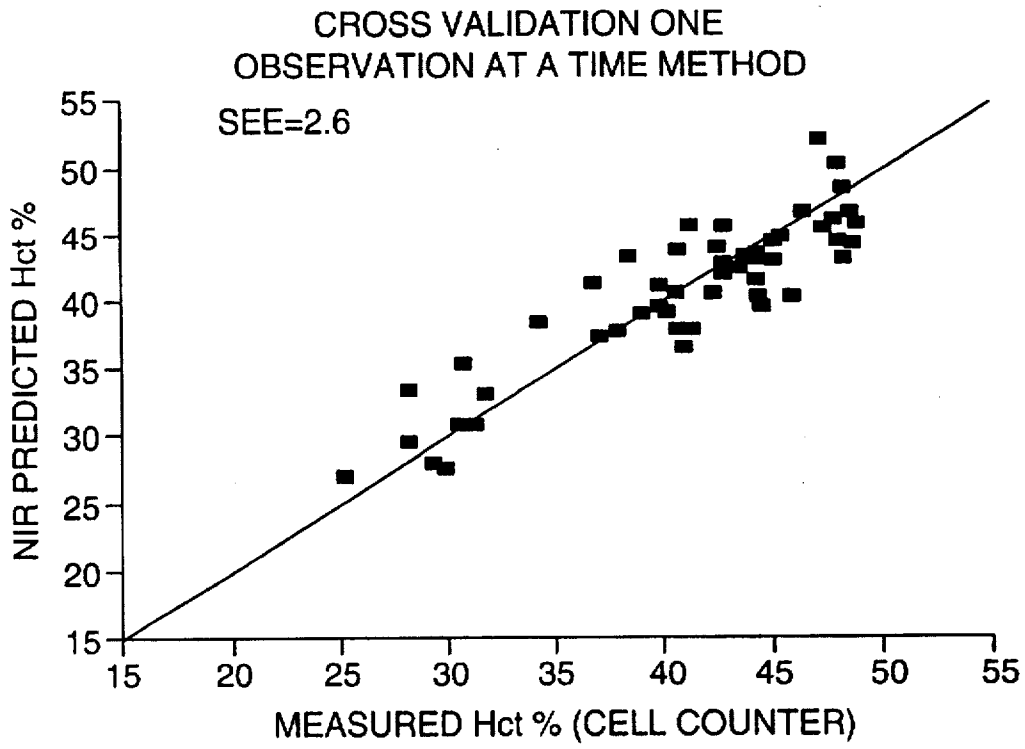


Fig. 24A

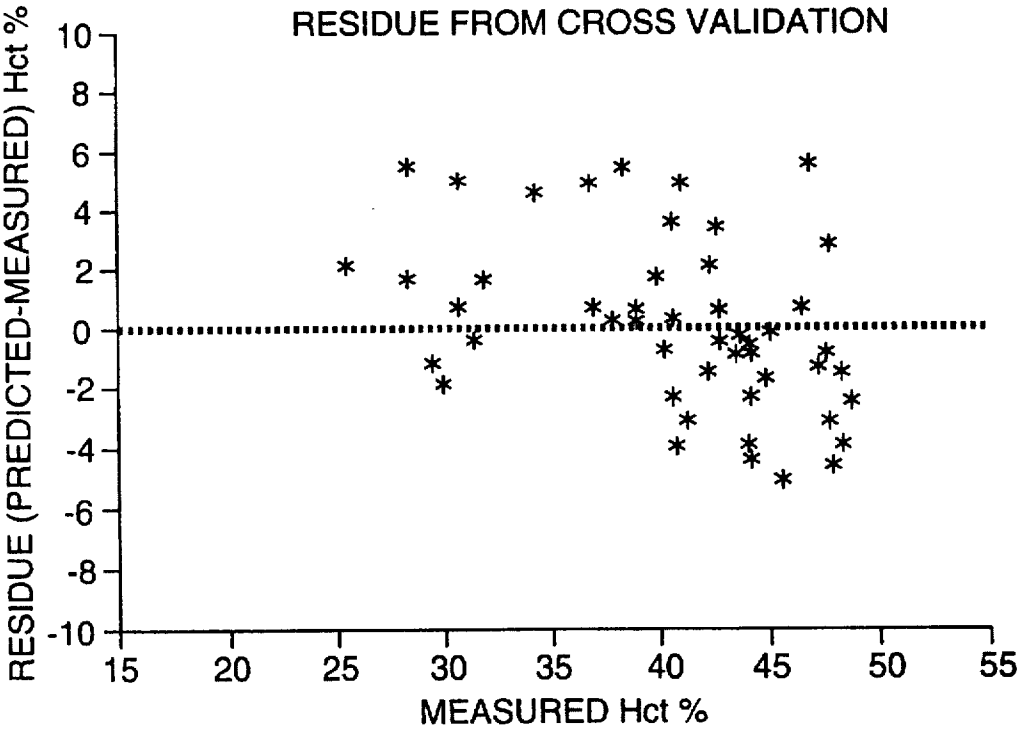


Fig. 24B

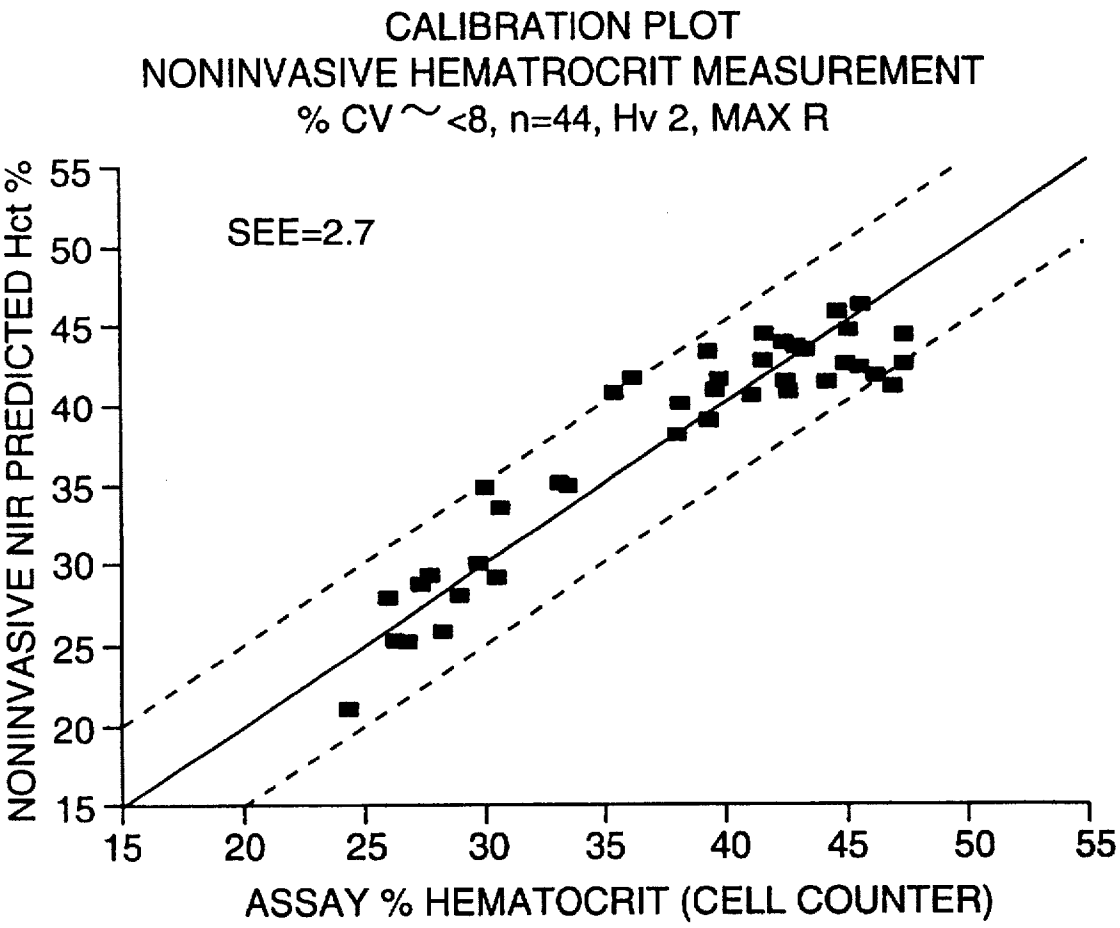

CALIBRATION PLOT
NONINVASIVE HEMATROCRIT MEASUREMENT
% CV ~ <8, n=44, Hv 2, MAX R
SEE=2.7
NONINVASIVE NIR PREDICTED Hct %
ASSAY % HEMATOCRIT (CELL COUNTER)
15
20
25
30
35
40
45
50
55

Fig. 25

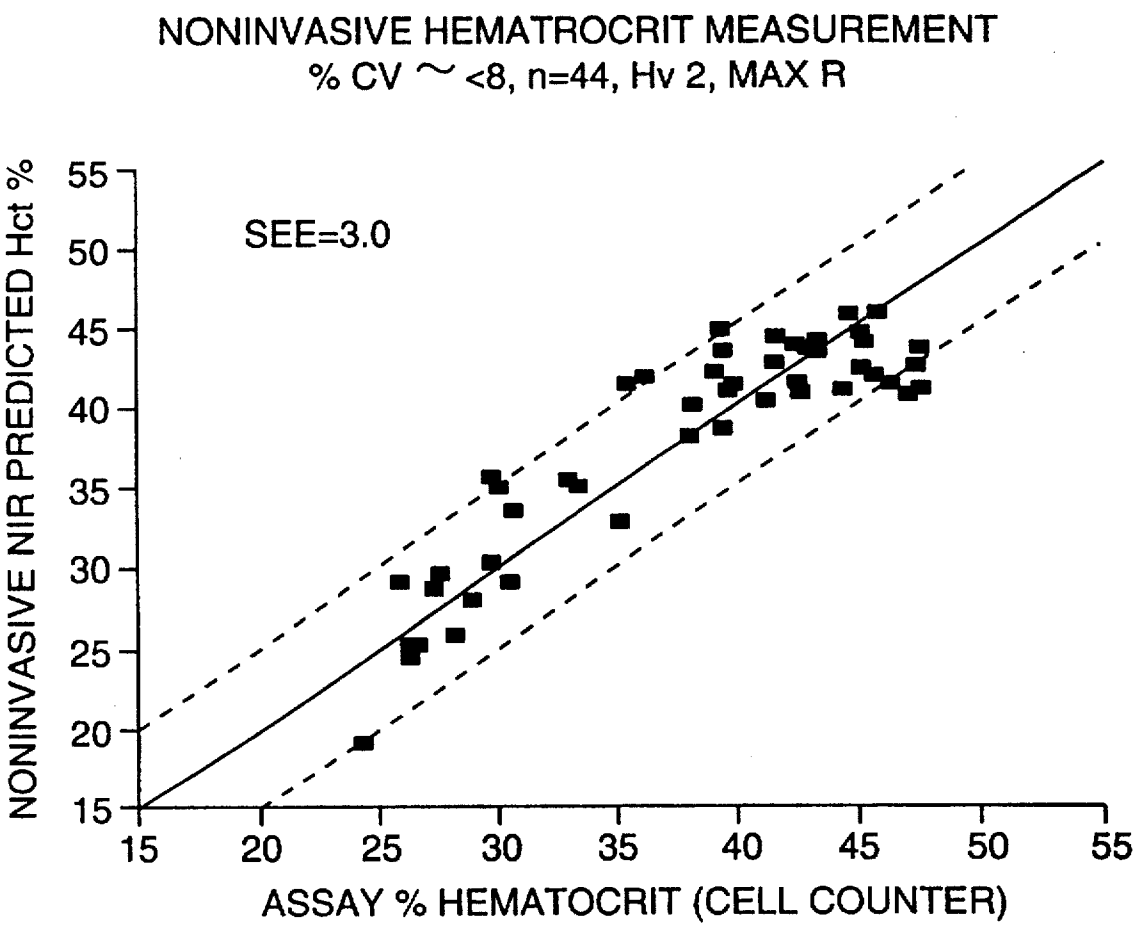

NONINVASIVE HEMATROCRIT MEASUREMENT
% CV ~ <8, n=44, Hv 2, MAX R
SEE=3.0
NONINVASIVE NIR PREDICTED Hct %
ASSAY % HEMATOCRIT (CELL COUNTER)
15
20
25
30
35
40
45
50
55

Fig. 26

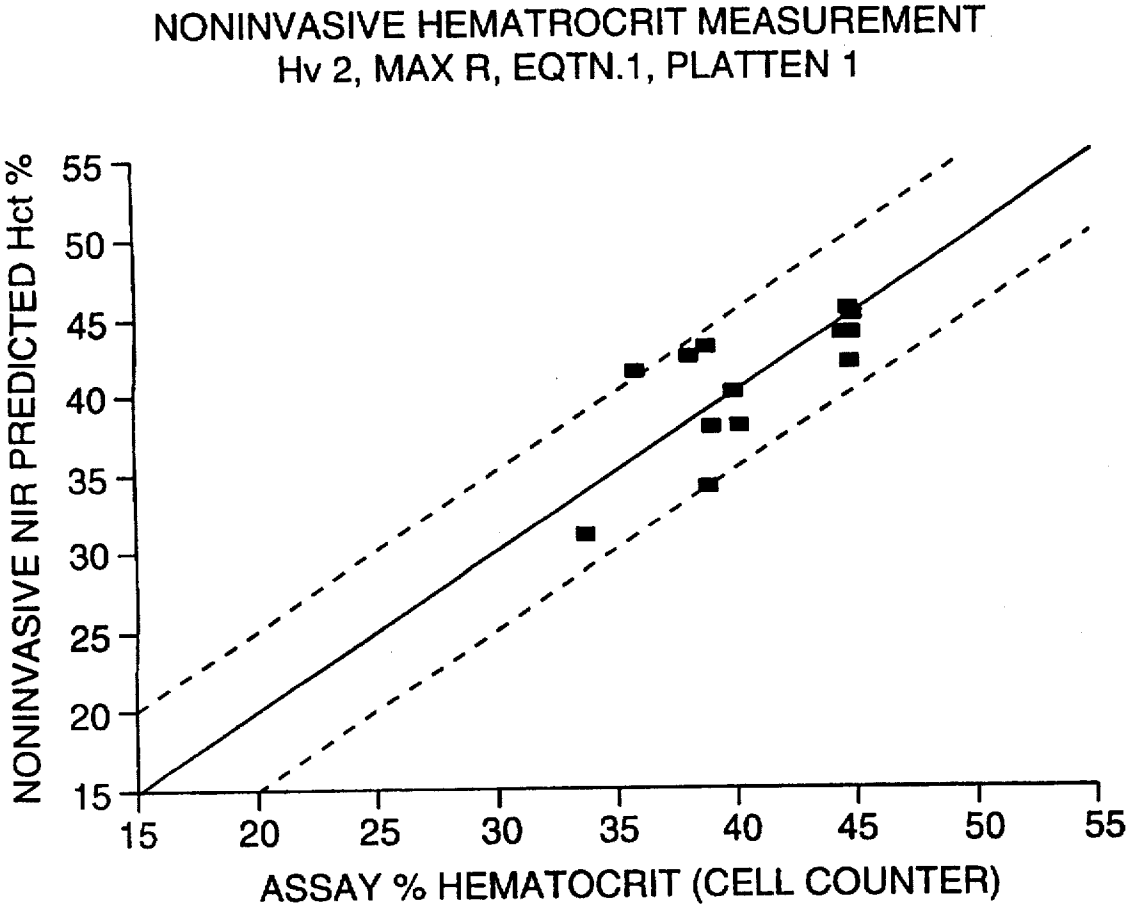

NONINVASIVE HEMATROCRIT MEASUREMENT
Hv 2, MAX R, EQTN.1, PLATTEN 1
NONINVASIVE NIR PREDICTED Hct %
55
50
45
40
35
30
25
20
15
15
20
25
30
35
40
45
50
55
ASSAY % HEMATOCRIT (CELL COUNTER)

Fig. 27

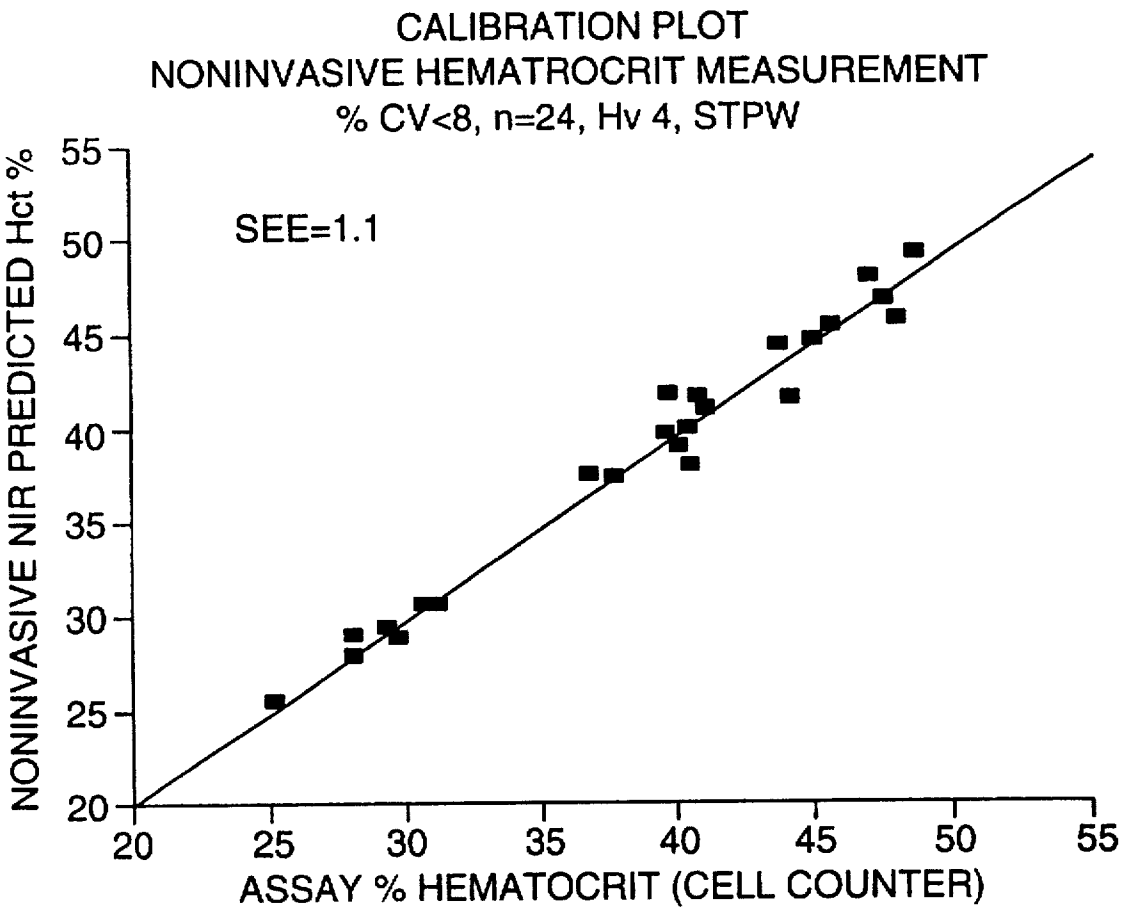

CALIBRATION PLOT
NONINVASIVE HEMATROCRIT MEASUREMENT
% CV<8, n=24, Hv 4, STPW
SEE=1.1
NONINVASIVE NIR PREDICTED Hct %
ASSAY % HEMATOCRIT (CELL COUNTER)
20
25
30
35
40
45
50
55

Fig. 28

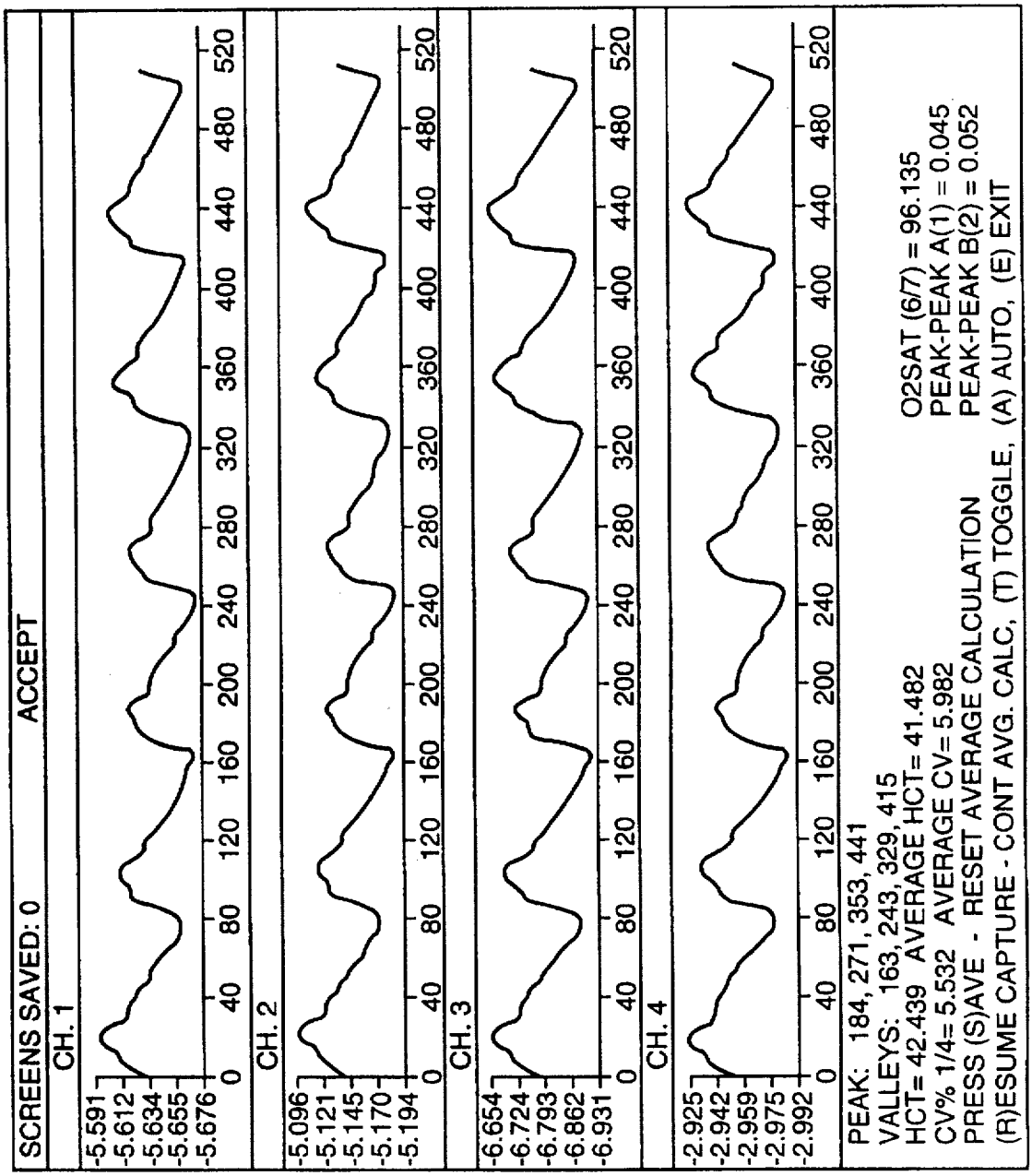

SCREENS SAVED: 0
ACCEPT
CH. 1
-5.591
-5.612
-5.634
-5.655
-5.676
0 40 80 120 160 200 240 280 320 360 400 440 480 520
CH. 2
-5.096
-5.121
-5.145
-5.170
-5.194
0 40 80 120 160 200 240 280 320 360 400 440 480 520
CH. 3
-6.654
-6.724
-6.793
-6.862
-6.931
0 40 80 120 160 200 240 280 320 360 400 440 480 520
CH. 4
-2.925
-2.942
-2.959
-2.975
-2.992
0 40 80 120 160 200 240 280 320 360 400 440 480 520
PEAK: 184, 271, 353, 441
VALLEYS: 163, 243, 329, 415
HCT= 42.439 AVERAGE HCT= 41.482
CV% 1/4= 5.532 AVERAGE CV= 5.982
PRESS (S)AVE - RESET AVERAGE CALCULATION
(R)ESUME CAPTURE - CONT AVG. CALC, (T) TOGGLE, (A) AUTO, (E) EXIT
O2SAT (6/7) = 96.135
PEAK-PEAK A(1) = 0.045
PEAK-PEAK B(2) = 0.052

Fig. 29

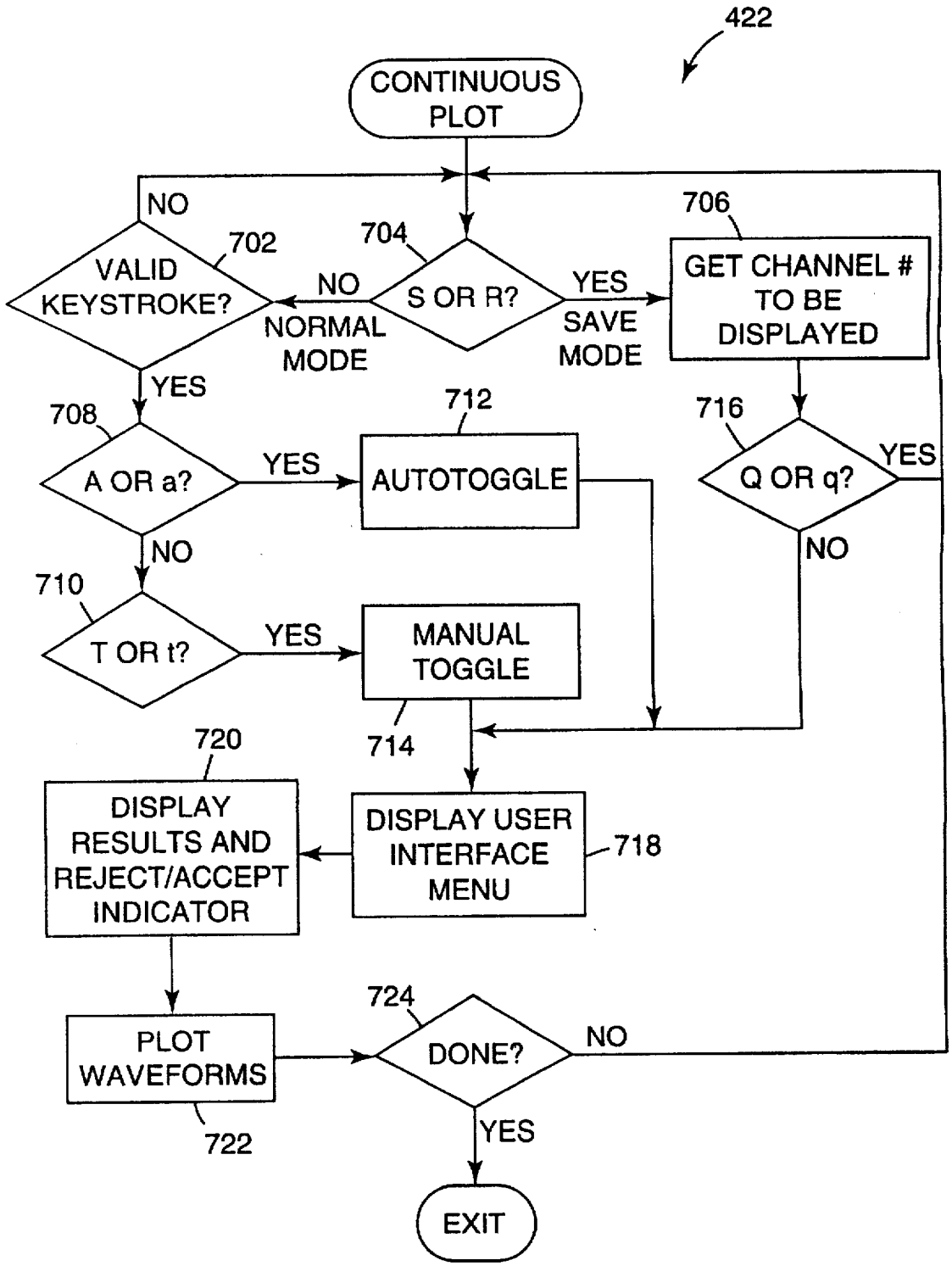

422
CONTINUOUS PLOT
NO
VALID KEYSTROKE?
702
704
S OR R?
NO
NORMAL MODE
YES
SAVE MODE
706
GET CHANNEL # TO BE DISPLAYED
YES
708
A OR a?
YES
712
AUTOTOGGLE
716
Q OR q?
YES
NO
NO
710
T OR t?
YES
MANUAL TOGGLE
714
720
DISPLAY RESULTS AND REJECT/ACCEPT INDICATOR
DISPLAY USER INTERFACE MENU
718
724
PLOT WAVEFORMS
722
DONE?
NO
YES
EXIT

Fig. 30A

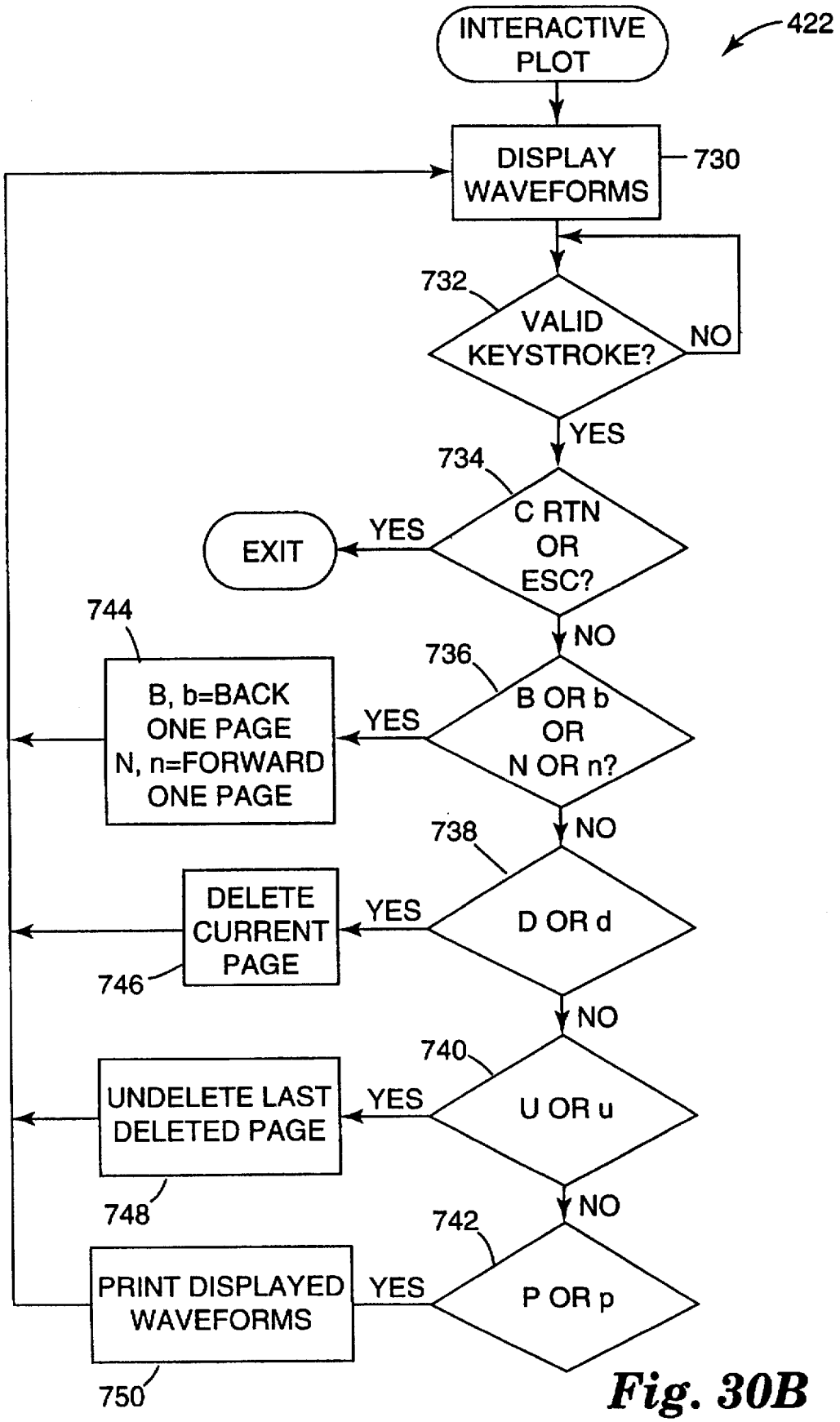

INTERACTIVE PLOT
422
DISPLAY WAVEFORMS
730
732
VALID KEYSTROKE?
NO
YES
734
C RTN OR ESC?
YES
EXIT
NO
736
B OR b OR N OR n?
YES
744
B, b=BACK ONE PAGE
N, n=FORWARD ONE PAGE
NO
738
D OR d
YES
DELETE CURRENT PAGE
746
NO
740
U OR u
YES
UNDELETE LAST DELETED PAGE
748
NO
742
P OR p
YES
PRINT DISPLAYED WAVEFORMS
750

Fig. 30B

METHOD AND APPARATUS FOR NONINVASIVE PREDICTION OF HEMATOCRIT

This is a division of application Ser. No. 08/189,600 filed Jan. 31, 1994 now U.S. Pat. No. 5,553,615.

GOVERNMENT RIGHTS

This invention was made with Government support under Contract N00014-89-C-0024. The Government has certain rights in this invention.

REFERENCE TO MICROFICHE APPENDIX

This application incorporates by reference the computer program listing in the attached microfiche appendix, which includes 2 microfiche and a total of 128 frames.

FIELD OF THE INVENTION

This invention relates to a method and apparatus for noninvasive prediction of hematocrit.

BACKGROUND OF THE INVENTION

Hematocrit, the fractional percent volume of erythrocytes (red blood cells) in total volume of blood, is a vital blood constituent to be monitored to determine the physiological condition of a mammalian patient.

Hematocrit has been traditionally measured by withdrawing or diverting blood from the body of a mammalian patient. Such in vitro or in vivo techniques that are invasive to body cause complications in the condition of the patient and those treating the patient. Any invasive diagnostic or monitoring procedure is less preferred by a mammalian patient than a noninvasive procedure. Blood-borne diseases are a source of concern for those treating the patient.

Invasive procedures for determining hematocrit where a sample of blood is withdrawn are disclosed in U.S. Pat. Nos. 3,923,397 (Shuck) and 5,200,345 (Young) and in European Patent Publication 0 419 222 A2 (Callis et al.)

Invasive procedures for determining hematocrit where a sample of blood is diverted from the bloodstream of a patient are disclosed in U.S. Pat. Nos. 4,227,814 (Soodak et al.); 4,303,336 (Cullis); and 4,447,150 (Heinemann); and in European Patent Publication 0 419 223 A2 (Callis et al.).

Invasive procedures for determining hematocrit where a probe is inserted into the body is disclosed in U.S. Pat. Nos. 4,776,340 (Moran et al.) and 4,936,679 (Mersch).

Noninvasive procedures for predicting hematocrit can employ magnetic resonance, as disclosed in U.S. Pat. No. 5,233,991 (Wright); or impedance plethysmography, as disclosed in U.S. Pat. Nos. 4,562,843 (Djordjevich et al.) and U.S. Pat. No. 4,548,211 (Marks).

Noninvasive procedures for predicting percent oxygen saturation employing photoplethysmography, commonly called pulse oximetry, are disclosed in U.S. Pat. Nos. 4,819,752 (Zelin) and 5,193,543 (Yelderman). In Zelin, light emitting diodes at two different wavelengths are employed, with corrections made for the pulsatile nature of blood flow, variations in the strength of the light source, variations in the thickness of tissue through which the light passes, variations in placement of the detector in respect of the location of the light emitters, and changes in the physiology of the non-pulsatile component. In Yelderman, light emitting diodes at two different wavelengths are also employed, with corrections made to improve resistance to interference from ambient artificial light, BOVIE electrocautery interference using AM modulation/demodulation techniques.

Noninvasive procedures for predicting hemoglobin, arterial oxygen content and hematocrit employing photoplethysmography is disclosed in U.S. Pat. No. 5,101,825 (Gravenstein et al.). In Gravenstein et al., the blood constituents are predicted by measuring the change in the mass of hemoglobin resulting from a measured change in the volume of blood. After total hemoglobin is predicted, hematocrit is approximated by multiplying total hemoglobin by a factor of three.

None of the known invasive procedures are preferable to either patient or practitioner if a truly noninvasive technique were available that could predict hematocrit accurately. None of the known noninvasive procedures predict hematocrit directly.

European Patent Publications 0 419 222 A2; 0 419 223 A2 (both Callis et al.); and 0 476 192 A2 (Callis) disclose methods for prediction of hematocrit using chemometric techniques and regression analysis that uses the spectral absorbance of water in the near infrared spectrum to provide the basis of prediction based on a two compartment model where one compartment has a different amount of water than the other compartment. But none of the Publications disclose a method or apparatus to noninvasively predict hematocrit.

SUMMARY OF THE INVENTION

The treatment of patients needs a method and apparatus to predict hematocrit using photoplethysmography rapidly, directly, accurately, and mechanically noninvasively.

The present invention provides a method and apparatus for the mechanically noninvasive, rapid, direct and accurate prediction of hematocrit using photoplethysmography.

In one aspect of the invention, the method and apparatus also predicts oxygen saturation using photoplethysmography.

In another aspect of the invention, the method and apparatus also predicts methemoglobin using photoplethysmography.

In another aspect of the invention, the method and apparatus predict hematocrit and optionally oxygen saturation transcutaneously of a mammalian patient using algorithms that employ a plurality of wavelength ratio pairs.

In another aspect of the invention, the method and apparatus predict hematocrit and optionally methemoglobin noninvasively in blood stored in containers for later transfusion into a mammalian patient.

In another aspect of the invention, the method and apparatus provide corrections for oxygen saturation status in hematocrit to correct for variations in the amount of carboxyhemoglobin in the blood of a mammalian patient.

In another aspect of the invention, the apparatus provides a method for minimizing an undesirable effect of light causing an excessive change in the temperature in tissue being analyzed transcutaneously.

In another aspect of the invention, the apparatus provides a method for minimizing the effect of extraneous light interrogating mammalian tissue.

In another aspect of the invention, the apparatus provides a combination of fiber optics and lenses that maximize the shape and transmission of light emerging from interrogated mammalian tissue.

In another aspect of the invention, the apparatus optionally provides an order-adaptive filter for detrending photoplethysmographic signals.

In another aspect of the invention, the apparatus provides an adaptive peak and valley detector for waveforms generated in photoplethysmography.

In another aspect of the invention, the apparatus provides a high common mode rejection amplifier for use with photoplethysmographic signals.

In another aspect of the invention, the method and apparatus provide a method for estimating the confidence level of noninvasive photoplethysmographic signals.

In another aspect of the invention, the method and apparatus optionally provide quantifiable performance indices for photoplethysmographic waveforms.

In another aspect of the invention, the method and apparatus optionally provide a noise reduction technique for multi-wavelength photoplethysmography.

A feature of the invention is the ability to noninvasively predict hematocrit within plus or minus 5 hematocrit percent of the actual hematocrit value.

Another feature of the invention is the ability to noninvasively predict percent oxygen saturation within plus or minus 5 oxygen saturation percent of the actual oxygen saturation value.

An advantage of the invention is that the noninvasive prediction of hematocrit can proceed intermittently or continuously without disruption to the blood flow or blood stream of a mammalian patient.

Another advantage of the invention is that the noninvasive hematocrit prediction minimizes exposure of a health care practitioner to blood of the mammalian patient.

Another advantage of the invention is that the noninvasive hematocrit prediction can be made rapidly and accurately in intensive treatment environments, such as hospital emergency rooms, intensive care and surgical arenas, and in military triage.

Another advantage of the invention is that a simultaneous prediction of oxygen saturation and hematocrit can be made, thereby allowing the correction of one to allow for the effect of varying magnitudes of the other.

Another advantage of the invention is that the method and apparatus of the invention is adaptable to be miniaturized for portable use where health care is needed but facilities are unavailable.

Yet another advantage of the invention is that it allows the use of predicted quantities of hematocrit and percent oxygen saturation to calculate other meaningful predictions, such as the oxygen carrying capacity of mammalian blood, defined as the product of hematocrit and percent oxygen saturation assuming a normal amount of hemoglobin present in a red blood cell.

Other aspects, features, and advantages will become apparent as a description of embodiments proceeds with reference to the following drawings.

BRIEF DESCRIPTION OF THE DRAWINGS

FIG. **1** is a typical photoplethysmograph.

FIG. **2** is a simplified schematic illustration of a system of the present invention.

FIG. **3** is a simplified diagram of the method of the present invention.

FIG. **4** is a more detailed schematic illustration of an embodiment of the invention for interrogating mammalian tissue using photoplethysmography.

FIG. **5** is an illustration of a "chopper wheel" used in an embodiment of the present invention.

FIG. **6** is an electronic schematic diagram of the motor control circuit for the chopper wheel.

FIGS. **7A** and **7B** are perspective illustrations of a finger holding device in an embodiment of the present invention.

FIGS. **8A** and **8B** are illustrations of two plattens used in an embodiment of the present invention.

FIG. **9** is a schematic illustration of an embodiment of the invention for collimating and filtering light from interrogated tissue.

FIG. **10** is an illustration of one platten shown in FIG. **8**, showing photodetectors used in the present invention.

FIG. **11** is an electronic schematic diagram for amplification and filtering of the photoplethysmographic signals.

FIG. **12** is an electronic schematic diagram of the trigger control module.

FIGS. **13A** and **13B** show exemplary two dimensional arrays in which raw data and peak and valley locations are stored, respectively.

FIG. **14** is a flow chart of the user preconfiguration process.

FIG. **15** is a flow chart of the processing control steps of the present invention.

FIG. **16** is a flow chart of the detrending procedure of the present invention.

FIG. **17** is a graph showing the original, detrended and DC signals.

FIG. **18** shows an exemplary photoplethysmographic waveform and an associated differentiated photoplethysmographic waveform.

FIGS. **19A** and **19B** show the procedure for finding actual peak and valley locations.

FIG. **20** shows the procedure for finding the the values associated with peak and valley.

FIGS. **21A–21D** show exemplary waveforms associated with the template matching technique of the present invention.

FIG. **22** is a calibration plot of results using a first equation used according to the present invention for the direct prediction of hematocrit compared with actual hematocrit.

FIG. **23** is a validation plot of results using the first equation.

FIGS. **24A** and **24B** are a cross validation plot of results using the first equation.

FIG. **25** is a calibration plot of results using a second equation used according to the present invention.

FIG. **26** is cross validation plot of results using the second equation.

FIG. **27** is a validation plot of results using the second equation.

FIG. **28** is a calibration plot of results using a third equation used according to the present invention.

FIG. **29** shows an exemplary display screen of the present invention.

FIGS. **30A** and **30B** show control flow for continuous display of waveforms and interactive display, respectively.

EMBODIMENTS OF THE INVENTION

Photolethysmography

In photoplethysmography, visible and near infrared (NIR) light is transmitted through mammalian blood to predict hematocrit and other analytes of interest in such blood. The

transmission is noninvasive without diversion of the blood from the vessels in which the blood is contained.

In the embodiment of transcutaneous photoplethysmography, one must account or discount for a number of factors that are not encountered in the use of photoplethysmography in an in vitro or diverting in vivo environment used in the prior art. Nonlimiting factors one must consider are: oxygen saturation; the absorbance characteristics of mammalian tissue, mammalian bone, venous blood, and the capillary bed; the distance of light transmission; the avoidance of ambient light; the pigmentation of skin; blood pressure; and tissue temperature and compression.

In the embodiment of assessing the quality of mammalian blood stored for later transfusion, one must consider a number of factors that are not encountered in the use of photoplethysmography in noninvasive, transcutaneous embodiments. Nonlimiting factors one must consider are: size of the vessel; distance of light transmission; the absorbance characteristics of the containing vessel; temperature of blood; and substances added to blood to preserve blood acting as interferents.

Once the transmitted light is detected, one must consider the effects of noise; the effects of ambient light; and the effects of the settling rate of particulates and cells (i.e., scatterers of light).

Once the transmitted light is treated to maximize its usefulness in hematocrit prediction, then the prediction must be sufficiently accurate and precise to be useful as a substitute for invasive or diverting procedures. Nonlimiting factors one must consider are the robustness of the calibration equation, the inclusiveness of a broad representation of the general population when forming the training set; and a reliable reference method that also is accurate and precise.

The present invention has overcome these factors to provide a method and apparatus to noninvasively and directly predict hematocrit using photoplethysmography.

The Beer-Lambert law relates the light intensity exiting an optical absorber Io, to the light intensity incident on it, Ii, according to the following equation:

$$Io=Ii(e^{-k*l*c})$$

where k is the extinction coefficient of the absorber, l is the pathlength traversed by the light through the absorber and c is its molar concentration.

Optical absorbance A is therefore defined as:

$$A=ln(Ii/Io)=k*l*c$$

where ln is the natural logarithm. In traditional spectroscopy instruments the intensity Io represents the intensity of light that has gone through the sample (absorber) holder such as a cuvette and the absorber itself; and therefore a reference absorbance of the empty cuvette is taken prior to filling it up with the absorber and subsequently subtracted. In other instruments, two beams of light are used, with one going through an empty cuvette and the other through a cuvette filled with the absorber but otherwise identical to the first cuvette. The difference of absorption values then gives the true absorption of the absorber under test. In other words one needs to measure the intensity of light with and without the presence of the absorber in the path of the light.

In this invention, as is required in the field of pulse oximetry (c.f., U.S. Pat. Nos. 4,653,498; 4,621,643; and 4,685,464; among others) the light intensities Io and Ii as defined above are obtained from a well-vascularized body part such as a finger by measuring the light emerging from the finger at the points in time identified above in the photoplethysmograph as the "peak" and "valley" respectively.

It must be emphasized that any measurement of light attenuated by tissue in vivo is the result of the incident light being reflected, absorbed and significantly scattered. This last phenomenon, especially as it is spatially co-mingled with absorption inside the absorber has the multiple effects of:

(1) increasing the path length of photons relative to the geometric distance between the source and detector in contact with the finger;

(2) as a consequence of (1) above the optical absorption cross section is increased (i.e., the photons are bounced around inside the absorber increasing chances of being absorbed in it); and

(3) the collimated or directional beam of incident light emerges from the finger as from a diffuse source.

Particularly, this scattering is also a function of the wavelength, and therefore the measurement of absorption at a given wavelength needs to be normalized by another wavelength to neutralize the effect of scattering. "Attenuated light" means the light emerging from mammalian tissue in a form diminished from irradiated light by the effects of reflection, refraction, absorbance, and scattering.

FIG. **1** shows a typical photoplethysmograph plotted in amplitude vs. time. Typical photoplethysmographs can be comprised of a desired pulsatile signal **10**, a Direct Current (DC) average **20**, various noise and other physiological and mechanical artifacts. Nonlimiting examples of these artifacts are physical movement between the sensor and interrogated mammalian tissue, respiratory-induced variations, and other artifacts. Repetitively within the pulsatile signal **10** are locations of peaks **30** and valleys **40**, and their corresponding amplitudes or intensities I_P and I_V, respectively. Pulsatile average **50** is the average AC value (I_P–I_V) over a defined number of pulse periods.

While it is possible to visually evaluate the quality of a desired signal embedded in artifact and noise, such as using a digital oscilloscope, the process requires a repetitive application of an empirically derived and applied standard.

The present invention provides a repeatable, quantifiable method of prediction that evaluates the waveform for peaks, valleys, DC averages, and pulsatile averages. The method of prediction is predicated on proper selection of wavelengths related to the analytes of interest.

Selection of Appropriate Wavelengths

European Patent Publication 0 419 223 A2, corresponding to U.S. patent application Ser. No. 07/995,951 (Callis et al.), the disclosures of which are incorporated by reference, discusses both ratios of wavelength pairs and taking a multiple derivative of the relationship between the absorption as a function of the wavelength as alternative preprocessing techniques useful for the prediction of hematocrit. In both methods, wavelengths chosen are associated with absorbance peaks of water in blood where the two compartments of blood have differing amounts of water. In the ratio method, a second wavelength chosen preferably corresponds to an isosbestic point for absorbance of oxyhemoglobin and deoxyhemoglobin. A second ratio for correction of oxygen saturation is optionally included.

This invention unexpectedly requires additional and different ratios for noninvasive, transcutaneous prediction of hematocrit. Irradiation and detection of transcutaneously transmitted light is exceedingly more complex than such irradiation and detection in a stationary cuvette or a nonin-

vasive but diverting blood flow loop with a viewing space of constant dimensions.

As in European Patent Publication 0 419 223 A2, corresponding to U.S. patent application Ser. No. 07/995,951 (Callis et al.), the selection of wavelengths for direct, noninvasive prediction of hematocrit is based on the components of water, oxyhemoglobin, and deoxyhemoglobin in mammalian blood.

But unexpectedly, the selection of wavelengths employs multiple wavelengths having significance for those components and their interrelationships. Depending on the mammalian species involved, the scope of the invention is not limited to a particular number of wavelengths employed. Desirably, from about 4 to about 14 wavelengths can be initially selected for statistical analysis to determine the best coefficients for prediction of hematocrit. Preferably between 5 and 8 wavelengths can be initially selected and used in statistical analysis for determining the best coefficients for prediction of hematocrit.

At a minimum, selection of wavelengths should include:

(1) a wavelength where the absorbance of water is at or near a measurable peak;

(2) at least one wavelength where the absorbance of oxyhemoglobin (oxyHb) and deoxyhemoglobin (deoxyHb) are predictable and represent total hemoglobin (Hb) content, i.e., the isosbestic region of hemoglobin (Hb Isos), it being preferred to use two wavelengths from this region;

(3) a wavelength where the absorbance of water greatly exceeds the absorbance of all forms of hemoglobin; and

(4) a wavelength where the absorbance of all forms of hemoglobin greatly exceeds the absorbance of water.

One wavelength can satisfy two or more of the selection criteria. In European Patent Publication 0 419 223 A2, two wavelengths satisfied all four selection criteria.

Desirably, selection of wavelengths also includes:

(5) a wavelength where the absorbance of oxyhemoglobin greatly exceeds the absorbance of deoxyhemoglobin; and

(6) a wavelength where the absorbance of deoxyhemoglobin greatly exceeds the absorbance of oxyhemoglobin.

Again one wavelength in the set can satisfy two or more of the selection criteria. A ratio of the two selection criteria (5) and (6) is conventionally used for pulse oximetry. Unexpectedly, use of selection criteria (5) and (6) can correct for the effects of the presence of differing amounts of carboxyhemoglobin in mammalian blood as result of whether the patient smokes tobacco products or has inhaled smoke.

Preferably, the selection of wavelengths also includes:

(7) at least one different wavelength from selection criteria (1) where the absorbance of water is at or near a measurable peak or shoulder and is subjected to differing interferences than selection criteria (1); optionally

(8) a wavelength where the absorbance of water is in or near a valley between peaks.

Optionally the selection of wavelengths can also include (9) a wavelength where water and hemoglobin are in an isosbestic relationship.

As stated above, optical absorbance is a natural logarithmic relationship. Discussion of the selection of wavelengths herein refer to absorbance intensity of ln(Io/Ii) or ln(Ii/Io) or other relationships between the analogues of Ii and Io, i.e., Iv and Ip, respectively, that may additionally involve I_{DC} described below as forms of H Values described below.

Use of these selection criteria does not mean that the wavelength will be used in the ultimate prediction equation. Statistical analysis described below may be used to choose ratios among these selection criteria wavelengths to determine the best correlation.

Based on the required, desirable, and preferred selection criteria, Table 1 shows ranges and preferred wavelengths for use in the present invention.

TABLE 1

Wavelength Criteria	Acceptable Range (nm)	Desirable Range (nm)	Preferred Range (nm)
1. Water Peak	1160–1230	1180–1215	1195–1207
2. Hb Isos	800–850	800–840	805–837
3. Water >> Hb	1150–2100	1290–1500	1300–1315
4. Hb >> Water	450–690	600–685	630–680
5. Deoxy Hb >> Oxy Hb	650–690	655–685	660–680
6. Oxy Hb >> Deoxy Hb	890–920	895–925	900–910
7. Other Water Peak(s)	960–990	970–990	972–985
8. Water Valley	1100–1120	1105–1115	1110
9. Water & Hb Isos	1130–1170	1140–1165	1160

For each of the pulses in an optical train at each wavelength selected, the apparatus picks out the numerical values at the locations of the photoplethysmograph peak, valley and the average value which represents the DC component. This is done for the simultaneously recorded pulse at each of the several wavelengths used.

Selection of "H Value" Equations

Because of the scattering encountered in the mammalian tissue, it is a discovery of the present invention that only a pseudo-absorption can be calculated by the natural logarithmic ratio of the light intensities Io and Ii.

For purposes of this invention, this pseudo-absorption is termed the "H Value" or "HV". In European Patent Publication 0 419 223 A2, where one ratio of two wavelengths is disclosed to predict hematocrit and one ratio of two other wavelengths is disclosed to optionally correct the hematocrit for oxygen saturation, a ratio of ln(Io/Ii)@ wavelength **1** divided by the ln(Io/Ii)@ wavelength **2** is used. But the effects of pulsatile flow in mammalian tissue were not considered in the static or dynamic conditions disclosed.

It is understood that ratios can be calculated by using ln(Io/Ii) or ln(Ii/Io). It is further understood that the H Values can be calculated by interchanging the numerator and denominator, each identified as ln(Io/Ii), or by forming other non-logarithmic and linear and nonlinear ratios as shown below.

Unexpectedly, the present invention has selected four H Values that approximate the effects of pulsatile blood flow in mammalian tissue. Depending on the mammalian species involved and the area of the patient being interrogated, any of these H Values could provide an acceptable result. But an H Value that takes into consideration pulsatile nature of the mammalian tissue during light interrogation and the effect of the DC component is preferred over an H Value that does not.

The four H Values equations useful in the present invention are shown below as equations. Moreover, the present invention contemplates that other H Values can be calculated empirically according to techniques known to those skilled in the art of waveform processing.

HV1 = ln(Ip/Iv)@w1 / ln(Ip/Iv)@w2
HV2 = {ln(Ip/Iv)@w1/ln(Ip/Iv)@w2}*{Idc@w2/Idc@w1}
= HV1*{Idc@w2/Idc@w1}.
HV3 = {(Ip–Iv)@w1/(Ip–Iv)@w2}*{Idc @w2/Idc@w1}.
HV4 = ln{(Ip–Iv)/Idc}@w1/ln{(Ip–Iv)/Idc}@w2

where Idc is the DC or average value of the light intensity for a pulse, w1 and w2 are two independent wavelengths, Ip is intensity at a peak, Iv is intensity at a valley, and the subscripts 1 to 4 for the H values HV are identifiers but do not indicate any ascribed wavelength. The difference between Ip and Iv is a single pulse peak to peak intensity; the average of several of these is the pulsatile average (AC).

HV1 is a ratio for two different wavelengths of a logarithmic relation between peak and valley of a pulse.

HV2 multiplies HV1 by an inverse ratio of the average DC value at the two wavelengths to normalize the AC component of the signal.

HV3 multiplies a ratio of the single pulse peak to peak intensity at two wavelengths by the same inverse ratio as used in HV2; an AC/DC ratio. The differences between HV2 and HV3 is the absence of any logarithmic relationship in HV3.

HV4 is a ratio for two different-wavelengths of the natural logarithm of the single pulse peak to peak intensity over DC average; a logarithmic AC/DC ratio.

Thus, for purposes of this invention, the term $HV3_{2,7}$ indicates a pseudo-absorbance calculated according to the formula for HV3 shown above with the two wavelengths w1 and w2 being identified as wavelengths 2 and 7, respectively.

Such pseudo-absorbance values are obtained from a broad cross-section of mammalian patients of the same species and preferably stored electronically. A look-up table can be prepared according to the teaching of European Patent Publication 0 419 223 A2 and patent application Ser. No. 07/995,951 identified above in conjunction with statistical analysis as described below.

As identified in European Patent Publication 0 419 223 A2 and patent application Ser. No. 07/995,951 identified above, the use of second derivative absorbance values at wavelengths in the regions of interest can be used and substituted for H Values to derive a multi-parameter regression equation for hematocrit prediction. A larger number of measurements is required. But the method of obtaining the pseudo-absorbance values of hematocrit is derived from pulsatile flow as treated according to the present invention.

Selection of Statistical Analysis

Generally, one of the four HV formulae, i.e., HV1 or HV2 or HV3 or HV4 is chosen for the purpose of approximating the absorption equation coefficients with the best correlation coefficient and standard error of prediction possible.

Statistical analysis can take several mathematical forms known to those skilled in the art. Nonlimiting examples include linear regression, non-linear regression, multiple linear regression, step-wise linear regression, partial least squares, principal component analysis, chemometrics, and other regression techniques as well as curve-fitting, neural networks, and other non-regression techniques.

For example, linear regression can be employed as disclosed in European Patent Publication 0 419 223 A2. If H Value, HV3, is chosen, then all possible wavelength pairs xy are chosen to form numerous HV3 values of the form $HV3_{x,y}$.

As disclosed in European Patent Publication 0 419 223 A2, one can calculate all possible wavelength pairs of a spectrum. But using the wavelength selection criteria of the present invention, one can confine the wavelength pairs only to those wavelengths actually selected for formation of the prediction equation.

This reduction in the number of wavelength pairs selected reduces the complexity of the light transmission and optics apparatus to require only those wavelengths actually used for statistical analysis of the H Value chosen.

For example, if photoplethysmographs were recorded at four wavelengths simultaneously, then the following HV3 values would be computed $HV3_{1,2}$; $HV3_{1,3}$; $HV3_{1,4}$; $HV3_{2,3}$; $HV3_{2,4}$ and $HV3_{3,4}$. Each of these H Values is computed for a large number of individual pulse pairs (recorded substantially simultaneously), generally 40, for a given patient, and the average is used as part of the equation to predict hematocrit. A smaller number of pulse pairs can be used if the variance from pulse to pulse is acceptably small. The aggregate of the H Values recorded establish a training set of H Values.

The average values of the H Values of each of the possible wavelengths of interest can be treated as variables for statistical analysis. The data can be analyzed using a personal computer, such as an IBM personal computer, utilizing commercially available computer software, such as the statistical computer software SAS/STAT (R) , Version 6, Fourth Edition sold by SAS Institute Inc., Cary N.C. 27512.

Data can be analyzed using various techniques including Forward Selection, Stepwise Regression, and Maximum R^2 Procedure. The latter two are preferred.

Ordinarily the FORWARD SELECTION (FS) technique begins with no variables in the mathematical model used to form the prediction equation. For each of the independent variables, FS calculates F statistics that reflect the variables' contribution to the model if it is included. The p-values for these F-statistics are compared to the significance level defined for entry into the model, "SLENTRY=" value that is specified in the Model statement. If no F statistic has a significance level less than the SLENTRY=value, FS stops. Otherwise, FS adds the variable that has the largest F statistic to the model. FS then calculates F statistics again for the variables still remaining outside the model, and the evaluation process is repeated. Thus variables are added one by one to the model until no remaining variable produces a significant F statistic. Once a variable is in the model it stays.

The STEPWISE REGRESSION method is a modification of the FS technique and differs in that variables already in the model do not necessarily stay there. As in the FS method, variables are added one by one to the model, and the F statistic for a variable to be added must be significant at the SLENTRY=level. After a variable is added, however, the SR method looks at all the variables already included in the model and deletes any variable that does not produce an F statistic significantly lower than the chosen significance level for staying in the model. Only after this check is made and the necessary deletions accomplished can another variable be added to the model. The SR process ends when none of the variables outside the model has an F statistic significant at the entry significance level and every variable in the model is significant at the staying significance level, or when the variable to be added to the model is the one just deleted from it.

The Maximum R^2 (MAXR) improvement technique does not settle on a single model. Instead it tries to find the best one variable model, the best two variable model, and so forth, although it is not guaranteed to find the model with the largest R^2 for each size. R^2 or R sqd. refers to the square of the correlation coefficient R.

The MAXR method begins by finding the one variable model producing the highest R^2. Then another variable, the

one that yields the greatest increase in the R^2, is added. Once the two variable model is obtained, each of the variables in the model is compared to each variable not in the model. For each comparison, MAXR determines if removing one variable and replacing it with the other variable increases R^2. After comparing all possible switches, MAXR makes the switch that produces the largest increase in R^2. Comparisons begin again, and the process continues until MAXR finds that no switch could increase R^2. Thus, the two variable model achieved is considered the "best" two variable model the technique can find. Another variable is then added to the model, and the comparing-and-switching process is repeated to find the best three variable model, and so forth.

The difference between the Stepwise method and the MAXR method is that all switches are evaluated before any switch is made in the MAXR procedure. In the Stepwise method, the 'worst' variable can be removed without considering what adding the 'best' remaining variable might accomplish.

Selection of Prediction Equations

Using a statistical analysis described above on one or more H Value equations described above that employ wavelengths chosen according to the Selection Criteria described above, an equation for the prediction of hematocrit can be obtained.

When using MAXR or stepwise analysis to find the best correlation coefficients and R^2 value, the prediction equation can have a linear or nonlinear combination of n regression coefficients for n variables constituting the H Values at the pairs of wavelengths selected from the wavelength selection criteria. These regression coefficients are stored in a look-up table on the computer and are combined with the realtime photoplethysmograph to predict hematocrit.

Thus, an hematocrit prediction equation can be a plurality of ratios linearly or nonlinearly combined depending on the best correlation using statistical analysis to actually measured hematocrits for the same patients. Actual values of hematocrit are measured and stored according to a standard, accepted technique. Nonlimiting examples of such measurement techniques include cell counters, centrifuges, and indirectly from the amount of total hemoglobin measured on a co-oximeter.

Broadly, a prediction equation according to the present invention is represented by:

$$HCT=\alpha(HV_{a,b})^A+ \ldots \omega(HV_{x,y})^Z+\phi$$

where HV is the H Value for wavelengths pairs a,b to x,y selected by the statistical analysis according to the step (e); A through Z are exponents of any value; α through ω are regression coefficients determined by the statistical analysis; and ϕ is the intercept also determined by the statistical analysis.

For example, the following equation shows an exemplary prediction equation according to the present invention:

$$HCT=\alpha HV2_{1,4}+\beta HV2_{2,3}+\chi HV2_{2,7}+\delta HV2_{3,7}+\epsilon HV2_{4,6}+\phi$$

where HV2 is the H Value described above for various wavelengths selected **1**, **2**, **3**, **4**, **6**, and **7**; α,β,χ,δ, and ϵ are regression coefficients determined by statistical analysis; and ϕ is the intercept also determined by statistical analysis. $\alpha,\beta,\chi,\delta,\epsilon$, and ϕ can be positive or negative.

Depending on the mammalian species involved and the location of noninvasive hematocrit prediction transcutaneously, it is possible that one or more wavelengths selected for formation of a prediction equation are not in the ultimate prediction equation. That fact does not diminish the need for use of the wavelength selection criteria described above. From the presentation of wavelengths shown above, it is possible in the present invention to employ a wavelength, i.e., wavelength **5** or wavelength **8**, that is not ultimately used in the prediction equation.

Once a prediction equation is established, it is validated. The accuracy in formation and performance is reviewed to assure reproducibility. European Patent Publication 0 419 223 A2 discloses the techniques for calculating standard error of calibration and standard error of prediction, also known as standard error of estimate.

It is desired to have a standard error of estimate of less than about 5% hematocrit and preferably less than about 2.5% hematocrit.

Use of A Prediction Equation

With the equation established and standard error of estimate confirmed to be acceptable, then the equation can be used to predict unknown hematocrit values noninvasively. Preferably an equation is stored electronically with the established regression coefficients from the training set and the specific wavelengths are irradiated and detected and analyzed according to the H Value(s) in the prediction equation.

Having provided a description of the establishment and rationale for a direct hematocrit prediction equation, an overview of the apparatus and method to achieve and use that equation follows.

System Overview

FIG. **2** shows a simplified block diagram of the present system **100** for noninvasive determination of hematocrit. System **100** includes an optics module **200**, an electronics module **400** and a processing module **500**. As described above, the present system measures hematocrit noninvasively by measuring absorbance of light through blood perfused tissue at appropriate wavelengths. The amount of light absorbed at each wavelength of interest is used to determine a correlation between the amount of light absorbed and the hematocrit level.

The present invention samples the blood perfused tissue at a predetermined rate. The minimum frequency at which the tissue is sampled must satisfy the Nyquist sampling criteria of at least twice the highest frequency present in the signal to be sampled. For purposes of the present invention, the signal of interest is the pulsatile blood flow through the mammalian tissue. This signal contains frequencies such as the pulse rate (1–2 Hz in humans) and other higher frequency components such as those present in the dichrotic notch. A preferred sampling frequency of 100 Hz was therefor chosen for purposes of the present invention to ensure capture of all relevant plethysmographic information.

A mammalian sample **328**, such as a human finger, is interrogated by a modulated light source **102**, which is controlled as described below with respect to FIG. **4**. The light is modulated at the preferred sampling frequency of 100 Hz. The modulated light travels down fiber bundle **326** and is transmitted through the sample **328**. The transmitted light is collected by a plurality of photodetectors **338**, each of which corresponds to a different one of the wavelengths of interest.

The optical radiation collected by each photodetector is converted into a photocurrent by the electronics module **400**. Each photocurrent is filtered and amplified by one of a plurality of amplifier/filter electronics **120**, one for each wavelength of interest. The amplified and filtered signals are then digitized, stored and processed by processing module **500** as described in more detail below.

Method Overview

FIG. 3 shows a simplified block diagram of the control flow through the system of FIG. 2. The preprocessing control **162** steps are performed as described above by optics module **200** and electronics module **400**. The post-capture processing steps **164–180** are performed on the digitized photoplethysmographic signals by the processing module **500** to determine and extract the desired information. The sampled signals may be smoothed and/or detrended in control block **166** to remove undesirable low frequency components, such as DC drift, which may be induced into the photoplethysmographic signals due to artifacts such as respiration and movement of the subject. The location and magnitude of the peaks and valleys of the photoplethysmographic signals for each wavelength of interest are determined in control block **168**.

Absorbances for each wavelength of interest are calculated in control block **172**, as well as absorbance ratios of different wavelength pairs to form the H Values described herein. The H Values are then combined in control block **176** as described herein to predict the hematocrit.

Once the hematocrit is predicted, a measure of the level of confidence of the estimate is determined at control block **178**. This is important in establishing confidence limits a clinician may have in the hematocrit estimate, and may indicate whether further tests or measurements need to be made. The waveforms, hematocrit, confidence value, oxygen saturation and other information determined by the present system are displayed as required at control block **180**.

Having provided system and method overviews of the invention, a specific embodiment of the apparatus and methods follow.

Light Transmission and optics

FIG. **4** provides a schematic illustration of one embodiment of the invention that demonstrates how the invention has overcome difficulties in noninvasive photoplethysmography. FIG. **4** shows a system **310** for transmitting light transcutaneously and the optics for maximizing the reception of transcutaneously transmitted light. Briefly, light from a lamp **312** is chopped by disc **314** as detected by a LED-photo-detector pair **316** electrically connected to an electronics and processing module **500**. The light is reflected by a mirror **320** and sent through an aspheric lens **322**, past a mechanical shutter **324**, into a light source fiber optic bundle **326** where it reaches mammalian tissue **328**.

After transversing the mammalian tissue **328**, the light is received into a light collection fiber optic bundle **330** and divided into between 6 and 10 channels **332**, one or each wavelength of interest. Each channel **332** merges into a fresnel lens collimator **334** (as shown ore completely in FIG. **9**), which directs the interrogated light in each channel through an interference filter **336**. The filtered light from each channel **332** shines on a photodiode **338** for each channel, each diode configured to receive light in a specific light range. Each photodiode **338** converts the received light to an electronic signal which is filtered and amplified as described below with respect to FIG. **11**. Software executed by the computer processes the signals as described herein to predict hematocrit, determine a confidence level, and display the photoplethysmographic waveforms and other information of interest.

Transmission of light begins with the generation of broad wavelength light by an incandescent lamp **312**. Lamp **312** is commercially available from a number of commercial sources. Preferably, the lamp **312** has multiple filaments and is a unit similar to ones used in overhead projectors commercially available from Minnesota Mining and Manufacturing Company (3M), and is identified as 3M part no. 78-8000-7618-0.

Lamp **312** from 3M was chosen because it has a large filament area which is advantageous for further optical processing of this light, and also has a high energy output being rated at 900 watts at 120 V of supply. In addition this halogen-gas-filled lamp **312** has a built in metal reflector behind the filament, as is commonly employed in overhead projectors. Because the lamp **312** is used in the system **310** at a supply voltage of about 73 V from the power supply (not shown), its output is 37% of the rated output at 120 V (power is proportional to the square of the voltage). This increases the life of lamp **312** significantly.

A precision DC power supply at about 73 V is preferably used. Thus, the power fluctuations in the output of the lamp **312** are minimized to acceptable levels. It is an aspect of the invention to recognize that the relative spectral power output of the lamp **312** should not vary significantly every time it is used. Otherwise, the calibration constants used in the algorithm used to predict hematocrit do not maintain accuracy and precision.

Because the relative spectral output is also a function of the temperature of the filament, by assuring a constant power output, this condition is satisfied.

Alternatively, one could provide a diode feedback loop (not shown) to assist in controlling the relative spectral output.

The incandescent light in the range of 300 nm to greater than 20,000 nm from the lamp **312** is periodically interrupted by a 10 cm (4 inch) diameter disc **314** rotating at high speed about 1 cm above the lamp **312** that has pie-shaped open sectors for transmission of light, as seen in FIG. **5**. The disc **314** is preferably made from a metal such as aluminum and preferably has two diametrically-opposed open pie sectors of about 66° opening each. Thus, the disc blocks light during about 228° of each revolution. It is within the scope of the invention to vary either the rotation speed or the amount of blockage, size, and number of the open sectors in order to adjust the amount and duration of light passing disc **314**. It is also within the scope of the invention to use opto-electronic shutters such as those that vary the light transmitted through them between various levels depending on the applied electrical signal and at the rate of change of the applied signal.

The light from the lamp **312** is "chopped" for several reasons. The "chopping" of the optical beam sing open pie-shaped sectors on disc **314** unexpectedly reduces excess heating of mammalian tissue that could alter the conditions affecting a noninvasive, transcutaneous prediction of hematocrit. This chopping can also be used to facilitate a lock-in amplification of the signal, thus increasing signal to noise ratio. During the "off" period of the disc **314** when the light from lamp **312** is blocked from the optical train, and a background reading of the signal indicating ambient noise can be subtracted.

A motor drives disc **314** at a speed of from about 2000 revolutions per minute to about 4000 revolutions per minute, and preferably 3000 revolutions per minute. Rotation at the preferred rate gives one open slot passing over the lamp at a preferred sampling frequency of 100 Hz (cycles per second, here 100 pulses/flashes of light per sec.) Each open sector allows about 3.33 milliseconds of complete filament exposure. This time period is referred to as the "sample window". The computer is synchronized as described below such that the computer samples the photoplethysmographic waveform of each wavelength of interest during this 3.33 millisecond sampling window.

Thus, the preferred total duty cycle or light "on" time is about 33.3%. Configuration of lamp **312** and disc **314** in this manner minimizes the undue heating of the rest of the components **320**, **322**, **324**, and **326** in the optical train that follows as shown in FIG. **4** and more importantly limits the temperature rise of the mammalian tissue **328**, e.g., the finger which this chopped light eventually interrogates.

The disc **314** is spun by a motor (not shown), preferably obtained from an optical chopper unit model SR540 sold by Stanford Research Systems Inc., of Sunnyvale. Calif.

Preferably, the disc **314** is gold plated on the upstream side exposed to lamp **312** and has an anodized black matte finish on the other or downstream side. The gold plating, by virtue of its low emissivity, minimizes heating of the disc **314**, and the black matte maximizes loss of any acquired heat.

Motor Control and Trigger Module

To ensure that the light from the lamp **312** is modulated at the preferred sampling frequency of 100 Hz, the motor control circuit **114** shown in FIG. **6** controls the speed at which the motor rotates disc **314**. A panel mounted potentiometer and corresponding meter readout shown in the upper right portion of FIG. **6** allow the clinician to adjust the motor speed by setting the frequency desired. An precision 10 Volt source LH0070 is buffered by amplifier LM324. A motor driving stage consisting of a transistor, Schottky diode and a nonlinear resistor RXE-030 converts this voltage into a corresponding current which is sensed by a 1.7 ohm resistor and LM324 amplifier. This current is connected to pin **4** of a standard RJ11 telephone jack. A photodiode **316** embedded in the motor senses the transitions at which the chopper wheel shutter begins to open over the lamp. The photodiode produces a corresponding pulsed signal which is connected to the motor control circuit via pin **3** of the RJ11 jack. This pulsed signal is used to determine and display the frequency on the aforementioned meter, and also produces the signal SHUTTER OPEN.

The SHUTTER OPEN signal is isolated from the rest of the circuit by optoisolator HP2231. The SHUTTER OPEN signal is used to synchronize the CPU such that the CPU samples the photoplethysmographic signals of all wavelengths of interest during the 3.33 millisecond sampling window.

Referring again to FIG. **4**, the light allowed through an open disc sector of disc **314** is then reflected off a "hot" dichroic mirror **320** set at a 45 degree angle to the light beam. This mirror preferably has an area of about 6.5 cm square (2 inches square) and preferably is constructed of a pyrex base and coated with dielectric films manufactured by Omega Optical, Inc. of Brattleboro, Vt. that allows it to transmit through light impinging on it at a 45 degree angle and consisting of wavelengths that are both (a) less than about 650 nm in the visible region and (b) greater than 1350 nm in the near infrared region. The mirror reflects, therefore, preferably all wavelengths in the bandwidth of about 650 nm to 1350 nm onto a about 7.6 cm (3 inches) diameter pyrex glass aspheric condenser lens **322** of about 7.6 cm (3 inches) focal length, i.e., an f/1 lens. Thus, only that light used in predicting hematocrit is processed; extraneous light that might interfere with the prediction or heat the mammalian tissue **328** is discarded through the mirror **320**.

The light from the lens **322** is focussed onto one end face of a fiber optic bundle **326** about 0.9 meter long (3 feet) and having about 1.0 cm (0.39 inch) core diameter. This bundle **326** consists of thousands of individual fibers whose jacketing was removed to improve the "packing fraction". Packing fraction refers to the ratio of the true geometrical area computed by adding together the area of each individual fiber to total area occupied by the individual fibers at the end face and the dead space between them. The higher the packing fraction, the more efficient the use of the core diameter. Bundles are made by Fiberguide Industries Inc. of Sterling, N.J.

Another feature of the fibers is that they are made from low water (OH—) content silica. This is important because this invention relies on the efficient measurements of light absorbed by the tissue water. Hence losses of light at wavelengths corresponding to water absorption wavelength bands in other parts of the system are undesirable.

The fibers in the bundle **326**, and therefore the bundle's numerical aperture or its light collection ability is chosen to be high, at least 0.5 and preferably about 0.52 so that maximal light is gathered from a wide angle of an acceptance cone of light striking the bundle face from the lens.

Another feature of the optical system **310** is a mechanical shutter **324**. This is a piece of metal sheet painted flat black and placed between the lens **322** and the face of the fiber bundle **326** about 3 to 4 mm away from the bundle **326**. The shutter can also be made from opaque materials with a plurality of holes or openings of varying intensity such as a wire mesh. This shutter **324** is operated by a small metal rod lever (not shown) so that it can be positioned to partially cover or open a fraction or all of the face of the bundle **326**. This allows one to mechanically interrupt the amount of light entering the bundle **326** from the lamp **312**. The importance of the shutter **324** lies in the fact that it is possible to vary the light intensity interrogating the mammalian tissue (e.g., a finger) without altering the relative spectral intensity of the light. If the power to the lamp **312** were altered, then the filament temperature and hence the relative spectral intensity would change which would cause an alteration of the system **310** calibration constants used in the prediction of hematocrit. The need to alter the light intensity arises due to the large differences in the thickness of fingers in the general population. Thin fingers that allow more light to be transmitted can saturate the electronic amplifiers **340**. Thus, the amount of light used to interrogate a finger must be reduced without changing the relative spectral intensities that could otherwise affect the accuracy and precision of the prediction of hematocrit.

All of the above described components **312**, **314**, **316**, **320**, **322**, and **324** can be mounted using optical and ordinary laboratory fixtures and mounts. All of the above components can be enclosed in a sheet metal housing (not shown) which is preferably painted flat black to minimize multiple light reflections and effectively remove heat. All the holders of the components of system **310** are preferably similarly painted for the same reason. The housing preferably also includes a 20 watt fan blowing air over the components to maintain an acceptable temperature condition of about 65° C. and minimize a rise in temperature of greater than about 80° C. during operation of the system. The housing and the enclosed components can be mounted on a larger plate, preferably made of aluminum about 0.7 cm (0.3 inch) thick.

Loss of available light for interrogation of tissue **328** is a factor to be overcome. Because of the limited wavelengths needed (650–1330 nm) and because of the use of various components to attain, with stability and reproducibly, light of a relative spectral intensity, loss of light is a necessary compromise for the effectiveness of the system. Mirror **320** loses about 10% of the light intended for lens **322**. Lens **322** loses about 20% of the light intended for bundle **326**. Within bundle **326**, more than 40% of the light intended for tissue **328** is lost. It is understood that other schemes such as

allowing light from lens **322** to directly impinge on finger **328** by removing fiber bundle **326** would significantly increase the light but decrease the flexibility of using the device. In all cases, particularly the bundle, the amount of loss is function of the wavelength.

Transmitted Light Reception and Data Acquisition

The optical fiber bundle **326** carrying the selected wavelength light from the lamp **312** has its other end terminating in a finger holder device **327**. Referring to FIGS. **7A** and **7B**, this device **327** preferably comprises two vertical plates of acrylate plastic. The first plate receives the light emitting bundle **326** into an about 1.2 cm (0.5 inch) diameter hole in it, anchored by a set screw, such that the bundle **326** is in a horizontal position with its end protruding on the other side of the plate. This acrylate plate also swivels around a vertical axis located at the hole. A second acrylate plate with a hole similar to the first receives a second bundle **330**, that collects light after transmission through the finger **328**.

While in the embodiment shown in FIG. **7**, a finger is chosen as the mammalian tissue through which light travels from bundle **326** to bundle **330**, it is understood that system **310** and particularly device **327** can be modified to interrogate other types of mammalian tissue. In the case of humans, the device **327** can be reconfigured to an earlobe, the bridge of a nose, or buccal mucosa inside a mouth without departing from the scope of the present invention.

While in the embodiment shown in FIGS. **7A** and **7B**, a transmission system is shown, it is to be understood that the scope of the present invention includes the use of optical reflectance techniques in order to noninvasively predict hematocrit.

The finger holding device **327** allows one operating system **310** to position a finger in it, such that the light emitting bundle **326** from the lamp **312** is in contact with the nail of the finger and the second bundle **330** is in contact with the palmar side of the finger opposite the nail. A screw with a thumbwheel allows the two plates to be brought together so that the finger **328** is squeezed gently in the device **327** between the two bundles **326** and **330**. A swivel on the first plate (not shown) is used so that the bundle **326** face is parallel to the nail of finger **328** due to the fact that the finger **328** is almost wedge-shaped at its extremity.

The collecting bundle **330** is also about 0.9 meter (36 inches) in length and made from high numerical aperature (NA) fibers similar to those of the first bundle **326**. After about 330 cm (12 inches) from the common end (core diameter of about 1.2 cm) of bundle **330** that collects light from the finger **328**, the bundle **330** splits into several smaller-diameter channels that can transmit light in different channels to specialized photodetectors **338** for spectral intensity detection. Each channel and associated photodetector corresponds to a different one of the wavelengths of interest.

Preferably the bundle **330** splits into as many channels **332** as are needed to transmit light to photodetector **338**. As the core area of the bundle **330** at the common end is split into multiple smaller core area channels **332**, using too many channels **332** can further cause a loss of interrogated light. Using too few channels **332** will not provide sufficient number of wavelengths in the system **310**.

The total number of channels **332** and photodetectors **338** depends on the number of discrete wavelengths used in the algorithm to predict hematocrit. The number of wavelengths can range from about 2 to about 12 as described below. The number of wavelengths desirably ranges from about 5 to about 10, with 8 discrete wavelengths preferred. Thus, in a preferred embodiment shown in FIGS. **8A** and **8B** (also shown in FIG. **4**), there are eight channels **332** of bundle **330**, each providing light into a discrete channel.

As seen in FIGS. **8A** and **8B**, because the light incident on the mammalian tissue **328** has unequal intensities at the various wavelengths and because the wavelengths longer than 1000 nm are more strongly absorbed by mammalian tissue, the channels **332** carrying the light intended for analysis at these wavelengths exceeding 1000 nm have a larger core diameter. In channels **332**, two channels **332** have a core diameter of about 7 mm for use with Germanium photodetectors described below for wavelengths greater than 1000 nm, while six channels **332** have have a core diameter of about 2.5 mm for use with silicon detectors, as explained below for wavelengths less than 1000 nm.

All bundles **326** and **330** and channels **332** preferably have a braided cloth covering and enclosed in a stainless steel flexible monocoil sheathing. The end faces of each bundle **326**, **330** and channels **332** are preferably made from stainless steel and utilize medical grade epoxy with an ability to withstand high temperatures (up to 80° C.). All bundles **326** and **330** and channels **332** were made by Fiberguide Industries of Sterling, N.J.

As seen in FIGS. **8A** and **8B**, the eight channels **332** of the collecting bundle **330** terminate at a platten holder **360**. This platten holder **360** is preferably a vertical piece of about 1.2 cm (0.5 inch) thick aluminum with eight holes, four in each of two columns.

As seen in FIG. **9**, on one side of the holder **360** are affixed cylindrical tubular pieces **362** that receive a lens-bundle assembly **364**. Each lens-bundle assembly **364** can be adjusted to fit inside the tubular piece **362** at variable depths and fixed in position by set screws **366**. Each assembly **364** preferably comprises a ferrule **368** that accepts the end face of one channel **332** of the collecting bundle **330**; at the other end of ferrule **368** is a lens **334** (as seen in FIG. **9**), preferably a circularly cut 0.158 cm (1/16 inch) thick acrylate Fresnel lens **334** (as seen in FIG. **9**) held in place by a retaining ring (not shown). All machined parts are preferably made from black anodized aluminum. First, the Fresnel lens **334** is set in the ferrule **368**, and then the channel **332** is inserted into the other end of the ferrule **368**, such that the distance between the lens **334** and the inserted channel **332** face is exactly equal to the focal length of the Fresnel lens **334**.

This arrangement in ferrule **368** produces a shaped beam (e.g. a fairly collimated beam) of light exiting from the Fresnel lens **334**. This lens-assembly ferrule **368** is inserted into the tubular piece **362** on the platten holder **360** and preferably fixed at a distance such that the light striking the photodetectors **338** on the other side of the platten **360** gives a maximum optical signal.

Considering the platten holder **360**, on the side opposite the channels **332**, there is affixed a removable platten **374**, preferably a metal machined plate that is easily screwed on to the platten holder **360** by thumbscrews (not shown) that has machined wells **376**: one opposite each hole that correspond to the eight channel-lens assemblies **362**. In each well fits a module **378**.

Each module **378** preferably comprises an interference filter **336** (as seen in FIGS. **4**, **8**, **9**, and **10**), each generally of a specified, known center wavelength and about 10 nm full width at half power. These filters **336** are about 2.5 cm (1 inch) in diameter and 2 to 5 mm in thickness. The center wavelengths vary as specified. In a preferred embodiment, the filters **336** include the water band in the 1165 to 1330 nm range, the oxyhemoglobin-deoxyhemoglobin isosbestic points in the 800 nm range, the arterial blood oxygen

saturation measurement wavelengths in the vicinity of 660 nm and 910 nm, and the water band wavelengths in the 965 nm range.

As seen in FIG. **10**, each platten contains germanium photodetectors having a 10 mm diameter and 79 mm^2 active area and upper water band filter (1165–1330 nm) **336** in each of the first two wells. The other six wells contain square silicon photodetectors having 100 mm^2 active area and filters **336** for wavelengths under 1000 nm.

The germanium photodetectors are commercially available from EG&G Judson of Montgomeryville, Pa., while the silicon photodetectors are commecially available from Hamamatsu Corporation of Bridgewater, N.J. The interference filters are commercially available from Omega Optical Inc., of Brattleboro, Vt.

In a preferred embodiment, the two, upper water band filters filter for 1300 nm and 1195 nm light plus/minus 2 nm for each. The commercially available Germanium photodetectors used with such filters are Model #RJ16R10MSC sold by EG&G Judson.

Also in the preferred embodiment, the other six filters filter for 972 nm, 1100 nm, 820 nm, 805 nm, 910 nm, and 660 nm light, respectively, plus/minus 2 nm for each filter. The commercially available silicon photodetectors used with such filters are S2387-10.10R sold by Hamamatsu Corporation.

The selection of wavelengths depends on the choice of the equations used to predict hematocrit or other analytes of interest as described above. Preferably, the selection of wavelengths can be each of the Preferred Range wavelengths described in Table 1 above. More preferably, the wavelengths can be the set of 680, 810, 837, 900, 972, 985, 1207, and 1315 nm. Most preferably, the wavelengths can be the set of 660, 805, 820, 910, 972, 1100, 1195, and 1300 nm.

Referring again to FIG. **4**, as stated previously, there is known to be a severe loss of light intended to interrogate tissue **328**. Within tissue **328**, there is considerable light scattering of the interrogating light. Only about 5% of the light entering a finger **328** is collected by bundle **330**. Then bundle **330** splits that diffusely transmitted light from the tissue **328** into several channels **332**, eight in a preferred embodiment based on the number of wavelengths to be analyzed. Lenses **334** and filters **336** also have some loss of light transmitted.

Thus, from lamp **312** to the photodetectors **338**, the drop in wattage of light is severe, to the range of nanowatts of light detected. Unexpectedly, the system **310** can use such miniscule amounts of light in several, discrete wavelengths to provide a prediction of hematocrit. Alteration of system **310** to provide an increased amount of light reaching photodetectors **338** could change the temperature of tissue **328** being interrogated. Thus, the method and apparatus of the present invention unexpectedly achieves delivery of an effective amount of interrogated light to photodiodes for signal processing and prediction of hematocrit.

Referring again to FIG. **10**, all eight photodetectors **338** are connected by shielded wires to a miniature **20** pin connector (not shown) for electrical connection to amplifier **340** (See FIG. **4**). An easily removable electrical connector with a cable attaches the platten **374** to the electronics box containing amplifier **340**. The photodetectors **338** convert the time variant wavelength specific optical signals contained in the light collected from the finger **328** into equivalent electronic signals to be processed by the rest of the system **310**. The output from the photodetectors **338** (photocurrent) goes to the input of the electronics portion of the system **310** through a shielded twisted pair cable; the photocurrent is input to a differential pre-amplifier as described below with respect to FIG. **11**.

Alternatively, the present invention can replace the broad band light source **312**, disc modulator **314**, fiber bundles **326** and **330** and optical wavelength filters **336** and Fresnel lenses **334** with small solid state modulated monochromatic light sources such as light emitting diodes, super light emitting diodes, laser diodes and similar devices in order to achieve a more compact and less mechanically and optically cumbersome system **310**.

Signal Processing

FIG. **11** shows an electrical schematic diagram of the amplifier and filter electronics **120** shown in FIG. **2** corresponding to one of the wavelengths of interest. Each set of amplifier and filter electronics **120***a–n* are preferably implemented with the identical circuitry as shown in FIG. **11**. However, in some circumstances it may be desirable to tune the electronics to the specific type of photodetector used.

In FIG. **11**, the optical radiation from the fiber bundles is incident on a photodetector **338**, which converts the optical radiation into a corresponding photocurrent. The photodetector is connected to the inputs of an instrumentation amplifier **134** via individual, shielded twisted pair wires **132**. The cable shields are connected to chassis ground to reduce common mode noise. The instrumentation amplifier **134** is comprised of a differential pre-amplifier and a precision device (INA106). The differential pre-amplifier configuration also results in very high rejection of common mode signals, and includes two operational amplifiers U1 and associated circuit components. A 167K ohm feedback resistors is coupled to the inverting input of each operational amplifier U1. An 24nF capacitor in parallel with each feedback resistor reduces the high frequency content (i.e., reduces high frequency peaking) of the signal at the output of each operational amplifier U1. The cutoff frequency of this RC pair is 40.8 Hz. 10K ohm resistors connected to the non-inverting terminals of the operational amplifiers U1 reduce noise by compensating for unequal operational amplifier bias currents. The output of the pre-amplifier stage is a differential signal comprised of a negative voltage at the output of the top operational amplifier and a positive voltage at the output of the bottom operational amplifier.

In the preferred embodiment, low noise operational amplifiers are used for the pre-amplifiers. Low current noise operational amplifiers are preferred for high shunt resistance photodetectors, while low voltage noise operational amplifiers are preferred for low shunt resistance photodetectors.

Immediately following the pre-amplifier stage is a precision device (INA106) which converts the differential signal from the preamplifier stage into a single ended electrical output. When properly configured, this device subtracts the output of the top operational amplifier from the output of the bottom operational amplifier, resulting in a conversion of the two individual signals to one voltage signal. This device also amplifies the converted signal by a factor of ten.

Two operational amplifier circuits U2 configured as a fourth order low pass Butterworth filter **136** further reduce the high frequency content of the signal. The low pass filters are preferably comprised of two consecutive second order Butterworth filters U2, each having a cutoff frequency of 33.8 Hz. The frequency response of the combined filters U2 is a fourth order low pass filter with a cutoff frequency of 33.8 Hz.

An RC filter, comprised of **10** ohm resistor and capacitor **150**, further low pass conditions the signal. The RC filter ground is tied to the ground of the processing module **500**. The resistor, R, also serves to decouple the distributed

capacitance of the cable that connects the electronics to the processing module **500**. The cable is 360 degree shielded with the shield tied to ground at the ground of Butterworth filter **136**.

The processing module **500** is preferably implemented with a Keithley-Metra Byte Analog to Digital Converter board and a Toshiba 3200 portable computer. The computer includes a 80386 microprocessor augmented by the Keithley-Metra Byte analog-to-digital (A/D) converter board. The processing module **500** receives the analog signal and converts it to a digital representation via the A/D board.

Samples of the digitized plethysmographic waveforms are preferably captured by the CPU during the 3.33 milliseconds of complete lamp filament exposure (the sampling window). As described above with respect to FIG. **6**, the SHUTTER OPEN signal is used to synchronize the CPU such that the CPU samples the photoplethysmographic signals of all wavelengths of interest during the 3.33 millisecond sampling window. The SHUTTER OPEN signal corresponds to the time at which the pie-shaped sectors of disc **314** just begin to open over lamp **312**. After receipt of the SHUTTER OPEN signal, the CPU waits for a delay corresponding to the time between receipt of the SHUTTER OPEN signal and the time when the lamp filament is completely exposed. After that delay has elapsed, the CPU generates the signal DELAY BURST TRIGGER, shown in FIG. **12**. Upon receipt of the DELAY BURST TRIGGER signal, the trigger control circuit **116** of FIG. **12** generates a series of burst pulses.

Upon receipt of each burst pulse, the CPU samples the waveform for one of the wavelengths of interest. In the preferred embodiment, for example, eight burst pulses, each corresponding to one of the eight wavelengths of interest, are generated by trigger control module **116** over a period of about 60 microseconds. Upon receipt of each burst pulse, the CPU samples the corresponding waveform of interest.

Thus, in the preferred embodiment, all eight waveforms are sampled in a serial fashion over a time frame of approximately **60** microseconds during each 3.33 milliseconds of complete lamp filament exposure. Although all wavelengths are not sampled simultaneously, the samples are taken over a time frame of about 60 microseconds in the preferred embodiment. This 60 microsecond time frame is very small when compared to the time frame of any relevant photoplethysmographic information in the signal of interest, such that for practical purposes, the samples are essentially captured "simultaneously". However, it shall be understood that the waveforms for all wavelengths of interest could also be sampled in parallel without departing from the spirit and scope of the present invention.

Data Storage

After the waveform samples are captured, the raw data is converted to volts and is stored in two-dimensional arrays **210** such as that shown in FIG. **13A**. This structure is an array of pointers **212**, one for each channel, to an array of raw data such as array **214**. In the preferred embodiment, the total number of channels is stored in the variable "Numbchans" and in the preferred embodiment is equal to eight. Also in the preferred embodiment, each array can store up to **512** data points per channel, so the variable "ArraySize" in FIG. **13A** is equal to 512 in the preferred embodiment.

The memory used for the actual sampling is preferably configured to act as a ring buffer. The DMA buffer used by the Keithley-MetraByte A/D card is split into two blocks. Using the DMA, the processing control procedures described below read from one block of DMA while writing into another. When one block has been completely written, post-processing is performed on that block of data. All of this is accomplished while the CPU continues to sample data into the next block of dynamic memory.

Processing Control

FIG. **14** shows the process by which a user is able to configure several system parameters. First, while it is possible to visually evaluate the quality of the waveforms obtained, it is a feature of the present invention to provide and apply repeatable, quantifiable measures which evaluate the waveforms and produce numerical "figures of merit" which are displayed to the screen. To this end, the user is able to set quantifiable performance indices against which the waveforms are evaluated for their ability to convey an accurate prediction of hematocrit. In the preferred embodiment, the two parameters used for this are the peak to peak voltage of two user configurable channels, and the coefficient of variation of a user configurable parameter.

In general, the two channels having the lowest pulsatile power (and hence a low signal to noise ratio) are specified for the former purpose at blocks **618** and **620**. If the peak to peak amplitude of these channels falls below the user specified minimum, a REJECT message is displayed, indicating to the user that further data should be obtained.

The other performance index of the preferred embodiment is the coefficient of variation of at least one H Value (described in more detail below). If the CV of the specified H Value exceeds the limit set by the user at blocks **622** and **624**, the REJECT message will be displayed. If both the peak to peak amplitudes and the CV are within the user specified limits, an ACCEPT message is displayed (see FIG. **28**).

FIG. **14** also shows that the user is also able to select which channels are to be sampled at block **606**, and which channel is to be used for peak and valley detection at block **608**. This designated "peak channel" is typically the isosbestic channel as described in more detail below with respect to FIGS. **19A** and **19B**.

If upon visual inspection the displayed waveforms are excessively noisy or contain considerable drift, or where the displayed peak to peak amplitudes and/or coefficient of variation measure are unacceptable, the user may, on a channel by channel basis, choose to process the signals further in an attempt to improve the confidence in the hematocrit prediction. When the signals for one or more channels appear excessively noisy, the user may elect to smooth the raw data for those channels before the signals are further processed. In doing so, the user selects which channels are to be smoothed and the order of the tap filter that is to be used on the raw data for the channels selected at block **610**.

On channels where considerable drift or baseline trend is present, the user may, on a channel by channel basis, detrend those channels at block **612**. The detrending procedure is described in more detail below with respect to FIG. **16**.

On channels having a low signal to noise ratio (SNR), the user may elect, on a channel by channel basis, to template match the low SNR signals to a higher SNR signal (usually the designated peak channel) at block **614**. The template matching procedure is described in more detail below with respect to FIG. **20**.

The user is also able to input the equations which are used in the hematocrit prediction at block **616**.

FIG. **15** shows a simplified flow chart of the control software for the present apparatus for noninvasive determination of hematocrit. A detailed computer program listing of the control software can be found in the attached Microfiche Appendix.

As shown in FIG. **15**, the CPU first captures the raw data for each of n channels (eight in the preferred embodiment). The raw data is converted to volts and is stored in memory as described above. Control block **408** will smooth and/or detrend selected channels if so configured by the user as described above with respect to FIG. **14**. Next, the location of the peaks and valleys of the designated "peak channel" are computed and stored by control block **410**. In control block **412**, the amplitude, or voltage value, of the peaks and valleys for the photoplethysmographic waveform for each wavelength of interest are computed.

Once the values of the peaks and valleys for each channel are known, a pseudo-absorbance for each peak/valley pair is calculated in control block **414**.

Also, the values of these pseudo-absorbances are combined in control block **414** to compute the H Values, which are combined in a prediction of the hematocrit in control block **418**. The peak to peak voltages (the AC component) of the user selected channels, most preferably the two channels with the lowest pulsatile power and/or lowest signal to noise ratio, are also calculated. These peak to peak voltages are used by the present system as described above to reject the data if the peak to peak value falls below a user settable threshold.

If the data is not rejected for the reasons cited above and because of patient movement artifact, instrument disconnection, or unacceptable coefficient of variation, as described below, control block **420** computes the average hematocrit, average oxygen saturation and an average coefficient of variation.

Whether or not the data is rejected, the waveforms and results are displayed at control block **422**. The entire process continues while the CPU continues to sample each channel until the user signals to quit sampling data.

Detrending

Although non-invasive measurement of hematocrit can be accomplished by measuring the transmission of light through blood perfused tissue at appropriate wavelengths, in practice these measured signals can be corrupted by artifact due to respiration and movement, particularly when collected in a clinical environment. This artifact is a form of low-frequency noise that can also be described as data trend or baseline drift. When this drift or trend is significant the hematocrit measurement is subject to error. The present invention therefor provides an order-adaptive filter for de-trending data to improve the accuracy and precision of hematocrit measurement via photoplethysmography.

The de-trending process itself is straightforward and the processing steps are shown in FIG. **16**. First, the average pulse period is found over the data interval of interest. Typically, the data is detrended in blocks of from 4 to 8 pulse periods. The measured pulse period 'x' in seconds corresponds to N discrete time steps in the sampled waveform. More precisely, N='x'·fs where fs is the sampling frequency in Hz (100 Hz in the preferred embodiment. N is then rounded to the nearest odd integer. Next, the pulsatile signal is filtered with a Moving Average (MA) filter of length N using the following equation:

$$\mu(n) = 1/N \sum_{k=n-\frac{(N-1)}{2}}^{k=n+\frac{(N-1)}{2}} x(k)$$

The detrended signal x*(n) is then obtained by subtracting the filtered signal from the original signal using the equation:

$$x\cdot(n)=x(n)-\mu(n)$$

By tuning the MA filter to the pulse period, the moving average is always calculated over a pulse period. This blocks the pulsatile variation from leaking into the baseline waveform μ(n) leaving only the true drift or trend signal component. When the filter length N (averaging interval) is equal to the pulse length, the pulse frequency and its harmonics are essentially nulled. This approach has a significant advantage in that nulling of the pulse frequency is guaranteed. Other filtering approaches will not necessarily null the pulse frequency and therefore their baseline waveforms may be contaminated with residue of the pulsatile waveform. Additional advantages of this MA filter include ease of implementation, unconditional stability, and linear phase response.

If the data has been detrended, the calculation of H Values for detrended data requires that the intensity values be calculated in a specific manner. The detrended peak and valley levels I^*_p and I^*_v are determined from the detrended signal x*(n). Then the baseline component I_{BL} is added back on in order to provide the appropriate offset:

$$I_p=I^*_p+I_{BL}$$
$$I_v=I^*_v+I_{BL}$$

The particular baseline value for a peak-valley combination is the value of μ(n) that is halfway between the peak and valley time indices. For example, if valley I occurs at time p and peak I occurs at time q then I_{BL} is given by:

$$I_{BL}=\mu\left(\frac{q-p}{2}\right)$$

It shall be understood that these peak and valley intensity values are not the same as those calculated from the original data. It may appear that the baseline value is removed and then simply added back on again. This is not the case. When the data is de-trended, the MA value μ(n) that is subtracted from the peak is different from the MA value subtracted from the valley, because μ(n) is a time-varying waveform. However, when the intensity values are reconstructed, the baseline value is the same for both the peak and the valley.

Table 2 shows H Value data for two patients. The asterisk on the H Value indicates that it is calculated on detrended data. Note that in all cases the de-trended H Values have a lower coefficient of variation.

	Patient A								
	hv1	hv1*	hv2	hv2*	hv3	hv3*	hv4	hv4*	Wavelength Ratio
Mean	0.2409	0.2518	0.0360	0.0376	0.2409	0.2517	1.3220	1,3106	1–3
SD	0.0485	0.0205	0.0072	0.0030	0.0485	0.0205	0.0434	0.0179	
CV	20.1261	8.1553	20.0565	8.0755	20.1261	8.1610	3.2848	1.3680	

-continued

Mean	0.3357	0.3499	0.2761	0.2787	0.3356	0.3498	1.2299	1.2203	1–4
SD	0.0620	0.0277	0.0509	0.0226	0.0620	0.0277	0.0369	0.0163	
CV	18.4633	7.9080	18.4207	7.8579	18.4642	7.9137	2.9977	1.3394	
Mean	1.2417	1.2378	1.5355	1.5308	1.2418	1.2380	0.9551	0.9554	2–4
SD	0.0301	0.0260	0.0372	0.0323	0.0301	0.0261	0.0043	0.0043	
CV	2.4205	2.1026	2.4237	2.1115	2.4241	2.1065	0.4549	0.4535	

Patient B

	hv1	hv1*	hv2	hv2*	hv3	hv3*	hv4	hv4*	Wavelength Ratio
Mean	0.2986	0.2992	0.3391	0.3399	0.2985	0.2991	1.2938	1.2926	1–3
SD	0.0243	0.0111	0.0272	0.0137	0.0243	0.0111	0.0183	0.0143	
CV	8.1384	3.7115	8.0129	4.0221	8.1349	3.7087	1.4146	1.1091	
Mean	0.2587	0.2595	0.1459	0.1463	0.2586	0.2593	1.3405	1.3390	1–4
SD	0.0217	0.0106	0.0121	0.0066	0.0217	0.0106	0.0209	0.0179	
CV	8.4011	4.0954	8.2977	4.5419	8.3992	4.0950	1.5586	1.3346	
Mean	0.8367	0.8375	1.0921	1.0932	0.8365	0.8374	1.0449	1.0446	2–4
SD	0.0120	0.0108	0.0159	0.0148	0.0120	0.0108	0.0044	0.0041	
CV	1.4333	1.2900	1.4604	1.3564	1.4386	1.2951	0.4179	0.3905	

The plot shown in FIG. **17** shows the three relevant signals for a typical case. The original signal x(n) is shown by a solid line, the MA filtered signal μ(n) shown by a dashed line, and the de-trended signal x*(n) shown by a dot-dashed line. In FIG. **17**, the de-trended signal x*(n) has been offset so that the three graphs can be shown on the same page. It shall be understood, however, that the de-trended signal is zero-mean.

Adaptive Peak and Valley Detector

Once the sampling of each channel is complete and the raw data is stored and detrended, the present invention processes the captured data to estimate hematocrit and other characteristics of interest. The preferred method used to determine the correlation between absorbed light and hematocrit is the ratio of the photoplethysmographic values at the peak and valley for an individual heartbeat. An exemplary photoplethysmograph **210** is shown in the upper portion of FIG. **18**. One full heartbeat is indicated by reference numeral **208**. It is very important that the actual peaks, such as peak **204**, of the waveform **210** are detected and the false peaks due to noise and the dichrotic notch **206** are ignored. A dichrotic notch **206** is created by the closure of the aortic valve and can be more pronounced in some individuals. In some individuals, the dichrotic notch is very weak during sampling. The present invention provides a real time adaptive peak and valley filter which determines the actual peaks **204** and valleys **202** of the waveform **210** while filtering out any false peaks and valleys. This is an important feature of the present invention as the underlying pulsatile signal, and hence the associated peaks and valleys, are highly variable and potentially non-periodic.

FIG. **19A** shows the process **410** by which the actual peaks and valleys are found. First, the sampled waveform is differentiated. An exemplary differentiated photoplethysmographic waveform **216** is shown in the lower portion of FIG. **18**. An 11 tap smoothing filter is applied to the differential waveform at block **632**. Next, all peaks in the differentiated waveform are found, and the value of the maximum peak in the differentiated waveform, peak **218** in FIG. **18**, is determined at block **638**. A threshold value is calculated for comparison purposes at block **640**. In the preferred embodiment, the threshold value is 50% of the value of the maximum peak **218** in the differentiated waveform. This threshold value is also shown on the differentiated waveform in FIG. **18**. Valid peaks in the differentiated waveform are determined from invalid peaks in the differentiated waveform by comparing the actual value of each peak with that of the threshold value at block **642**. If the peak in question has a value less than that of the threshold value at block **644**, that peak is determined to be due to noise or the diacrotic notch and is therefore an invalid peak at block **648**. Any peak that is determined to be part of an incomplete pulse is also as designated invalid to avoid false peaks. If the peak in question has a value at block **644** greater than the threshold value, that peak is a valid peak at block **646**.

After determining valid peaks in the differentiated waveform at block **649**, the actual peaks and valleys for the original waveform are determined as shown in FIG. **19B**. The differentiated waveform is scanned looking for points at which the differentiated waveform amplitude equals zero, such as point **214** in FIG. **18**. This corresponds to the point where the slope of the actual waveform equals zero, thus, the location of an actual peak or a valley. The process starts at a peak in the differentiated waveform at block **652**, for example, peak **218** in FIG. **18**, and examines data points to the right of this peak at block **654**. The zero crossing point is determined to be the data point at which an actual peak at block **656**, **205** in the example of FIG. **18**, occurs. If this point has been already found from previous peak candidates the duplicate peak is discarded at block **658**. Otherwise, the location of the actual peak is stored in a one dimensional array **220** at block **660** such as that shown in FIG. **13B**. This process is continued for all candidate peaks through blocks **664** and **662**.

The right portion of FIG. **19B** shows the process by which valid valley locations are found. After all peaks are tested, the valleys are found by scanning to the left of a determined peak at blocks **666** and **668** (such as peak **204** in FIG. **18**) in the differentiated waveform for the zero crossing point at block **670** (point **212** in FIG. **18**). This zero crossing point is determined to be a valley (valley **202** in FIG. **18**), and this valley location is also saved for further calculations at block **674**. The process continues through blocks **678** and **676** for all candidate valleys.

The locations of all valid peaks for each wavelength of interest are stored in a one-dimensional array such as that shown in FIG. **13B**. The number of elements in this array is equal to the maximum number of valid peaks (100 in the preferred embodiment) which can be stored. The location of each actual peak is stored in the array. For example, if a peak is determined to exist at the 23rd and 60th data point, the array would contain 23 and 60. The same is true for each

valley found. If a valley is determined to be at the 19th and 48th data points, then a similar array for storing valley locations would contain 19 and 48, etc.

Peak and Valley Value Determination

Once the location of the peaks and valleys is determined and stored, the voltage values or amplitude of the peaks and valleys are determined.

For each wavelength band there is a time dependent voltage level corresponding to the energy received in that band. The correlation between voltage value and location is maintained in the array where the raw data is stored.

Where the signal levels are relatively high, i.e., a high signal to noise ratio (SNR), a direct reading of the raw data of the voltage value of a peak or valley of a particular location can be confidently made. Due to differences in absorption and, scattering for the various wavelengths, however, the pulsatile signals for some channels have weaker signal to noise ratios than others. The underlying signals in the absence of noise all have the same underlying shape, since each channel will yield a photoplethysmograph having the characteristic shape of the pumping and flowing bloodstream. The only difference between signals for different channels is their pulsatile amplitude and DC offset. It is this amplitude and DC offset that are critical to the accurate measurement of hematocrit. However, on low SNR signals the peak and valley values contain significant noise and this inaccuracy leads to error in the hematocrit calculation. The present invention therefore provides a technique for improving the measurement of amplitude of the peaks and valleys for channels with low SNRs. This technique is called "template matching" and is shown in FIG. **20**.

FIG. **20** shows the present template matching technique **412** for finding the values of peaks and valleys at low SNRs. In the preferred embodiment, the user is able to select whether template matching should be performed on a channel by channel basis.

For example, if the peak to peak voltages of the user selected channels falls below the specified threshold, the user may infer that template matching may be appropriate.

The present template matching technique **412** has the advantage that peak and valley voltage measurement need only be performed on the wavelength with the highest SNR (in the preferred embodiment, this is most typically the isosbestic channel, corresponding to a wavelength in the range 800–840 nm). The high SNR wavelength is scaled to determine the values of peaks and valleys at wavelengths having low SNRs.

For purposes of illustration and the processing steps shown in FIG. **20**, assume channel A is the high SNR signal and channel B is a low SNR signal. Exemplary waveforms of signal A and signal B are shown as waveforms **510** and **512**, respectively, in FIG. **21A**. The first step is to band pass both signal A in block **680** and signal B in block **684**. The band passed waveforms of signal A and signal B are shown in FIG. **21B** as waveforms **518** and **520**, respectively. The linear phase band pass filter removes the DC offset, rejects high frequency noise and detrends the signals such that only the AC or pulsatile portion of the waveform remains.

Both signal A and signal B are also low pass filtered in blocks **682** and **686**, respectively. The low passed waveforms of signal A and signal B are shown in FIG. **21C** as waveforms **514** and **516**, respectively. The low pass filter rejects the AC component and passes the DC offset and any trend or low frequency noise such as respiratory artifact. The signal $\mu(n)$ described above with respect to FIG. **16** can be used for the low passed signal.

Next, a least square fit between band passed signal A and band passed signal B is calculated. This consists of scaling band passed signal A such that it is the best match for band passed signal B in the least square sense at block **688**. As previously stated, the signals for all channels of interest have the same underlying pulsatile waveform. The least square fit approach of the present invention simply exploits this fact. The advantage is that the location and amplitudes of the peaks and valleys need only be performed on the highest SNR signal at blocks **690** and **692**. The amplitudes of the peaks and valleys for the lower SNR signals are found by scaling the high SNR peaks and valleys with the scale factor from the least square fit optimization.

In the preferred embodiment, the scale factor is calculated in a block fashion. The block approach operates on signals that are segmented into blocks of data or vectors, as follows:

Let

$x_A(n)$=high SNR signal;

$x_B(n)$=low SNR signal;

$x^*_A(n)$=band passed high SNR signal;

$x^*_B(n)$=band passed low SNR signal;

$\mu_A(n)$=low passed high SNR signal;

$\mu_B(n)$=low passed low SNR signal; and

γ=scale factor,

where $x^*_A(n)=x_A(n)-\mu_A(n)$.

The least square minimization is defined as

$$\min_{\gamma} \|x^*_B(n) - \gamma x^*_A(n)\|^2$$

and the solution is given by

$$\gamma = \frac{x^{*+}_A(n)x^*_B(n)}{x^{*+}_A(n)x^*_A(n)}$$

where $x^{*+}_A(n)$ and $x^{*+}_B(n)$ are the transpose of $x^*_A(n)$ and $x^*_B(n)$, respectively.

The "clean" or noise reduced version of $X_B(n)$ at block **694** then becomes

$$\begin{aligned} x_{B(clean)} &= \gamma(x_A(n) - \mu_A(n)) + \mu_B(n) \\ &= \gamma(x^*_A(n)) + \mu_B \times (n) \end{aligned}$$

FIG. **21D** shows the "clean" version of signal B as waveform **522**.

Note that the clean version of $x_B(n)$ is a linear (affine) transformation of $x_A(n)$. Therefore, the peaks and valleys of the noisy vector $x_B(n)$ can be calculated from the peaks and valleys of the clean vector $x_A(n)$. In a multichannel system, this means that the peaks and valleys (both location and amplitude) need only be calculated for the channel with highest SNR (typically the isosbestic channel). The values of the peaks and valleys for those channels having low SNRs can be calculated using the above affine transformation.

Although the preferred embodiment is described as calculating the scale factor in block fashion, it shall be understood that the scale factor could also be calculated in many other ways, such as by recursion, without departing from the scope of the present invention.

In practice, there are several options for adding the low pass filtered signals μ_A and μ_B back into the AC pulsatile signals before calculating hematocrit. In the simplest case, the low pass signals may be added back to the AC signal without further processing. If the baseline value drifts considerably during a pulse, the baseline waveform could be set to the average value during that pulse. This would produce a stair-step DC waveform if considerable drift was present.

In U.S. Pat. No. 4,869,254, the equivalent DC value is set to either a peak or valley value of the unfiltered waveform. Then a peak or a valley value is adjusted to correspond to the DC shift. This is an alternative approach.

Determination of Prediction Equation

Using the MAXR statistical analysis method described above, and selecting from the Preferred Range of wavelengths described above in Table 1, and using either HV1 or HV2, the following equations can be used alternatively in the direct prediction of hematocrit of humans, noninvasively and transcutaneously:

$$HCT=55.3(HV1_{1207,660})-563(HV1_{1302,805})+596(HV1_{1302,910})-58(HV1_{837,805})+93.2$$

This equation was developed using data collected from about 53 healthy individuals, chronic renal failure patients, and postoperative patients to form the training set. FIG. **22** shows a calibration plot with an R^2=0.83 and all hematocrit values within +/−5 hematocrit percent. To validate this prediction equation, the hematocrit of 10 new individuals was predicted noninvasively and transcutaneously using the apparatus and method described above. The prediction equation for these 10 individuals was plotted and is shown as FIG. **23**. All prediction points fell within +/−3 hematocrit percent.

Another technique of validating the prior equation of FIG. **22** is to use a statistical program that removes one datum and predicts its value based on a regression equation derived from the remaining data points. This procedure is repeated for all data points in the set. The results are shown in FIGS. **24**A and **24**B.

The following equation below used the apparatus and method described above, HV2, MAXR, and the most preferred set of wavelengths: 660, 805, 820, 910, 972, 1100, 1195, and 1300 nm.

$$HCT=-54.85(HV2_{1300,1100})-34.72(HV2_{1195,972})+26.38(HV2_{1195,660})-7.418(HV2_{972,660})+3.105(HV2_{1100,910})+71.03$$

A complete calibration/validation sequence was run, using about 40 healthy volunteers and 25 chronic renal failure patients to provide a wider range of actual and training hematocrit values to establish the training set. FIG. **25** shows the calibration plot using the above equation with an R^2 of 0.85 and virtually all hematocrit values within +/−5 hematocrit percent. This equation was validated using the cross-validation, one point at a time method, which gave a prediction plot seen in FIG. **26** with an R^2 of 0.80 and only a slight increase in the spread of hematocrit values. FIG. **27** shows the results of an on line prediction performed by programming the coefficients of the above equation into the computer. Volunteer human subjects' photoplethysmographs were recorded and individual hematocrit values were displayed and recorded "online". As usual, venous blood samples withdrawn from the subjects were analyzed with a cell counter reference method. The results are displayed in FIG. **26**.

Once the prediction equation is established, the geometry of the device shown in FIG. **4** needs to remain fixed. Alteration of the device requires recalculation of the prediction equation.

The sensitivity of the above is dependent upon changes in individual H Values, shown in the sensitivity equation below.

$$Sensitivity=[-54.85-34.72+26.38-7.418-3.105]^T$$

e.g., a change of 10% in $HV2_{1300,1100}$ results in a change of 3 HCT %.

Another example of a calibration plot is shown in FIG. **28**. Data was taken on subjects and the data set reduced to include those with H Values corresponding to a H Value Coefficient of Variation of less than 8 percent. Statistical analysis using a stepwise regression was used, resulting in the following multiple wavelength calibration equation shown below with R^2=0.97.

$$HCT=-126(HV4_{805,660})-573(HV4_{1302,680})-1366(HV4_{1302,837})+1966(HV4_{1302,805})-643(HV4_{680,837})-1209(HV4_{837,910})+2297(HV4_{805,910})-123(HV4_{978,680})-259(HV4_{805,905})+1483.$$

It is understood that although nine wavelength ratios are used, a correlation coefficient R^2 of about 0.9 can obtained with only four of the nine ratios, i.e., the ratios vary in their contribution to the final correlation coefficient.

It is also understood that a cross validation of this equation may not produce hematocrit predictions of satisfactory accuracy because the small number sample of data points do not adequately represent the population. Nevertheless, this equation shows that data collected over a larger population with care to provide a low H Value coefficient of variation should provide a hematocrit prediction with low error.

Yet another example of a calibration equation was obtained with a data sample of a percent H Value Coefficient of Variation of less than 8, n (number of data points)=24, and R^2=0.92, utilizing the MAXR procedure to produce the following equation.

$$HCT=-17.6(HV_{1163,820})-166(HV2_{820,910})+22(HV2_{1302,805})+50.4(HV2_{805,910})+15.2(HV2_{978,680})+22.$$

Determination of Confidence Level Calculation of Coefficient of Variation

Once the hematocrit is predicted, a measure of the level of confidence of the prediction is desired. The reason for this is that there is uncertainty in the calculation. This variability, while ignored in many devices, can be used to indicate the confidence of the measurement.

One such method of estimating the confidence is to compute the distribution of a measured parameter about the mean a measured parameter. As an example, assume the measure of parameter measurement is normally distributed about the mean (v) with a standard deviation (σ). This is given by:

$$N(v,\sigma)=e^{-(x-v)^2/(2\sigma^2)}$$

$$\text{where } v=\frac{1}{n}\sum_{i=1}^{n} HV[i]$$

$$\text{and } \sigma=\left\{ 1/n \sum_{i=1}^{n} (HV[i]-v)^2 \right\}^{0.5}$$

Assuming a distribution about a central value, a valuable measure of the distribution of data about that value is the standard deviation (σ) or the standard deviation normalized to the mean and converted to a percentage, assuming a normal distribution. When the standard deviation is normalized to the mean the measurement is called the coefficient of variation (CV). The CV is computed as follows:

$$CV=\frac{\sigma}{v}\times 100\%$$

The CV provides an average of the measured parameter and number indicative of the distribution of the measured parameter about the average. For example, for a normal

distribution, a CV=5% means that 68.27% of the measured parameter (the data +/−1 standard deviation) lie in a band +/−5% of the measured parameter value.

For purposes of the present invention, the CV of several different parameters are applicable. One is the coefficient of variation of one or more H Values used to predict hematocrit. The preferred H Value for coefficient of variation purposes corresponds to the ratio of an isosbestic wavelength and the upper water band. Since an isosbestic wavelength and the upper water band are typically the strongest and weakest signals, respectively, the corresponding H Value is preferred since that ratio will generally give the worst case coefficient of variation.

Another useful measure which can be used is the CV of hematocrit prediction.

The significance of this calculation is not limited to normal distributions of data and coefficient of variation. In fact, the distribution about the mean of the preferred H Value in the present invention is not a normal distribution. However, the calculated CV is nevertheless a reliable indicator of the confidence level of the hematocrit prediction.

The CV of the preferred H Value is displayed as shown in FIG. **28**. If this CB exceeds the threshold specified by the user as described above with respect to FIG. **14**, a "REJECT" message will be displayed. If the CV does not exceed the user specified threshold, an ACCEPT message, as shown in FIG. **14**, is displayed. The displayed CV value, in combination with the ACCEPT or REJECT message and peak to peak voltages which are also displayed as described herein, allow the user to make a value judgment concerning the confidence of the hematocrit prediction.

Display of Waveforms and Results

The waveforms and computed results such as hematocrit, coefficient of variation, oxygen saturation, peak to peak voltages, etc. are displayed at control block **422** of FIG. **15**.

FIG. **29** shows an exemplary screen display of the apparatus of the present invention. The, display includes a plot of channels **1–4**. The waveforms are plotted as amplitude (volts) vs. time (hundredths of seconds). Also displayed are the locations of the peaks and valleys, the hematocrit prediction (HCT) for the currently displayed screen, the average hematocrit over all screens obtained, the coefficient of variation of the preferred H Value ($HV_{1,4}$ in FIG. **28**). The oxygen saturation and peak to peak voltages of channels **1** and **2** are also shown on the exemplary display of FIG. **29**.

The minimum peak to peak values (AC pulsatile component) of two channels and maximum CV of the H Values are configurable by the clinician as described above with respect to FIG. **14**. If, the peak to peak values are below the minimum, then a REJECT message is displayed. Similarly, if the CV is greater than the user specified threshold, then the data set is rejected. Thus, when used together, the displayed CV, Peak to Peak measurements and the ACCEPT/REJECT message form a figure of merit measurement which can be used to assess the quality of the hematocrit prediction.

FIG. **30**A shows the process by which waveforms are displayed to the screen during continuous capture of photoplethysmographic data. There are two display modes, normal display mode and save mode.

When in normal display mode, a number of saving and displaying options are available through a combination of keystrokes. The user is allowed to change the actual channels that are displayed while sampling (due to screen size limitations, a maximum of five waveforms can be displayed at a time while sampling). The user can select "autotoggle", at blocks **709** and **172** during which the system will display different sets of channels on each loop through the procedure. For instance, if there are eight total channels after the first 512 samples for each channel are obtained, a group of channels including the designated peak channel, will be displayed. When the next complete sample is obtained, a group of four channels will be displayed. The second group of four channels will include the four channels which were not displayed the first time, and the designated peak channel. Preferably, the designated peak is always displayed for reference purposes.

The user can also manually toggle the display by pressing "T" or "t" at block **170** to toggle the channels to be displayed at block **714**. Every time the user enters a "t" or "T", the next displayed channels will be the previous undisplayed channels. Manual toggling basically performs the same function as autotoggle except that the user indicates when the display should be toggled.

The procedure also constructs a basic menu of commands at block **718** the user can enter to manipulate both the screen output and actual saving of the captured data. This menu is displayed at block **720** on the screen as shown in FIG. **28**.

Once one has entered "S" or "R" at block **704** to enter save mode, a different display is shown. In save mode, only two channels are displayed on the screen. The first channel is always the channel that was used to find the peaks and valleys. The second channel is user selectable at block **706**. While in save mode the user can also enter a "Q" to quit saving at block **716**.

An actual plot at block **722** to the screen consists of one page of data or 512 data points in the preferred embodiment. However, a complete waveform will consist of many more stored data points. The procedure of FIG. **30**B allows the user to interactively scroll back and forth through the file. The user can page backward through the waveform by pressing "B" or "b", or forward through the waveform by pressing "N" or "n" at block **736**. The user is also able to print a waveform or waveforms at blocks **742** and **750** or interactively edit the waveforms by deleting pages (defined as 512 data points) from the plot at blocks **738** and **746**. An undelete option is also available for those instances where pages are mistakenly deleted at blocks **740** and **748**.

Prediction of Other Analytes of Interest

As mentioned previously, other analytes of interest in mammalian blood can be predicted using the method and apparatus of the present invention. The most common prediction conventionally employed is that of oxygen saturation. Because some of the eight wavelengths preferably employed can provide a ratio of wavelength absorbances at 660 nm and 910 nm, percent oxygen saturation can be readily predicted modifying to or adding electronic circuitry known to those skilled in the art. In that instance, a single apparatus can be used to predict both hematocrit and percent oxygen saturation, providing in a single noninvasive, transcutaneous device the ability to predict accurately and precisely two of the more important "blood gases" used in diagnosis or monitoring of the physiological conditions of mammalian patients.

Also as mentioned previously, one can combine a prediction of hematocrit with a prediction of methemoglobin to noninvasively monitor the physiological condition of mammalian blood stored for transfusion into mammalian patients.

In an alternative embodiment of the present invention, it was observed that stored blood ages in a manner that can be measured by the changes in hematocrit content and in methemoglobin. Specifically, it is an aspect of the present invention that the content of methemoglobin rises and

hematrocrit also increases as stored blood ages. Those changes can be quantified according to the techniques of the invention as applied to a noninvasive interrogation of a storage bag of blood. In this embodiment, due to the desire for noncontact with the stored blood, the same considerations of noninvasiveness prediction apply. For example, the mean cell volume of a constant volume of blood stored at 4° C., as measured after equilibration at room temperature over an interval of two weeks increased from 86.9 cubic micrometers to 100.7 cubic micrometers.

Specifically, the quality of stored blood can be assessed by predicting changes in hematocrit and methemoglobin using the same wavelengths as described above for hematocrit and adding one or more or some combination of the wavelengths of about 420 nm, 540 nm, 580 nm, 630 nm, and 1224 nm; the individual wavelengths may represent peaks and valleys or the isosbestic point(s) of the absorption spectrum of methemoglobin (in its acid and base form) and the spectra of various forms of hemoglobin such as oxydeoxy-, carboxy-, and sulfhemoglobin, to predict methemoglobin. The use of the same statistical analysis can be employed, with a possible equation used as follows:

$$HCT=\alpha' HV_{n,y}+\beta' HV_{n1,y1}+\chi' HV_{n2,y2}+\delta' HV_{n3,y3}+\epsilon' HV_{n4,y4}+\phi$$

where the terms have the same meaning as in Equation 5 above but now in addition employ the above cited wavelengths for methemoglobin to form the HV ratios.

It is important in this embodiment when using the blood in the storage bag of blood to pulsate the blood in order to generate peaks and valleys for proper calculation. One method is to make two measurements, one at each of two different distances between the light source and light collecting fibers. The storage bag of blood is between the fibers.

The utility of this embodiment of the present invention can be vital to supply of mammalian blood to a patient in emergency conditions. Also inventories of stored blood can be analyzed for shelf life prior to use. Because methemoglobin affects human blood by increasing the fraction of the ferric form of iron over the ferrous form and thereby **30** decreasing the ability of hemoglobin to combine with oxygen, this embodiment has significant physiological value to a health care practitioner.

Within the scope of this aspect of the invention, other wavelengths sensitive to absorption changes due to the changes in scattering as a result of the increased size (or volume) of red blood cells due to aging of the stored blood can also be measured.

Because of the variable nature of the human population, and their habit of ingesting tobacco for relaxation or recreation, and/or inhaling smoke involuntarily, other mathematical variations can be introduced in the prediction equations in order to compensate for the presence of carboxyhemoglobin. For example, one can add to a prediction equation a correcting variable corresponding to the value for carboxyhemoglobin as provided by a co-oximeter or add additional wavelengths. A representative equation follows:

$$HCT=\alpha'' HV_{n,y}+\beta'' HV_{n1,y1}+\chi'' HV_{n2,y2}+\delta'' HV_{n3,y3}+\epsilon'' HV_{n4,y4}+\phi$$

where the terms have the same meaning as in Equation 13 above but now in addition employ wavelengths to include carboxyhemoglobin (between about 450 nm and 1000 nm and preferably between 480 nm and 650 nm) and to form the HV ratios.

As justification for this alternative embodiment, it was found that the smoking population had a carboxyhemoglobin content of between 1–10% of total hemoglobin, whereas the non-smoking population had a carboxyhemoglobin content of less than 1%–2%.

People exposed to smoke from fires, for example, may have elevated carboxyhemoglobin values of up to 15 to 30%.

Usefulness of the Invention

As stated previously, embodiments of the invention have great advantage in the ability to accurately and precisely predict hematocrit, methemoglobin, percent oxygen saturation in a noninvasive, nonintrusive manner.

Health care practitioners can employ the method and apparatus of the present invention to predict hematocrit and other optional analytes of interest within acceptable levels of prediction in substitution for more costly, more intrusive, more painful, and more dangerous conventional techniques.

Because of the truly noninvasive, painless method of the invention, a health care practitioner can continuously or periodically monitor hematocrit of a patient for changes or trends in physiological condition or can rapidly diagnose the immediate condition of a patient under severe trauma in a civilian or military situation.

The invention is not limited to embodiments described above. The following claims and their operative equivalents identify the scope of the invention.

What is claimed is:

1. An apparatus for the noninvasive prediction of hematocrit within mammalian tissue, comprising:

(a) a light source adapted to noninvasively interrogate the mammalian tissue with light of at least two wavelengths, wherein the at least two wavelengths are selected according to wavelength selection criteria, and wherein the wavelength selection criteria comprise:

(1) a wavelength where absorbance of water is at or near a measurable peak;

(2) at least one wavelength where absorbance of oxyhemoglobin and deoxyhemoglobin are predictable and represent total hemoglobin content;

(3) a wavelength where the absorbance of water greatly exceeds the absorbance of all forms of hemoglobin; and

(4) a wavelength where the absorbance of all forms of hemoglobin greatly exceeds the absorbance of water;

wherein each of the wavelength selection criteria must be satisfied, wherein each selected wavelength can satisfy one or more than one of the wavelength selection criteria, and wherein at least one of the selected wavelengths is in the range 1150–2100 nm;

(b) at least one detector adapted to receive light of the selected wavelengths transmitted through the mammalian tissue, the detector further adapted to convert the transmitted light of each selected wavelength from optical signals into electrical signals; and

(c) processing means, connected to receive the electrical signals from the detector, the processing means for:

determining the intensity of at least one peak, the intensity of at least one valley, and the intensity of at least one direct current value for the transmitted light of each selected wavelength;

determining at least one pseudo-absorption H Value for each selected wavelength, wherein each H Value is based on the intensities of the at least one peak, at least one valley, and the at least one direct current value; and

determining a prediction equation for the noninvasive prediction of hematocrit, wherein the prediction equation is based on true hematocrit values and the pseudo-absorption H Values determined for each selected wavelength.

2. The apparatus of claim 1, wherein the processing means is further adapted for noninvasively predicting hematocrit using the prediction equation.

3. The apparatus of claim 2, further comprising:

(a) means for calculating a coefficient of variation of the at least one H Value.

4. The apparatus according to claim 2, further comprising:

(d) means for displaying the prediction of hematocrit.

5. The apparatus of claim 1, wherein the modulated light source maintains relative spectral intensity.

6. The apparatus according to claim 1, wherein the wavelength selection criteria further comprises:

(5) a wavelength where the absorbance of oxyhemoglobin greatly exceeds the absorbance of deoxyhemoglobin; and

(6) a wavelength where the absorbance of deoxyhemoglobin greatly exceeds the absorbance of oxyhemoglobin.

7. The apparatus according to claim 6, wherein the wavelength selection criteria further comprises:

(7) at least one different wavelength from selection criteria (1) where the absorbance of water is at or near a measurable peak or shoulder and is subjected to differing interferences than selection criteria (1); and

(8) a wavelength where the absorbance of water is in or near a valley between peaks and where the absorbance of hemoglobin is minimal.

8. The apparatus according to claim 7, wherein the wavelength selection criteria further comprises:

(9) a wavelength where water and hemoglobin are in an isosbestic relationship.

9. The apparatus according to claim 8, wherein the wavelength selection criteria (1) has a range of about 1160–1230 nm; wherein the wavelength selection criteria (2) has a range of about 800–850 nm; wherein the wavelength selection criteria (3) has a range of about 1150–2100 nm; wherein the wavelength selection criteria (4) has a range of about 450–690 nm; wherein the wavelength selection criteria (5) has a range of about 650–690 nm; wherein the wavelength selection criteria (6) has a range of about 890–920 nm; wherein the wavelength selection criteria (7) has a range of about 960–990 nm; and wherein the wavelength selection criteria (8) has a range of about 1100–1120 nm.

10. The apparatus according to claim 1, further comprising a fresnel lens to shape the transmitted light of each selected wavelength.

11. The apparatus according to claim 1, further comprising

a high common mode rejection amplifier for amplifying and filtering the transmitted light of each selected wavelength.

* * * * *

UNITED STATES PATENT AND TRADEMARK OFFICE

CERTIFICATE OF CORRECTION

PATENT NO. : 5,755,226
DATED : May 26, 1998
INVENTOR(S) : Hatim M. Carim, et al.

It is certified that error appears in the above-identified patent and that said Letters Patent is hereby corrected as shown below:

On the title page, item [75] Inventors: Add Dirk R. Smith, Ramsey, MN.

Signed and Sealed this

Eleventh Day of May, 1999

Attest:

Q. TODD DICKINSON

Attesting Officer

Acting Commissioner of Patents and Trademarks